RSC Advances

REVIEW

View Article Online
View Journal | View Issue

Cite this: *RSC Adv.*, 2025, **15**, 43198

Green chemistry spotlight: metal-free organic transformations mediated by potassium persulfate

Rapelly Venkatesh[a] and Priyanka Chaudhary *[b]

Received 20th August 2025
Accepted 9th October 2025

DOI: 10.1039/d5ra06175j

rsc.li/rsc-advances

Potassium persulfate ($K_2S_2O_8$) has been used for the construction of carbon–carbon (C–C) and carbon–heteroatom (C–P/C–N/C–S/C–Se) bonds through metal-free oxidative transformations. This inexpensive oxidant has garnered significant attention in recent years as it is a green alternative for oxidative transformations. This review presents an update on the applications of potassium persulfate ($K_2S_2O_8$) in various transformations in the last six years (2018–2024). The key advancements in metal-free reactions driven by $K_2S_2O_8$ are highlighted, and critical discussions on their limitations are incorporated. Herein, this review focuses on presenting a perspective to organic chemists, encouraging the strategic development of unprecedented $K_2S_2O_8$-promoted oxidative methodologies by identifying the research gaps. Furthermore, it offers mechanistic insights into the underlying free-radical pathways of the reaction mechanism in detail.

1. Introduction

In synthetic organic chemistry, the formation of C–C and C–X (X = S, Se, O, P, and N) bonds has always been the central focus among researchers due to their fundamental importance in the synthesis of pharmaceuticals, agrochemicals and materials.[1] The construction of bonds and molecular architectures is critical, and this key step is used in the development of new molecules with desired properties. Significantly, over the years, the methods for forming these bonds have evolved, driven by the need for more selective and environmentally friendly methods.[2] Such organic transformations could be made environmentally friendly if the pre-functionalized substrates and byproducts are minimized. There are many organic and inorganic oxidants that have been explored by chemists. Among them, the most recently highlighted oxidant is potassium persulfate ($K_2S_2O_8$), which has shown a broad utility since its first report by Minisci in the early 1980s.[3] Potassium persulfate is an odourless and white crystalline solid. The individual sulphate groups of potassium persulfate are tetrahedral. The bond distance between dioxide (O–O) is 1.495 Å, and it is the redox active site. Its homolysis makes persulfate a powerful radical oxidant. In its structure, there are three short S–O bonds and one long S–O bond with lengths of 1.43 Å and 1.65 Å, respectively.[4] Its terminal S–O bonds have partial double bond character due to resonance. In the context of metal-catalyzed organic transformations for C–H functionalization, one of the challenges is the regeneration of the catalyst used in the reaction, which is achieved through oxidants. Furthermore, its reactivity can be enhanced by transition metal ions, making it a valuable tool in organic synthesis for metal oxidative organic transformations.[5] The antibonding orbitals of persulfate's O–O are responsible for bond cleavage and radical initiation. The formed $SO_4^{-\bullet}$ radical has a half-occupied orbital, which overlaps with the substrate orbitals and enables single-electron transfer (SET), hydrogen abstraction, radical addition, and annulation reactions.[6] Although the orbitals of the K^+ ion do not contribute to these reactions, the persulfate anion orbitals are directly responsible for its powerful oxidative and radical chemistry (Fig. 1).

Compared with other oxidants (*e.g.*, TBHP, H_2O_2, and selectfluor), potassium persulfate is a bench-stable oxidant, which offers a unique combination of high redox potential ($E^\circ \approx +2.01$ V) and clean byproducts. Hence, it is attractive for green and scalable synthesis. It avoids the generation of flammable organic peroxides in comparison with TBHP. Unlike H_2O_2, it does not require activation using any catalysts or acidic conditions, and no overreaction of the substrates occurs. $K_2S_2O_8$ enables selective radical transformations under mild

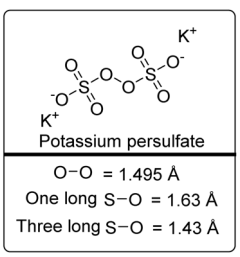

Fig. 1 Structure of potassium persulfate with bond distances.

[a]*Institute of Chemistry, Academia Sinica, Taipei 115201, Taiwan*
[b]*Department of Chemistry, University of Lucknow, Lucknow 226007, Uttar Pradesh, India. E-mail: priyankaciitbhu@gmail.com; chaudhary_priyanka@lkouniv.ac.in*

conditions. Selectfluor is more expensive and often results in the over-oxidization of substrates or introduction of fluorine inadvertently, while $K_2S_2O_8$ is cost-effective and highly atom-economical. Overall, $K_2S_2O_8$ balances reactivity, selectivity, and sustainability for radical-promoted oxidative couplings.

However, potassium persulfate is associated with a few practical limitations such as poor chemo selectivity in complex molecules with multiple oxidative sites and low solubility in non-polar solvents, often requiring the use of biphasic systems, which is challenging. Also, sulfate ions are generated as acidic byproducts, which may affect the basic sensitive reactants, and therefore neutralization would be required after completion of the reaction. These challenges indicate that although $K_2S_2O_8$ is a powerful tool for oxidative transformations, its use often demands fine-tuning of the reaction conditions, careful additive selection, and optimization for each substrate class to achieve high efficiency and selectivity.

For more than two decades, $K_2S_2O_8$ has been discussed as an environmentally friendly oxidative reagent because of its unique properties. It is a strong oxidant, capable of generating reactive oxygen species such as sulfate radicals, which can promote a variety of bond-forming reactions. Potassium peroxydisulfate ($K_2S_2O_8$) is a highly effective and versatile oxidizing agent.[3] It is a potential radical initiator. The peroxydisulfate ion $S_2O_8^{2-}$ decomposes to form the sulfate radical ($SO_4^{\bullet-}$), a potent one-electron oxidant with a very high redox potential of 2.01 V in aqueous solution.[3] Furthermore, its use can contribute to more sustainable chemistry by reducing the need for harsh reagents or excess catalyst as well as limiting the formation of toxic byproducts. It has great solubility in warmer water than colder water. These attributes make it a highly attractive option for researchers seeking efficient and environmentally friendly methods. Also, it has been reported that the usage of $K_2S_2O_8$ is very effective in the degradation of aromatic pollutants.[7]

An abundance of literature has been reported on metal-mediated and metal-free reactions. Based on this, a review has been reported in 2018,[5] but to the best of our knowledge, there has been no updated review in the literature to date. Here, metal-catalyzed reactions are out of the scope of this review. This straightforward strategy has shown great applicability in various metal-free oxidative reactions. Its synergistic approach to work with different additives and in the presence of water has been well explored in recent years. A systematic description of important substrates and their mechanism with underlining possibilities and shortcomings are presented. Herein, an update on the applications of the environment-friendly potassium persulfate in recent years is reported.

2. Metal-free oxidative transformations with $K_2S_2O_8$

Potassium persulfate has been explored as a principal and powerful oxidant for the construction of carbon–carbon (C–C) and carbon–heteroatom (C–O/C–P/C–N/C–S/C–Se) bonds through metal-free oxidative transformations. The range of bond construction has been further classified under various sections for oxidized, cyclized, and acyclized compounds, followed by the corresponding mechanism. These bonds are constructed through conventional, thermal, and photochemical approaches. The decomposition of $K_2S_2O_8$ leads to oxidation through the peroxodisulfate ion ($S_2O_8^{2-}$) or sulfate radical anion ($SO_4^{\bullet-}$).

2.1. C–C bond formation

A variety of substituted aldehydes, acids such as aliphatic/aromatic acids/keto acids/formic acids/salts of ketoacids/aryl acetic acid/sodium formate, carbamoyl moieties, benzoquinones, indazoles, and indoles, has been used for persulfate-mediated C–C bond formation. Herein, the C–C bond is formed simultaneously with a C–N or other type of bonds in the presence of a cheap inorganic oxidant ($K_2S_2O_8$).

In 2018, Airton G. Salles *et al.* reported photoredox catalyst (methylene blue) and potassium persulfate-mediated hydroacylation and epoxyacylation in basic aqueous medium under visible light (100 W irradiation).[8] They investigated a wide spectrum of aldehydes (aromatic and aliphatic), along with substituted olefins (conjugated and non-conjugated) to furnish ketones and epoxyketones, respectively.

The optimized reaction conditions for epoxyacylation were found to be the presence of 2.5 methylene blue (MB) with 2 equivalent of potassium persulfate, and alkaline aqueous medium (0.5 M K_2CO_3) under a 100 W household bulb at room temperature (25 °C) for 12 h (Scheme 1). This protocol led to the formation of a series of epoxides from varying olefins and aldehydes, all giving good to excellent yields (Scheme 1). It was noticeable to the authors that a nitrogen-bearing ring (pyridine) enhances the transformation process (Scheme 1, **3f**).

Considering that long-chain ketones have huge applications in medicinal and energy science, the authors investigated the hydroacylation using non-conjugated and long-chain olefins and aromatic aldehydes using 0.5 methylene blue (MB) with 1 equivalent of potassium persulfate, and alkaline aqueous medium (2.5 M K_2CO_3) in the presence of a 100 W household bulb at room temperature (25 °C) in 12 h (Scheme 2). This gave a series of desired compounds **5a–5c** in 69–89% yield. However, aliphatic aldehydes did not work with this methodology.

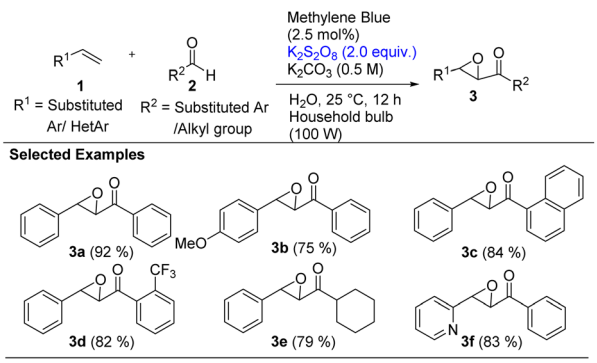

Scheme 1 Visible light-mediated epoxyacylation in an alkaline aqueous medium.

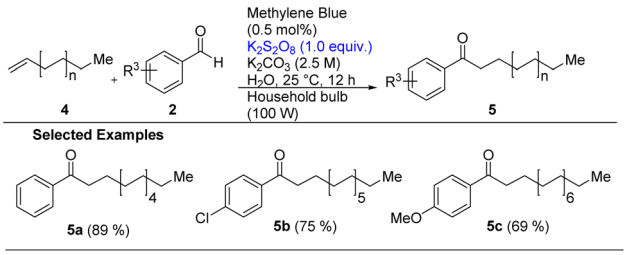

Scheme 2 Visible light-mediated hydroacylation in an alkaline aqueous medium.

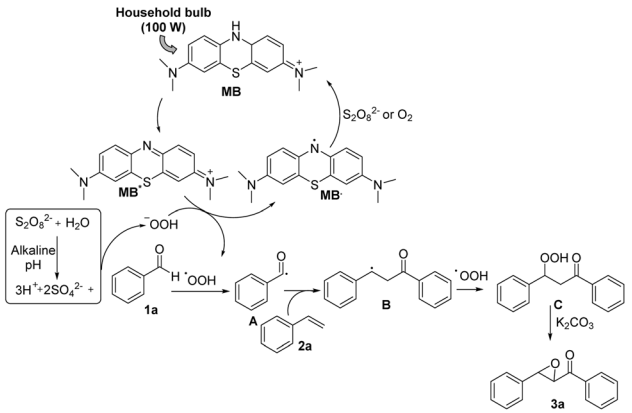

Scheme 3 Proposed mechanism for epoxyacylation.

The authors also evaluated the green chemistry metrics including carbon efficiency[9] and *E*-factor,[9] and later compared them with the respective reported reactions, as mentioned in Table 1. This indicates the importance of the designed methodology in the context of green metrics compared with previous literature reports.[10]

Mechanistic studies were performed by the authors to propose the mechanism for epoxyacylation (Scheme 3). Initially, the reaction was performed in the presence of 2 equiv. of TEMPO, under the standard conditions, which clearly showed the inhibition of product formation and free radical mechanism pathway. Further, the olefin was treated with electron-donating (ED) and electron-withdrawing (EW)-containing benzaldehydes, where the ED benzaldehyde gave the more favoured product. This proved that the addition of the acyl radical to olefin is a significant stage for the overall rate of reaction because of polar effects.

Decomposition of persulfate results in the formation of the hydroperoxide anion and sulphate under alkaline pH, as reported by Watts *et al.* Then, single-electron transfer (SET) from the hydroperoxide anion to methylene blue triplet (MB*) leads to the formation of the hydroperoxyl radical, as already reported. A 100 W household bulb was used to irradiate the photocatalyst (MB), which produces the excited MB state (MB*). As mentioned above, the generation of ˙OOH leads to hydrogen atom transfer from benzaldehyde (**1a**) to form the acyl radical (**A**), followed by its addition to styrene (**2a**) through SET. The formed radical **B** combines with the hydroperoxyl radical and forms peroxide (**C**). Finally, the hydroxide radical is eliminated using potassium carbonate (K_2CO_3), leading to the formation of epoxyketone (**3a**).

Later, in 2019, Jouffroy and Kong reported visible light-mediated C–H carbamoylation in the presence of 9-mesityl-3,6-di-*tert*-butyl-10-phenylacridin-10-ium tetrafluoro-borate (PC) of nitrogen-containing heterocycles.[11] They utilized bench-stable oxamate salts for the generation of carbamoyl radicals and amide functionalization of nitrogen-containing heterocycles. The rigorous standard reaction conditions were optimized using 4-chloroquinoline and potassium piperidine oxamate as the carbamoyl radical source, where 1.0 equivalent of potassium persulfate and 2.0 equivalent of trifluoroacetic acid (TFA) in a DMSO/H_2O mixture (1 : 1) in the presence of blue-LED irradiation at 30 °C gave the best results. The authors mentioned that maintaining the reaction temperature (30 °C ± 2 °C) with a fan and the solvent mixture of DMSO and H_2O in 1 : 1 ratio play a crucial and an important role in achieving the maximum product yield.

The versatility of the substrate scope for the oxamate part was explored with substituted alkyl groups on the nitrogen

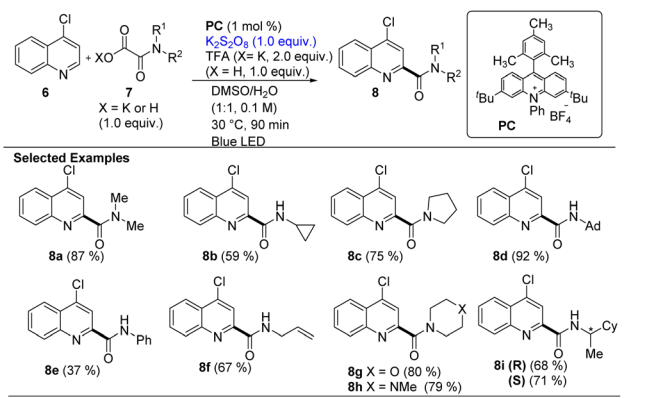

Scheme 4 Direct C–H carbamoylation of 4-chloroquinoline with various carbamoyl moieties.

Table 1 Comparison of the green metrics of the epoxyacylation and hydroacylation methods reported by Salles *et al.* with those of the previously reported methods

Green metrics	Salles *et al.* epoxyacylation	Previous literature on epoxyacylation[10]	Salles *et al.* hydroacylation	Previous literature on hydroacylation
Carbon efficiency	63%	27%	63%	28%
E-Factor	32	191	37	55

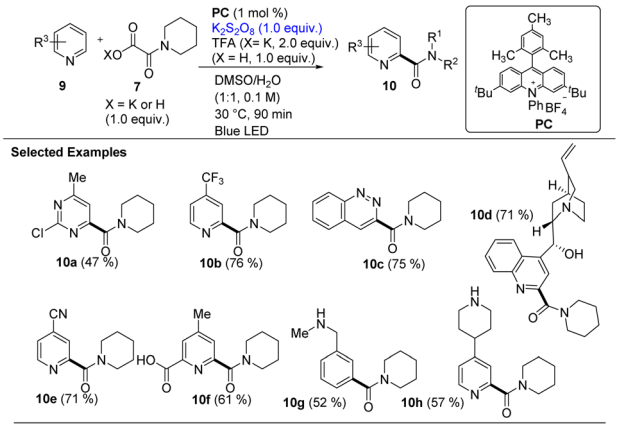

Scheme 5 Scope of the direct C–H carbamoylation of heterocycles.

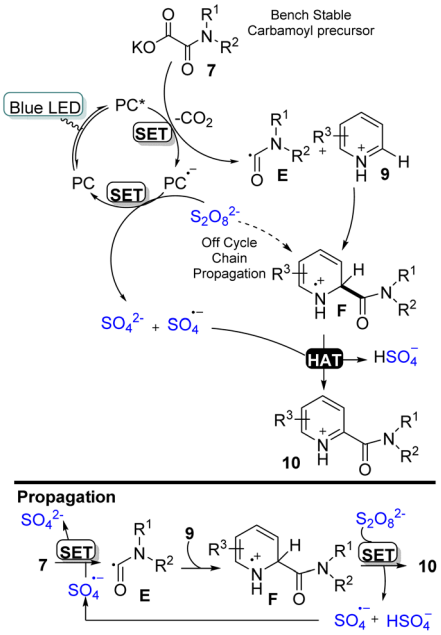

Scheme 6 Proposed mechanism for the direct C–H carbamoylation of heterocycles.

atom, as shown in Scheme 4. They showed great substrate compatibility with 37–92% yield. No C–H activation was observed in the case of nitrogen substituents of oxamate part. The chiral starting material in the case of **8i** gave the respective optically identical R and S products in quantitative yield (where no racemic products were observed) given that epimerization is a common phenomenon occurring in the case of amide bonds.

Later, the substrate scope was expanded for the heteroaryl part, where quinoline and different bicyclic systems such as isoquinoline, quinoxaline, phthalazine and caffeine showed remarkable tolerance under the standard conditions (Scheme 5). Following this, *Cinchona* alkaloid (**10d**) gave the desired product in good yield (71%), where hydroxyl groups, tertiary amines, and *exo* vinylic groups were found to be compatible with the reaction conditions. This complex synthesis of compounds has applicability in phase-transfer catalysis (PTC).[12] The authors discussed the advantages of the synthesis of amides *via* the carbamoylation method over the conventional method of synthesis by acids. Also, the desirable installation of amide functionality in complex molecules could be easily achieved, as shown by their methodology without affecting sensitive functionalities.

The authors reported the visible-light-promoted carbamoylation of heterocycles. The photocatalyst [PC] (9-mesityl-3,6-di-*tert*-butyl-10-phenylacridin-10-ium tetrafluoro-borate) reached its excited state in the presence of a blue LED as PC* in CH_3CN. It further undergoes oxidation for single-electron transfer (SET) from **7**. CO_2 was lost, generating nucleophilic carbamoyl radical **E**, which immediately adds to protonated heteroarene **9** to provide intermediate **F**. Simultaneously, the radical anion photocatalyst ($PC^{-\bullet}$) is oxidized by persulfate to generate $SO_4^{\bullet-}$, which also regenerates photocatalyst PC. $SO_4^{\bullet-}$ oxidizes intermediate **F** through HAT, which furnished the desired product **10** (Scheme 6).

An off-cycle radical chain process may take place in this reaction (Scheme 6, propagation). Intermediate **F** could be oxidized by the persulfate anion, generating the sulfate radical anion, which can perform SET oxidation from oxamate **7** to generate carbamoyl radical **E**. Combined with the above-mentioned photoredox cycle as a radical initiation cycle, this radical chain propagation would afford the desired product **10** efficiently.

Considering the importance of ketones, M. A. Rizvi's and B. A. Shah's group reported a photoredox-catalyzed approach for the oxidative coupling of acetylenes with 1,4-benzoquinones to synthesize various 4-hydroxyfunctionalized aryl/alkyl ketones.[13] The authors mentioned that synthesis of this class of cyclobutenes was not reported.

They used benzoquinone and phenylacetylene as model substrates in an AcCN/H_2O solvent system for the optimization of the reaction and irradiation of the reaction mixture with a blue light, resulting in 4-hydroxy benzophenone in 88% yield and no byproducts. The optimized conditions were $K_2S_2O_8$ (3 mmol), 1 mmol of trifluoroacetic acid (TFA) in 4 mL of AcCN/H_2O (1 : 1) under blue light irradiation at 25 °C for almost 10 h. The reaction also occurred in the presence of competitive oxidants such as $Na_2S_2O_8$ and $(NH_4)_2S_2O_8$, which gave lower yields compared to potassium persulfate. Also, the optimized conditions were examined under argon-degassed conditions instead of atmospheric O_2, where only traces of the desired product were observed (Scheme 7).

Under the standard reaction conditions, they moved ahead to investigate the substrate scope by varying the aromatic and aliphatic alkynes (**12**) with benzoquinone (**11**) and substituted 4-hydroxy benzophenone (**13**). The [2 + 2] reaction tolerated the EDG and EWG almost equally and gave the desired products in excellent yields. Further, the Paterno–Buchi reaction was expanded with 1,4-naphthoquinones and aryl/alkyl alkynes and provided substituted cyclobutenes. The dominant products were in *syn*-isomer form. The substrates were well tolerated and obtained in good yields. Only in the case of **14d** and **14e**, the

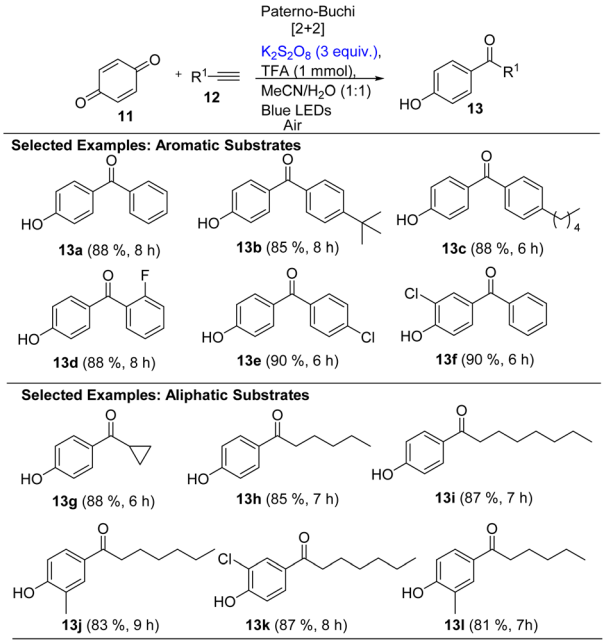

Scheme 7 Synthesis of aryl and alkyl ketones.

anti-isomers were obtained, which may be due to the axial interaction of the –OMe group of naphthoquinone and hydrogen atoms of the 3- and 6-membered substituent of alkynes (Scheme 8).

Before the proposed reaction pathway was studied, they performed pre-mechanistic studies involving TEMPO-mediated reactions and cyclic voltammetry. The reaction was inhibited in the presence of the radical scavenger TEMPO. The CV studies indicated that the phenylacetylene showed irreversible redox behaviour with only a single oxidation peak current starting at a potential close to 1.9 V (*vs.* SCE) and no reduction peak. This suggested that phenylacetylene can be oxidized by $SO_4^{2\bullet-}$, which is a generated photochemical with a higher reduction potential. These studies revealed that the reaction pathway is a free-radical approach with the help of TEMPO and consistent with the CV studies.

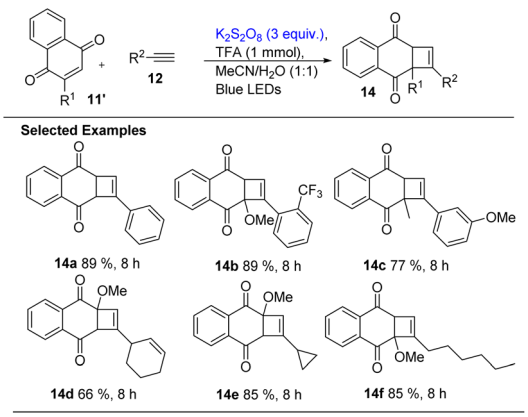

Scheme 8 Synthesis of cyclobutenes.

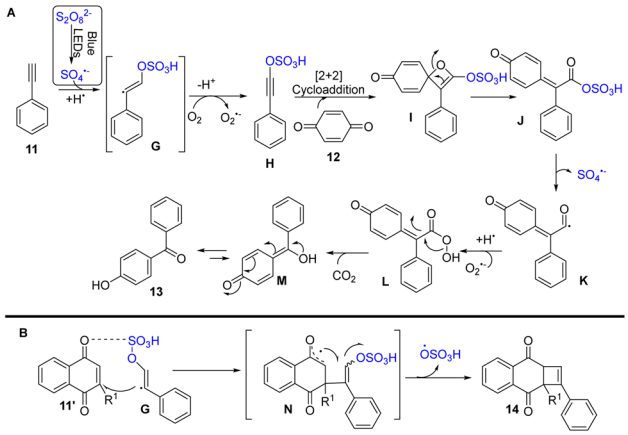

Scheme 9 Proposed mechanism: (A) synthesis of ketones and (B) synthesis of cyclobutenes.

The pre-mechanistic studies gave a platform to propose the mechanism (Scheme 9). The reaction proceeded with the homolysis of persulfate to form the sulphate radical anion in the presence of blue LEDs, which adds to the triple bond of the terminal alkyne and forms the vinyl transitory state (**G**). **G** in the presence of O_2 produces an intermediate (**H**) (comparatively stable). The reaction takes place between the carbonyl group of benzoquinone **12** and intermediate **H**, leading to the formation of oxetane **I**, which undergoes cyclic rearrangement to form intermediate **J**. This releases $SO_4^{\bullet-}$ to acyl radical intermediate as **K**. Then, $O_2^{\bullet-}$ reacts with intermediate **K**, followed by protonation by TFA, leading to per acid **L**, which further undergoes decarboxylation, and keto–enol tautomerization of *p*-quinone methides of **M** furnishes **13** as the desired product (Scheme 9A). In Scheme 9B, naphthoquinone undergoes addition to intermediate **G** through the C–C bond, leading to the formation of intermediate **N** with the loss of $SO_4^{2\bullet-}$, which gives substituted cyclobutenes **14**. This was confirmed through NMR data (especially *J* coupling values).

Considering the interest in the cyclization of enynes, the one-step synthesis of heterocycles using potassium persulfate through azidation was investigated by Wei *et al.* in 2019.[14] They reported that the transition metal-free, ligand-free, and regioselective cyclization of 1,6-enynes is promoted by $K_2S_2O_8$. For the optimization of the protocol, the chosen substrates were the model reaction of *N*-phenyl-*N*-(prop-2-yn-1-yl) methacrylamide with $TMSN_3$ (**16**) and the desired product was achieved under the optimal conditions of $K_2S_2O_8$ (3 equiv.) and acetonitrile (2 mL) at 85 °C in 24 h. The authors studied five different azide sources, azido-benziodoxolone, sodium azide, trifluoromethanesulfonyl azide, trimethylsilyl azide and tosyl azide, where $TMSN_3$ gave the highest conversion. The possible reason for the poor performance of the other azides besides $TMSN_3$ would be the trouble in the generation of the azide radical in the reaction medium.

Later, an array of substrates was investigated under the standardized reaction conditions (Scheme 10). *N*-Aryl-substituted 1,6-eynes with ED and EW groups at the *para*-

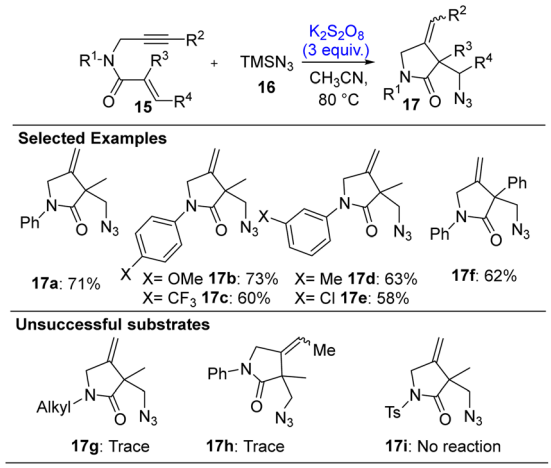

Scheme 10 Substrate scope of 1,6-eynes using $K_2S_2O_8$.

position gave good yields, whereas *meta*-substituted groups such as methyl (**17d**) and chloro (**17e**) groups in the aryl ring gave comparative lower yields. Also, it was observed that *N*-alkyl-bearing 1,6-eynes failed to produce the desired products, which may be possibly because the *N*-alkyl substituents/*N*-tosyl were not able to stabilize the alkyl azido radical intermediate in the reaction medium compared to *N*-aryl substituents. In most cases, almost 90% of the starting materials was recovered.

The mechanistic studies involved the addition of free radical trapping additives such as TEMPO, hydroquinone, and 2,6-di-*tert*-butyl-4-methylphenol (BHT), along with the standard reaction conditions, which gave traces of the desired products, which confirmed the formation of the azide radical. Also, the usage of anhydrous acetonitrile as the reaction medium led to lower yields of the desired products, which proved that the presence of water is a necessary condition for the reaction to occur. Later, the reaction of **15** with $TMSN_3$ was attempted using potassium persulfate, anhydrous AcCN and D_2O, which indicated that the H-atoms at the end of the olefin would be from water or the solvent.

In the proposed mechanism (Scheme 11), initially $K_2S_2O_8$ oxidized $TMSN_3$ to furnish azide radical intermediate **O** to alkene **15**, followed by the cyclization of the radical to alkyne group, leading to the formation of vinylic radical **P**. Later, it was observed that protons could be supplied by water or the solvent to intermediate **P** to form the desired product **17**.

Recently, A. Hajra *et al.* disclosed the $K_2S_2O_8$-mediated C-3 modification of 2*H*-indazoles using DMSO as a one-carbon source in chemodivergent transformations under aerobic conditions.[15] The conventional formylation processes are tedious, and therefore it is necessary to find interesting and economical routes for formylation strategies, leading to the design of formylation and esterification at C3 of indazoles using potassium persulfate.

The model substrate used is 2-(4-chlorophenyl)-2*H*-indazole with $K_2S_2O_8$ as an oxidant in a 1 : 1 mixture of DMSO and acetic acid. The optimal yield of 74% of the C-3 formylated product was achieved in DMSO/AcOH (19 : 1 ratio) at 100 °C. Variations in the solvent system ratio, temperature, and oxidant showed that $K_2S_2O_8$ and DMSO/CH_3COOH were the most efficient system. Interestingly, chemodivergence dependence was observed with an increase in $K_2S_2O_8$ (3 equiv.) content, which favoured the formation of ester derivatives, especially in a more acidic (1 : 3) DMSO/CH_3COOH reaction medium as the solvent at 100 °C.

A wide array of 2*H*-indazoles with various substituents at the N-2 position, including ED and halogen groups, underwent smooth formylation under the optimized conditions (Scheme 12). Also, the functionalized aryl groups at the indazole core were explored, which gave high yields of the products. It was noted that pyrazole derivatives did not give the desired product. In the case of ester formation at the C-3 position of indazole, various carboxylic acids such as acetic, propionic, and cyclohexane carboxylic acids were used and reacted successfully with indazole derivatives with moderate to good yields (Scheme 13). However, bulkier acids such as pivalic acid failed to react. Other nucleophiles such as phenol and aniline were unsuccessful, which indicated the specificity of the reaction to carboxylic acids.

To understand the reaction mechanism, control experiments were carried out. The reaction was carried out in the presence of N_2, which gave traces of product, indicating that O_2 is necessary for formylation but not for ester formation. Radical scavengers were also used under the standard reaction conditions, which inhibited both reactions, indicating a radical-based

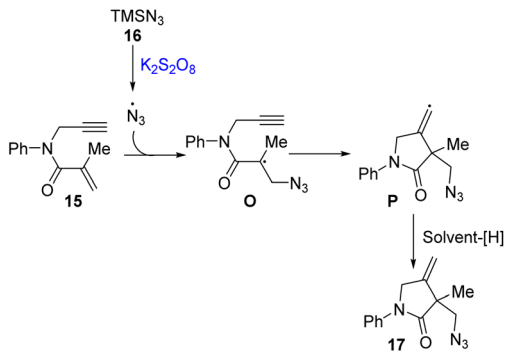

Scheme 11 Proposed mechanism for the radical cascade azidation and cyclization of 1,6-eynes.

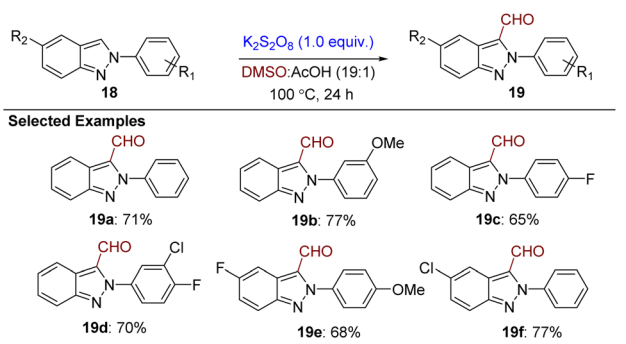

Scheme 12 Substrate scope for the formylation of indazoles.

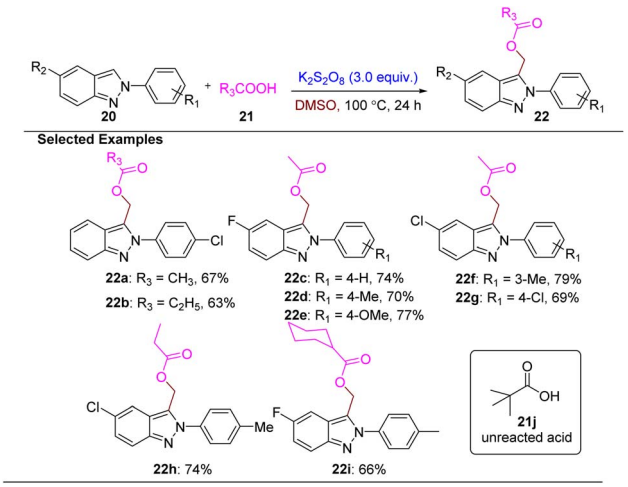

Scheme 13 Substrate scope of indazoles and aliphatic carboxylic acids.

mechanism. The DMSO source of the formyl and methylene groups was confirmed using isotopic labeling with DMSO-d_6 as the reaction medium.

The authors suggested the mechanism, where the $K_2S_2O_8$ underwent decomposition to generate sulfate radicals, which extract hydrogen from DMSO, forming α-sulfinyl radicals such as intermediate **Q**. **Q** attacks the nucleophilic 3rd carbon of indazoles to form intermediate **R**. The sulfate radical abstracts an H radical to form intermediate **S**, which undergoes rearrangement to form intermediate **T**. Further, in the presence of oxygen and carboxylic acid, intermediate **T** leads to either the formylated (**19**) or esterified (**22**) products. The formation of the ester product involved the generation of radical species from the carboxylic acids using an oxidant (Scheme 14).

As stated above, the C3-formylation of indazoles was performed using DMSO and acetic acid in the presence of $K_2S_2O_8$ as the formyl source. Encouraged by this work, in 2023, Sharma *et al.* disclosed the C3-formylation of varying imidazopyridines

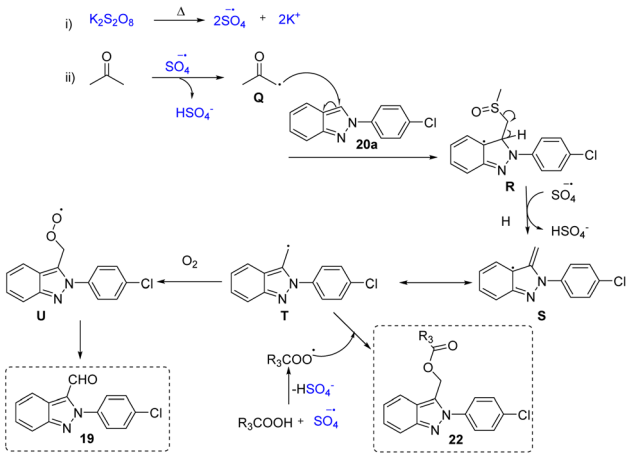

Scheme 14 Proposed mechanism for formylation and ester formation at the C3 site of indazoles.

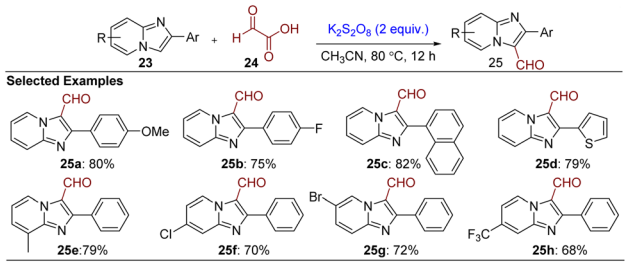

Scheme 15 C3-formylation of various imidazopyridines.

using glyoxylic acid and potassium persulfate under mild conditions.[16] The detailed optimization was conducted using 2-phenylimidazo[1,2-*a*]pyridine (1 mmol) and glyoxylic acid (1.2 mmol) with varying oxidants, solvents, temperatures. Alternative oxidants such as ammonium persulfate and oxone were also investigated but they failed to match the performance of $K_2S_2O_8$. The optimal conditions were $K_2S_2O_8$ (2 equiv.) in the presence of 3 mL acetonitrile at 80 °C, giving a high yield of the desired product in 12 h.

The feasibility of the standard reaction conditions was explored for substituted imidazopyridines and the C2-site using glyoxylic acid (Scheme 15). Electron-donating (**25a**) and electron-withdrawing groups (**25b**) at the C-2 aryl position gave good yields. Extended aromatic systems such as naphthyl (**25c**) and heteroaryl groups such as thiophene (**25d**) gave excellent yields. Similarly, substitutions of alkyl and halo/EW groups on imidazopyridines were well tolerated and furnished the products (**25e–25h**) in yields between 68–79%. This clearly indicates the benefits of the robust transformation with the compatibility of functional groups.

The authors supported the mechanism with free-radical trapping experiments and through experimental data with spectroscopic characterization. The reaction ceased in the presence of TEMPO and BHT, which confirmed that it proceeds *via* a radical pathway. As shown in Scheme 16, the mechanism was proposed by the authors, where the condensation intermediate (**V**) is formed from imidazopyridines and glyoxylic acid, which was detected through mass spectrometry. This intermediate undergoes decarboxylation commenced by the sulfate radical ($SO_4^{-\bullet}$), followed by the generation of intermediate **W**, which later loses a hydrogen atom to form the C-3 formylated product **25**.

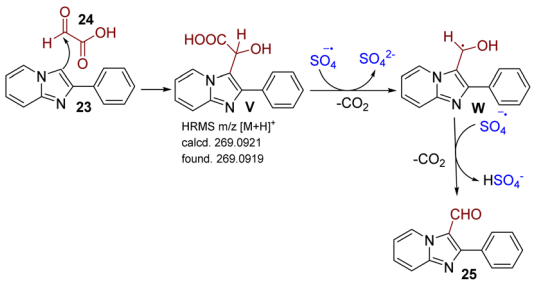

Scheme 16 Plausible mechanism for the C3-formylation of various imidazopyridines using glyoxylic acid.

In 2021, Laha and Hunjan disclosed glucose-promoted potassium persulfate C–C bond formation using substituted carboxylic acid and heteroarenes using any pre-functionalization in water as the reaction medium.[17] Glucose is an inexpensive sugar, which homolytically cleaves the peroxy bond of $K_2S_2O_8$, initiating the radical chemistry in aqueous media. This methodology enhances the sustainability given that the transformation was conducted in water.

The model reaction between phenylglyoxylic acid and pyrrole was conducted for optimization. It was performed in the presence of various sugars such as chitosan, galactose, raffinose, lactose and starch, which gave a lower yield of the desired product compared to glucose. The reaction in the presence of glucose gave good results, whereas without glucose, no product was formed. The solvent was screened based on the solubility of glucose from acetonitrile to water to a mixture of $CH_3CN : H_2O$, where H_2O was found to be the best. The addition of a mild base (NaOH) significantly increased the yield up to 85%. However, the standard reaction conditions chosen for further studies were 2 equivalents of $K_2S_2O_8$ and 1 equivalent of glucose in aqueous medium at room temperature.

With the optimized conditions in hand, the authors explored electron-rich heterocycles such as pyrrole, benzothiazole, and thiophene and electron-deficient heterocycles such as pyrazine, isoquinoline, and quinazoline with arylglyoxylic acid, which delivered the desired products in good yields (Scheme 17). A few failed to work for this methodology including indole, pyridine, and some indazoles. They also performed a gram-scale reaction using isoquinoline, which proved the scalability of this method. This transformation was further applied for the synthesis of benzimidazoles, benzothiazole, benzoxazole from *ortho*-substituted anilines and potassium salts of glyoxylic acids in quantitative yields (Scheme 18). Besides these amides, sulphonamide and amide derivatives were used to synthesize quinazolinones, benzothiadiazines and quinazolines. They gave yields between 75–89%, which are higher than that of the conventional approaches for their synthesis.

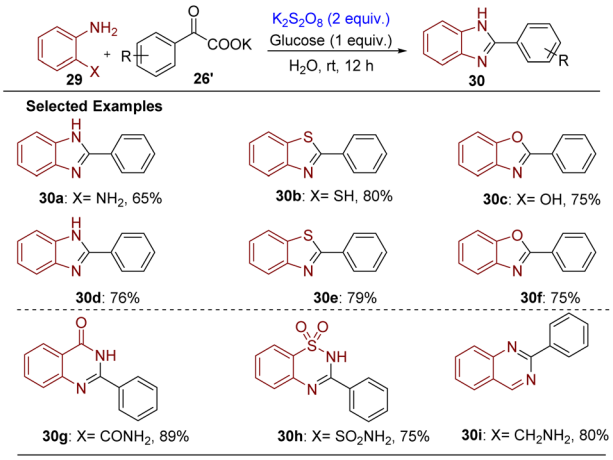

Scheme 18 Substrate scope for the synthesis of various N-heterocycles.

In the mechanistic studies, $K_2S_2O_8$ underwent heterolytic cleavage with the help of glucose at room temperature, resulting in the formation of a sulfate radical anion and sulfate anion, where the sulfate radical anion abstracts a hydroxyl radical from water (**I**). Herein, the presence of two reactive radicals was observed in the $K_2S_2O_8$-mediated transformation in water. However, $SO_4^{\bullet -}$ may result in the product formation depending on the nature of substrate (**II**). Glucuronic acid was produced by the HO$^\bullet$ radical *via* the oxidation of the –CH_2OH group of glucose (**III**). The aldehydic group of glucose underwent oxidation to produce gluconic acid in the presence of $SO_4^{-\bullet}$ and HO$^\bullet$ radicals (**III**). This suggested that the radicals cooperate in a unique way with the reactant and a difference in their behaviour would be observed based on the organic solvent used. Also, the radical scavenging experiment using TEMPO proved that the mechanism proceeds *via* a free-radical pathway. Therefore, the proposed mechanism led to the formation of the

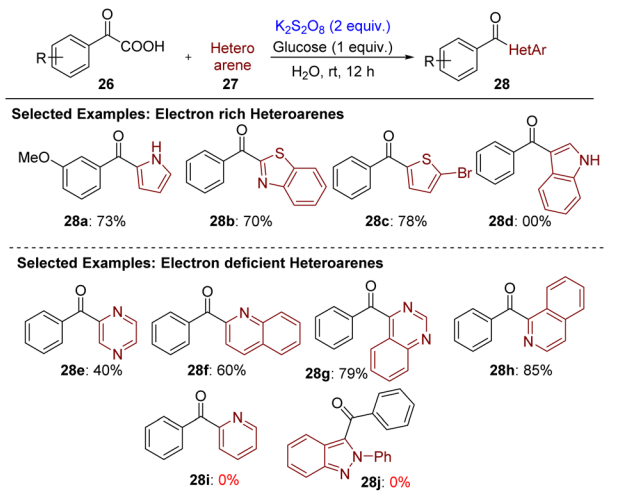

Scheme 17 Substrate scope for the aroylation of N-heterocycles using various ketoacids.

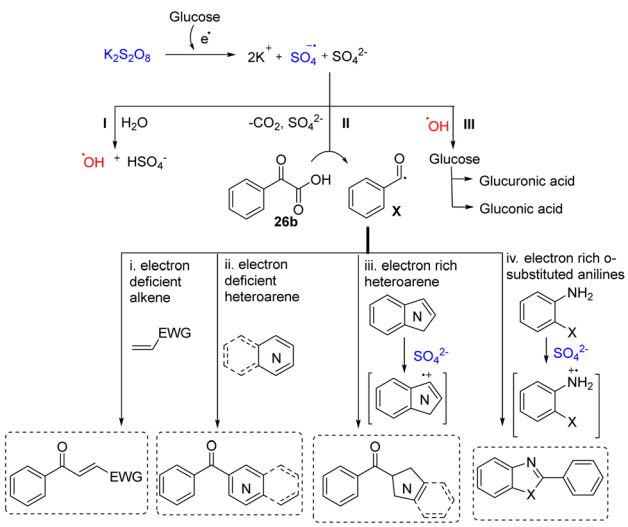

Scheme 19 Proposed mechanism for $K_2S_2O_8$-promoted aroylation.

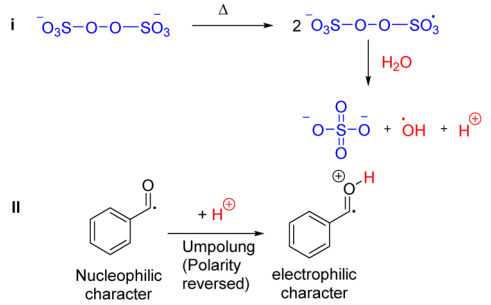

Scheme 20 Umpolung rule applied to an aroyl radical using $K_2S_2O_8$ in H_2O.

sulfate radical anion, further reacting with arylglyoxylic acid (**26b**) to form an aroyl radical (**X**) *via* decarboxylation, which further reacts with the electron-deficient alkene, electron-rich and deficient heteroarene, and electron-rich *ortho*-substituted anilines (**II**, Scheme 19).

The collaborative work of J. K. Laha and M. Breugst led to the investigation of the pH-controlled intramolecular cyclization of biarylacetic acid *via* decarboxylation by the application of the Umpolung rule[18] to the aroyl radical using $K_2S_2O_8$ in aqueous medium.[19] The authors hypothesized that the protonation of the carbonyl group of biarylacetic acid would reverse its nucleophilic character to electrophilic character by the decrease in pH after the generation of the aroyl radical. This could be achieved given that the decomposition of $K_2S_2O_8$ will lead to the formation of a sulphate anion, which reacts with water to produce protons, and hence the pH will drop naturally (Scheme 20). During the optimization of the reaction, they observed that presence of oxygen did not support the transformation, which is probably because it became a too oxidizing reaction. They isotopically labelled the oxygen as ^{18}O in H_2O, which confirmed the source of oxygen in the reaction through mass spectrometric analysis. The reaction was optimized, which gave the standard reaction conditions as 2 equivalents of $K_2S_2O_8$ in 1 mL of water as the reaction medium at 80 °C for almost 8 h, producing fluorenone in high yield.

Further, the protocol was investigated for electron-donating or electron-withdrawing substituents in biarylacetic acid either at the 2- or 4-position, which well tolerated the reaction conditions. Even disubstituted groups on the aryl group and the aromatic-extended group such as the naphthyl group (**32h**) gave good yields (Scheme 21). All the reactions proceeded smoothly under the standard reaction conditions to produce substituted fluorenone.

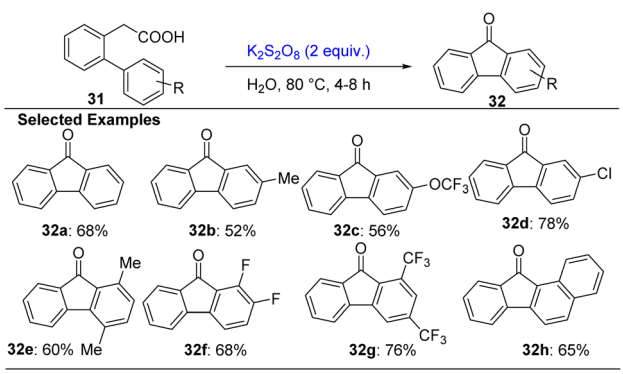

Scheme 21 Synthesis of fluorenone using biarylacetic acid.

The mechanistic studies initially involved the usage of TEMPO, a free radical scavenger, which completely inhibited the reaction and indicated the free-radical pathway of the reaction mechanism, trapping the benzyl radical intermediate in the reaction. The control experiments were conducted (a) by substituting the Brønsted acid with a Lewis acid ($AlCl_3$), (b) using *tert*-butyl hydroperoxide (TBHP), and (c) the combination of $AlCl_3$ and TBHP. In the case of (a), no product was formed, whereas in (b) only 15% of the desired product was formed with 55% of recovered starting material even after 24 hours. This proved that hydrogens are required for the formation of the product, where in the case of (c), almost 60% of the product was observed in 24 h given that the reactivity of TBHP was very slow (Table 2).

The mechanistic and computation studies helped in determining the underlying mechanism of the transformation. Biarylacetic acid in the presence of $K_2S_2O_8$ results in benzyl radical intermediate **Y**, which underwent oxidation to form benzyl carbocation **Z**. This intermediate forms [1,1′-biphenyl]-2-ylmethanol in the presence of water, which on oxidation led to the formation of [1,1′-biphenyl]-2-carbaldehyde. Further, this could form the desired product **32a** through three paths, as shown in Scheme 22. Through path **1a**, [1,1′-biphenyl]-2-carbaldehyde led to the elimination of the proton radical to form intermediate **A′** and underwent cyclization to from **B′**, followed by aromatization to form **32a** with the immediate removal of the H radical. Similarly, path **1a** was followed to obtain **A′**, where the eliminated H radical co-ordinates to carbonyl oxygen **D′** with the formation of cyclized intermediate **E′** through path **1b** and product **32a** was achieved. Also, in path **1c**, the carbonyl group of [1,1′-biphenyl]-2-carbaldehyde co-ordinates with the generated proton in the reaction medium as **C′**, followed by elimination of the H˙ radical and cyclization to form the final product **32a**.

In 2024, Indurthi *et al.* disclosed arylacetic acid as a coupling partner in a metal-free, room-temperature method from indoles and arylacetic acids using $K_2S_2O_8$ and glucose in water to synthesize 3,3′-bis(indolyl)methanes (BIMs).[20] This methodology was optimized using indole and phenylacetic acid. Different oxidants ($K_2S_2O_8$, $(NH_4)_2S_2O_8$, DDQ, $KHSO_5$) and sugar activators (glucose, galactose, maltose, and starch) were used in aqueous and acetonitrile solvents, where 2 equivalents of $K_2S_2O_8$ and 0.6 equivalents of glucose in water gave 78% yield of the desired product. A wide range of arylacetic acids (with both electron-donating and withdrawing groups) and functionalized indoles performed well, yielding BIMs in moderate to good yields (65–81%) (Scheme 23). This transformation was also utilized for the synthesis of bioactive compounds (**35e** and **35h**), which had great potential for pharmaceutical importance.

A few similar control experiments with radical scavengers (TEMPO and BHT) were performed as in earlier discussions above, which confirmed a radical mechanism. Glucose activates

Table 2 Control experiments for proposing the mechanism

S. no.	Reagents	Conditions	Yield [%] of **32a**
(a)	$AlCl_3$ (0.2–2 equiv.)	AcCN/DCM, 20–80 °C, 2–24 h	No reaction
(b)	TBHP (2 equiv.)	DCM, 80 °C, 24 h	15
(c)	$AlCl_3$ (1 equiv.), TBHP (2 equiv.)	AcCN/DCM, 80 °C, 24 h	60

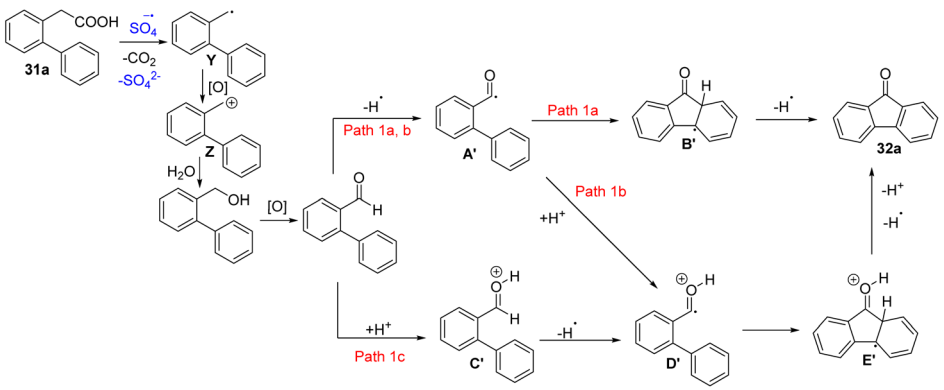

Scheme 22 Proposed mechanism for the formation of fluorenone.

persulfate, which facilitates the oxidative decarboxylation of arylacetic acids into aldehydes **K′**. The sulfate radical anion attacks **33a** to form nitrogen radical **L′**, which undergoes 1,3-hydrogen shift and isomerization, resulting in **L″**, and then **L″** reacts with **K** to form oxygen radical intermediate **M′**. The reaction of persulfate and water with intermediate **M′** led to the (3*H*-indol-3-yl) (phenyl)methanol intermediate, and its β-elimination formed the intermediate **N′**. Later, one more molecule of indole reacted with **N′** and resulted in **O′**, which steadily isomerizes to provide the desired product **35a.** Later, its condensation with indoles formed 3,3′-bis(indolyl)methanes (Scheme 24).

In 2023, Chen *et al.* developed a catalyst-free method using $K_2S_2O_8$ and tributylamine (Bu_3N) under mild conditions for the synthesis of oxindoles.[21] The authors investigated the optimization using *N*-arylacrylamide with *N*-Boc-4-iodopiperidine. $K_2S_2O_8$ was selected to oxidize Bu_3N and generate the α-

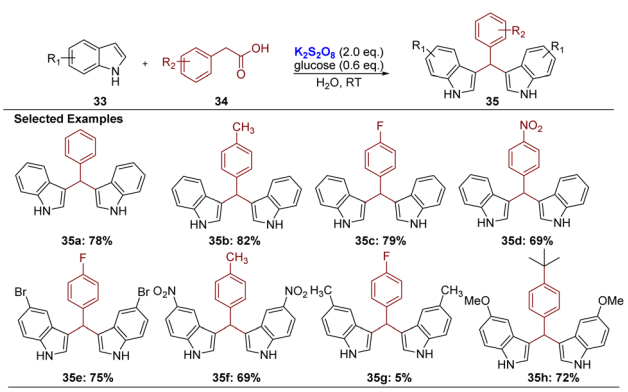

Scheme 23 Synthesis of 3,3′-bis(indolyl)methanes.

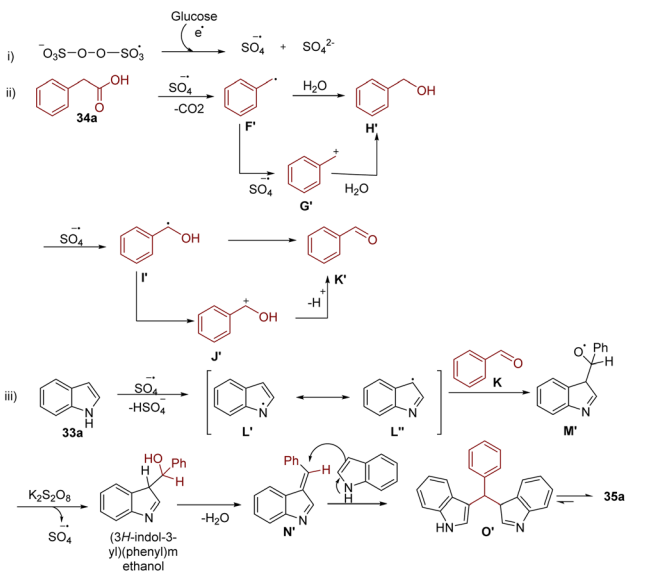

Scheme 24 Proposed mechanism for the synthesis of 3,3′-bis(indolyl) methanes.

aminoalkyl radical necessary for halogen abstraction. It was initially conducted in acetonitrile at 70 °C, and the desired oxindole product was obtained in 42% yield but the introduction of water as a co-solvent improved the solubility of $K_2S_2O_8$ and significantly boosted the yield in an AcCN : H_2O ratio of 4 : 1, resulting in 80% yield.

The versatility of this method could be explored with a series of *N*-aryl acrylamides. Various *N*-substituents such as bulky isopropyl, benzyl, and phenyl groups were well tolerated, which gave moderate to good yields. The reaction also accommodated a broad range of functional groups on the aryl ring, including halogens (F, Cl, Br, and I), trifluoromethyl, esters, and electron-donating alkyl groups. Interestingly, regioselective annulation occurred for *meta*-substituted arenes. In the case of halides, the reaction took place *ortho* to the substituent, while it occurred *para* to alkyl groups. Additionally, heterocycles such as pyridine (**38h**) and tetrahydroquinoline (**38i**) also participated successfully, giving moderate yields of the corresponding oxindoles. The versatility of this process was further demonstrated with a wide range of primary alkyl iodides. Linear alkyl chains of varying lengths (ethyl to octyl) and functionalized iodides with side chains all underwent efficient XAT-mediated coupling to yield the desired cyclized products. Thus, this approach enables the incorporation of diverse alkyl groups onto the oxindole core (Scheme 25).

Based on the experimental data and literature precedents, the authors proposed a plausible mechanism. Firstly, Bu_3N is oxidized by $K_2S_2O_8$ to generate α-aminoalkyl radical **P′**. This radical abstracts iodine from the alkyl iodide *via* halogen-atom transfer (XAT), forming alkyl radical **Q′**. **Q′** then adds to **36a**, producing intermediate **T′**, which undergoes intramolecular cyclization to form new radical species **U′**. This intermediate is finally oxidized and deprotonated to yield oxindole product **38** (Scheme 26).

Encouraged by this greener approach, Trinadh and Viswambharan constructed 2,2′-disubstituted-3-indolone derivatives from various substituted indoles using potassium persulfate ($K_2S_2O_8$) as the oxidant under aqueous conditions.[22]

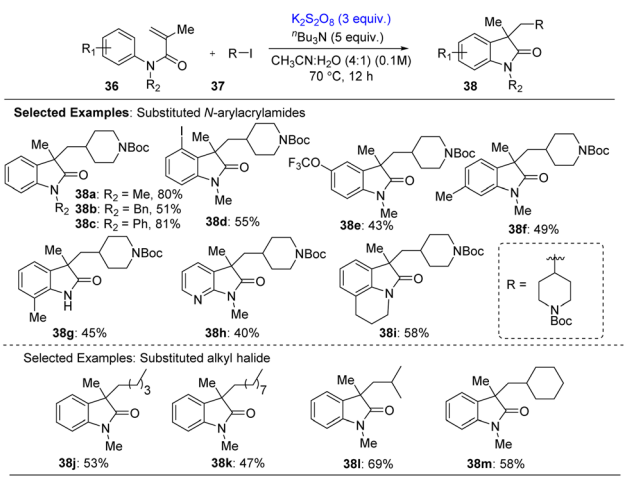

Scheme 25 Substrate scope of *N*-aryl acrylamides and alkyl halides.

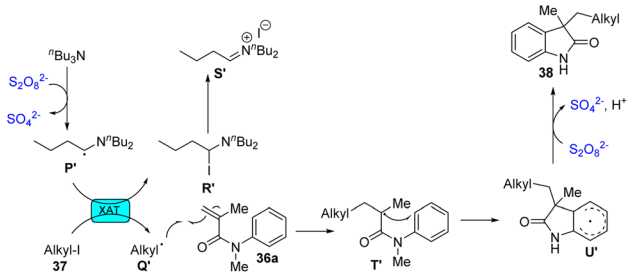

Scheme 26 Proposed mechanism for the synthesis of oxindoles.

The synthesized compounds were investigated for their photophysical properties, which could be used for bioimaging in cells. They explored the trimerization of 1-ethyl-1*H*-indole using $K_2S_2O_8$ in water, achieving 91% yield under open-air conditions. This reaction had not been reported before in aqueous media. They optimized various parameters and found that while some organic solvents gave lower yields, acetonitrile with molecular sieves under argon gave a similar 92% yield. The presence of oxygen did not significantly impact the reaction, and slow oxidation under heterogeneous conditions was crucial for high efficiency. All the substituted indoles containing electron-withdrawing groups (EWG) and electron-donating groups (EDG) gave good yields (Scheme 27) but a few indoles were insoluble in water due to which no products or low yield were obtained. Therefore, trimerization of water insoluble indoles was conducted in acetonitrile using $K_2S_2O_8$ with 4 Å molecular sieves (Scheme 28).

The pre-mechanistic studies confirmed the radical pathway, and EPR (electron paramagnetic resonance) studies were conducted using DMPO as a spin-trapping agent in both water and

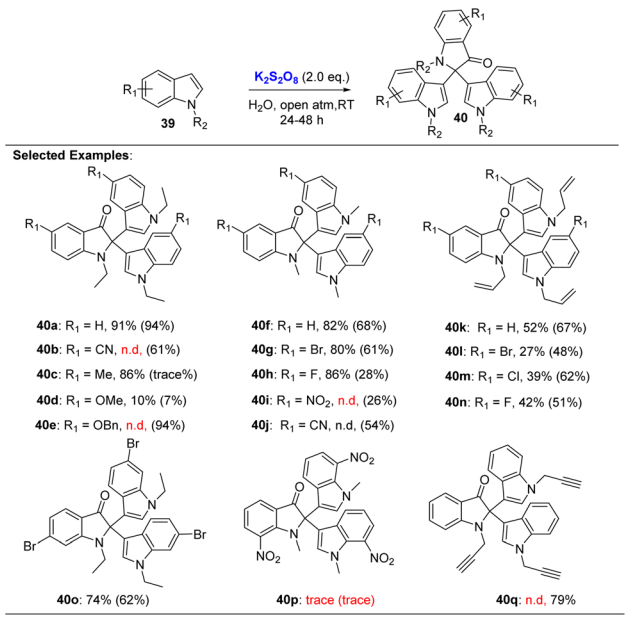

Scheme 27 Synthesis of 2,2-disubstituted-3-indolones in an aqueous medium.

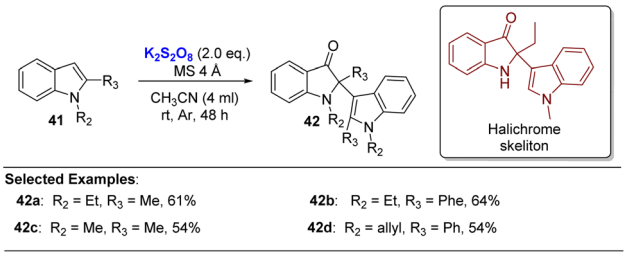

Scheme 28 Synthesis of 2,2-disubstituted-3-indolones in dry acetonitrile.

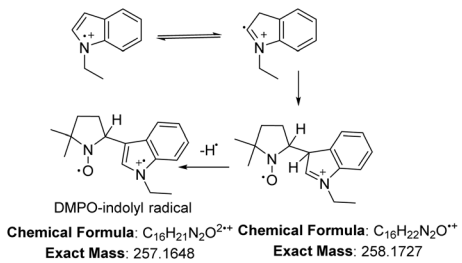

Scheme 29 DMPO-indolyl radical detected through mass spectrometry.

acetonitrile. In water, the EPR spectrum showed signals characteristic of a DMPO–OH adduct, indicating the formation of hydroxyl radicals. In acetonitrile, no signal was observed without DMPO, but with DMPO, a distinct septet pattern appeared, suggesting the formation of an indolyl radical cation at the C-3 position. The splitting pattern was influenced by hyperfine interactions with hydrogen and nitrogen atoms. Further validation was done through spectral variation and mass spectrometry, which confirmed the presence of the DMPO-indolyl radical adduct (Scheme 29).

EPR studies confirmed that both aqueous and acetonitrile-based reactions proceed *via* a radical mechanism. In water, sulphate radicals generate hydroxyl radicals, which react with indole to form radical intermediate (**W′**), which undergoes nucleophilic attack and oxidation to yield intermediate **Y′**. A similar process occurs in acetonitrile, where indole forms a radical adduct (**X′**) with sulphate radicals. This leads to intermediate **Z′**, which exists in keto–enol equilibrium with **Y′**. Under basic conditions, the reaction is suppressed. Further N–CH bond homolysis in intermediate **Z′** by hydroxyl (in water) or sulphate radicals (in acetonitrile) gives intermediate **A″**, which then reacts with another indole molecule to form the final trimer product (Scheme 30).

Metal-free cascade cyclized products were synthesized using readily available difluoroacetic acid derivatives ($ArSCF_2COOH$, $ArOCF_2COOH$, and $ArCF_2COOH$) for *N*-methacryloyl-2-phenylbenzimidazole by Ziwei Li *et al.* in 2022.[23] The role of the CF_2 group has been found to play an important role in the formation of benzimidazole[2,1-*a*]iso-quinoline-6(5H)-one derivatives. The authors investigated *N*-methacryloyl-2-phenylbenzimidazole and arylthiodifluoroacetic acid as model substrates for optimization. Varying the oxidants, bases, temperature, and atmosphere led to the standard reaction conditions of 2 equivalents of $K_2S_2O_8$ with 2 equivalents of $NaHCO_3$ in CH_3CN/H_2O (1 : 1) as the solvent system at 95 °C for 12 hours under N_2 gas with 73% yield.

With the optimized conditions in hand, they explored substituted 2-methyl-1-(2-phenyl-1*H*-benzo[*d*]imidazol-1-yl) prop-2-en-1-one with arylthiodifluoroacetic acids ($ArSCF_2COOH$), aryloxydifluoroacetic acids ($ArOCF_2COOH$), and α,α-difluorophenylacetic acids ($ArCF_2COOH$) (Scheme 31). The effect of various substituents on difluoroacetic acid derivatives is discussed in Table 3, whereas the variants of *N*-methacryloyl-2-phenylbenzimidazole involving the *para*-substituted rings with methyl, *tert*-butyl, methoxy, *etc.*, gave good yields, electron-withdrawing groups such as CF_3 and CN also worked reasonably, and substitution on the benzimidazole core (*e.g.*, 4,5-dimethyl) gave moderate yields. The reason behind the failure

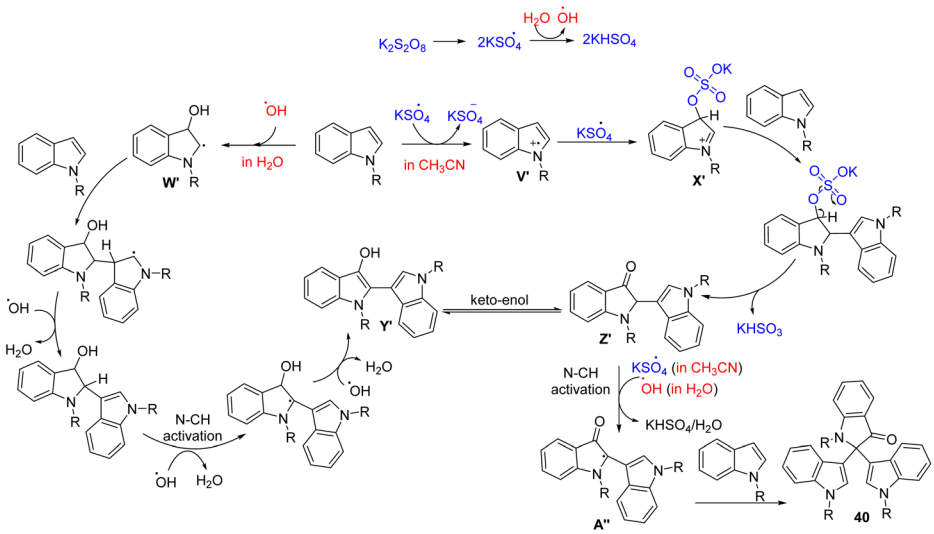

Scheme 30 Proposed mechanism for the formation of 2,2-disubstituted-3-indolones in H_2O and CH_3CN.

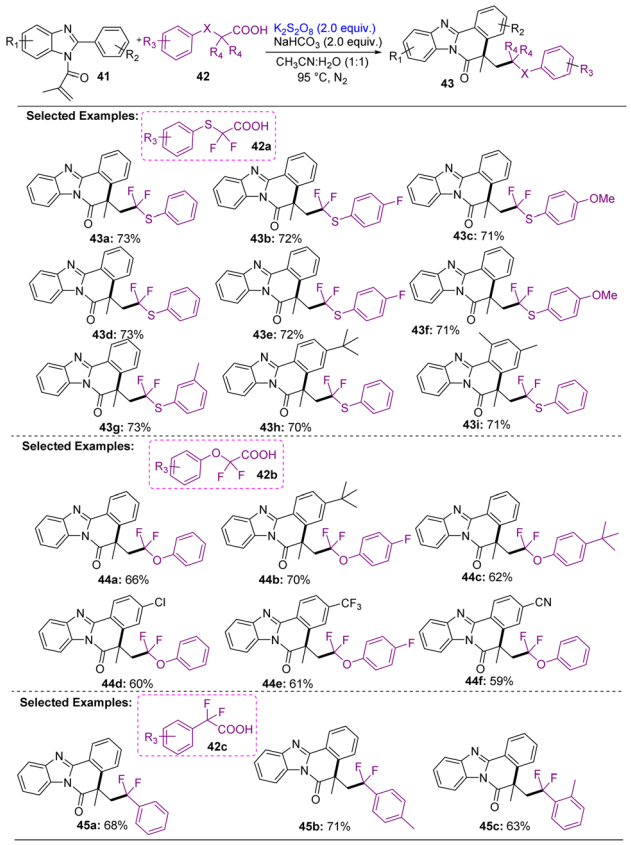

Scheme 31 Synthesis of aryldifluoromethylated benzimidazole[2,1-*a*] iso-quinoline-6(5*H*)-one derivatives.

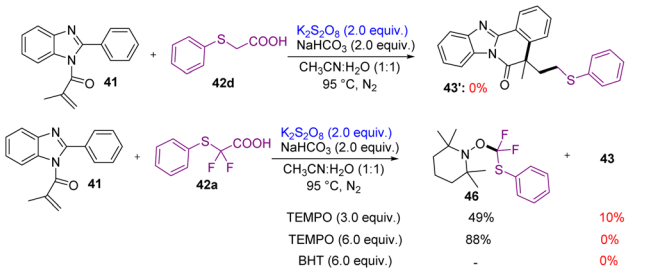

Scheme 32 Non-fluorinated analogue and radical scavenger-mediated reactions for mechanistic studies.

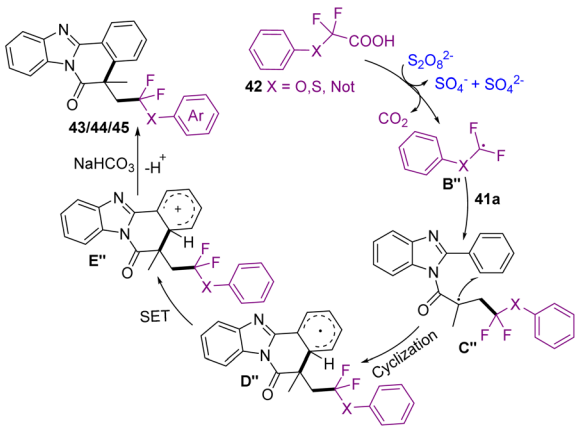

Scheme 33 Proposed mechanism for the synthesis of aryldifluoromethylated benzimidazole[2,1-*a*]iso-quinoline-6(5*H*)-one derivatives.

of restriction with strong electron-withdrawing groups such as NO_2, CF_3, and CN groups is the unstable methylene difluoro radical ($^{\cdot}CF_2$) in the course of the reaction. Mechanistic experimental studies were performed including the reaction of non-fluorinated analogue (**42d**), where no desired product was formed. Therefore, the presence of CF_2 is important for the completion of the reaction. Also, the reaction was performed in the presence of radical scavengers (TEMPO and BHT), which inhibited or lowered the product formation. These reactions confirmed that the reaction proceeded *via* a radical-based mechanism (Scheme 32).

The proposed mechanism involved the initial oxidative decarboxylation of **42** by $K_2S_2O_8$, generating aryldifluoromethylated radical **B**″. Then, **B**″ undergoes addition to the double bond of *N*-methacryloyl-2-phenylbenzimidazole (**41a**), forming intermediate **C**″, which underwent cyclization to form a six-membered ring as intermediate **E**″. This intermediate gets oxidized, and deprotonation yielded the final product (**43**/**44**/**45**) (Scheme 33).

The versatility of $K_2S_2O_8$ encouraged K. B. Schröder *et al.* to explore the capacity of photochemically activated persulfate to generate CO_2 radical anions from sodium formate, allowing their direct addition to electron-deficient alkenes such as vinylsulfones.[24] Initial optimization gave the standard conditions, where the reaction of phenyl vinylsulfone and sodium formate (HCOONa) using $K_2S_2O_8$ in aqueous acetonitrile under

Table 3 Substrate scope comparison of three different counter difluoroacetic acid derivatives

S. no.	Arylthiodifluoroacetic acids ($ArSCF_2COOH$)	Aryloxydifluoroacetic acids ($ArOCF_2COOH$)	α,α-Difluorophenylacetic acids ($ArCF_2COOH$)
1	Substituents such as F, Cl, and Br on the aryl ring were tolerated well	Substrates with F, Cl, CH_3, and *t*-Bu gave good yields	Standard conditions gave 63–71% yields
2	Strong electron-withdrawing groups (NO_2, CF_3, and CN) failed to give products due to radical instability	Methoxy and nitro groups led to no product, likely due to radical instability	Nitro substitution failed, again due to radical instability
3	Electron-donating groups (*e.g.*, OCH_3 and CH_3) had limited effects on yields		Methyl substitution at *meta*-position gave slightly lower yields due to steric hindrance

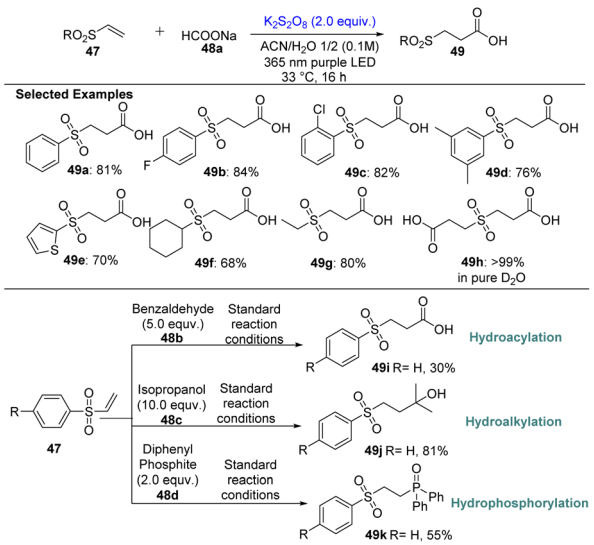

Scheme 34 Hydrocarboxylation, hydroacylation, hydroalkylation, and hydrophosphorylation of vinylsulfones using $K_2S_2O_8$.

blue LED irradiation efficiently produced the hydrocarboxylated product in 81% yield within 16 hours. Importantly, the reaction was tolerant to air and water, which offered a practical and scalable alternative to conventional CO_2-fixation strategies. The scope of the reaction included a variety of substituted vinylsulfones, with both aromatic and aliphatic derivatives having EDGs and EWGs species reacting effectively. Interestingly, this methodology was expanded beyond hydrocarboxylation to other hydrofunctionalizations, such as hydroacylation, hydroalkylation, and hydrophosphorylation, using different radical precursors in place of formate such as benzaldehyde, isopropanol, and diphenyl phosphite (Scheme 34).

The forgoing discussion led to pre-mechanistic studies depicting the possible mechanism. Suppressed product (**49a**) formation was observed in the absence of light, and hence light is necessary for the reaction. The addition of radical scavengers such as TEMPO completely inhibited the transformation, and the corresponding TEMPO-adducts were detected, which proved the involvement of carbon-centered radical intermediates. Deuterium-labeling experiments using deuterated formate provided strong evidence that the hydrogen atom incorporated into the product (**49a**) originates from the formate source rather than the solvent. UV-visible absorption studies ruled out the formation of electron donor–acceptor (EDA) complexes, and quantum yield analysis showed that the reaction was not a radical chain process but rather a stepwise photoinduced mechanism (Scheme 35).

The reaction mechanism revolves around the generation of CO_2 radical anions ($CO_2^{\bullet-}$), either through hydrogen atom abstraction (HAT) or *via* single-electron oxidation of formate (Scheme 36). One proposed pathway involves sulfate radicals produced from persulfate cleavage abstracting a hydrogen atom from formate, forming $CO_2^{\bullet-}$ directly. Alternatively, the oxidation of formate may yield a formyloxyl radical, which then decomposes to generate $CO_2^{\bullet-}$. This reactive species attacks the β-carbon of the vinylsulfone, producing a carbon-centered radical, which is eventually reduced to yield the final carboxylic acid product (**49a**). The persulfate acts as both an oxidant and initiator for radical formation, while visible light is crucial for driving the homolytic cleavage of the persulfate bond (Scheme 36).

In 2019, Xiao *et al.* emphasized the synthesis of chroman-4-one derivatives by potassium persulfate ($K_2S_2O_8$). The cascade radical cyclization reaction between aryl/aliphatic aldehydes and 2(allyloxy)aryl aldehydes was performed using a quaternary

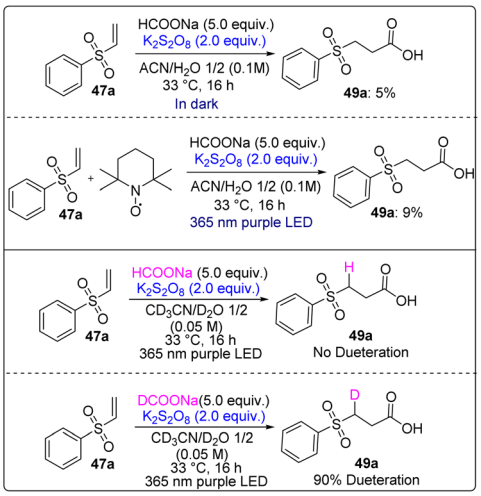

Scheme 35 Control experiments for the hydrocarboxylation of vinylsulfones.

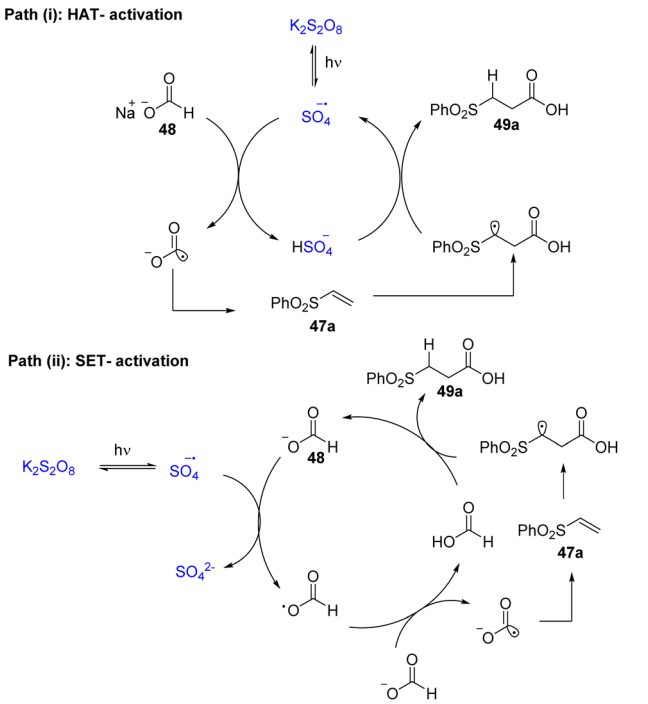

Scheme 36 Possible mechanisms for the hydrocarboxylation of vinylsulfones.

ammonium salt (TBAB) as an additive and $K_2S_2O_8$ as an oxidant.[25] This produced a chroman-4-one derivative in good yields by optimization, where 1 equivalent of TBAB and 2 equivalents of $K_2S_2O_8$ with dichloroethane (4 mL) gave the best results under a nitrogen atmosphere at 100 °C. It was also confirmed that the absence of TBAB or $K_2S_2O_8$ stopped the reaction completely as a control experiment.

These standard conditions were employed to investigate the substrate scope for aryl aldehydes and 2-(allyloxy)aryl aldehydes (Scheme 37). Electron-donating groups such as –Me, –OMe, and –SMe and weak electron-deficient groups such as –F, –Cl, –Br, and –I gave moderate to good yields, whereas electron-withdrawing groups such as nitro and cyano failed in the reaction. Interestingly, aliphatic aldehydes such as propionaldehyde and butyraldehyde worked very well. However, formaldehyde did not work under the reaction conditions (Scheme 37, **52l**). The sterically hindered substrates of 2-allyloxy aldehydes were also compatible.

The proposed mechanism initiated with the reaction of $K_2S_2O_8$ with TBAB, which generated sulfate radical anions. These radicals abstracted a hydrogen atom from the aldehyde (**50a**) and formed an acyl radical. The acyl radical adds to the double bond of 2-(allyloxy) arylaldehyde (**51a**) and anionic intermediate **F″**. This underwent intramolecular cyclization and generated intermediate **G″**. Later, the oxidation of **G″** by persulfate produced benzyl cation **H″**, which rapidly converted to the final chroman-4-one product (**52a**) (Scheme 38).

In 2020, H.-L. Huang *et al.* also developed a simple, one-step, transition metal-free method for the synthesis of chromenes

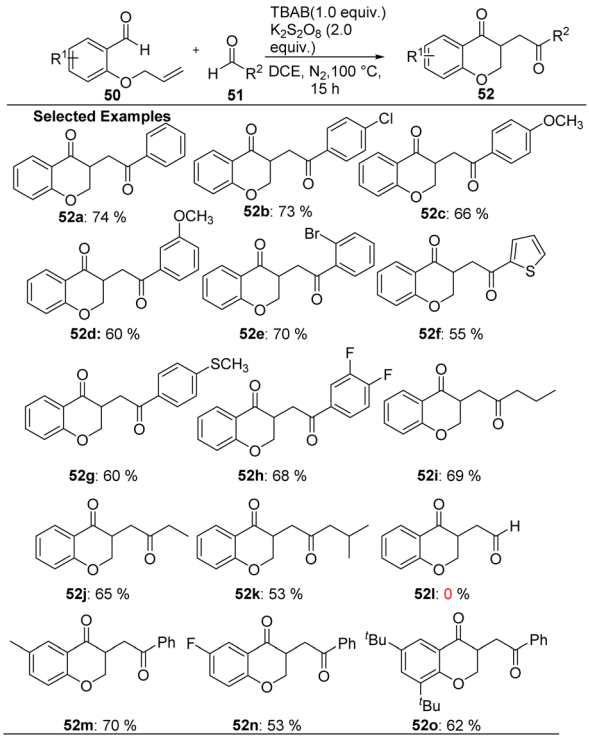

Scheme 37 Substrate scope of 2-(allyloxy) aryl aldehyde and aryl aldehyde for the synthesis of chroman-4-one derivatives.

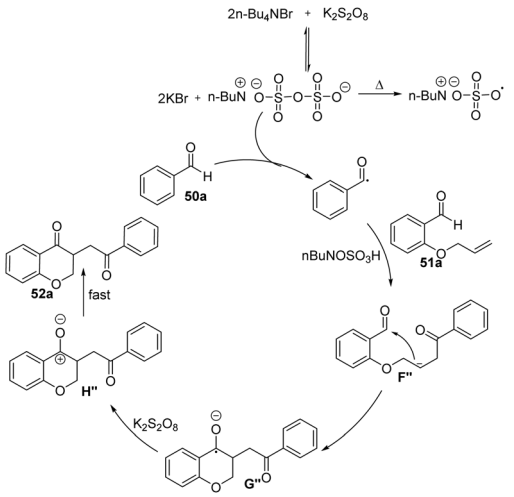

Scheme 38 Proposed mechanism for the synthesis of chroman-4-one derivatives using $K_2S_2O_8$ and TBAB.

containing CF_3 *via* the radical cascade cyclization coupling of 2-(allyloxy) aryl aldehydes with Langlois' reagent (CF_3SO_2Na).[26] The optimized conditions for the transformation involved 3.0 equivalent and 65% CF_3SO_2Na in 0.3 mmol, 0.1 M in DMSO due to the better solubility of both at 80 °C.

With the optimized reaction conditions in hand, a broad variety of electron-rich and electron-deficient aryl aldehydes were explored. The reactivity was enhanced with electron-withdrawing groups such as nitro, chloro, and bromo compared to electron-donating groups such as methyl and methoxy groups. In contrast, **54g** and **54h** gave traces of the product (Scheme 39).

The pre-mechanistic studies involved a radical trapping reaction using TEMPO, where the product formation was completely suppressed, confirming a radical pathway. It was also observed by the authors that chroman-4-one (**J″**) could be converted into **54a** under the reaction conditions (Scheme 40a). Based on these reactions, the mechanism was discussed. The Langlois reagent (CF_2SO_2Na) was oxidized *via* $K_2S_2O_8$ with the generation of CF_3 radical. The two pathways were mentioned by the authors (Scheme 40b). In path A, the addition of the radical to the C=C bond of 2-(allyloxy)arylaldehyde forms intermediate **I″**. Later, it underwent intramolecular cyclization to form chroman-4-one radical intermediate. Finally, oxidation and proton elimination furnished CF_3-substituted chromones. In alternative path B, it suggested that IT involved initial aldehyde oxidation *via* single electron transfer (SET) followed by further attack of the CF_3 radical, following similar path B, giving the desired product **54**.

In 2021, Zhou *et al.* disclosed the application of $K_2S_2O_8$ as a catalytic oxidant for the regioselective and efficient amidoalkylation between γ-lactams/amides and N-heteroaromatics in the absence of external photocatalysts or toxic solvents under visible light irradiation in water at room temperature.[27] For the optimization of the reaction, the authors chose 1-methylquinoxalin-2(1*H*)-one and 1-methylpyrrolidin-2-one (NMP) as model substrates and found that $K_2S_2O_8$ was indispensable

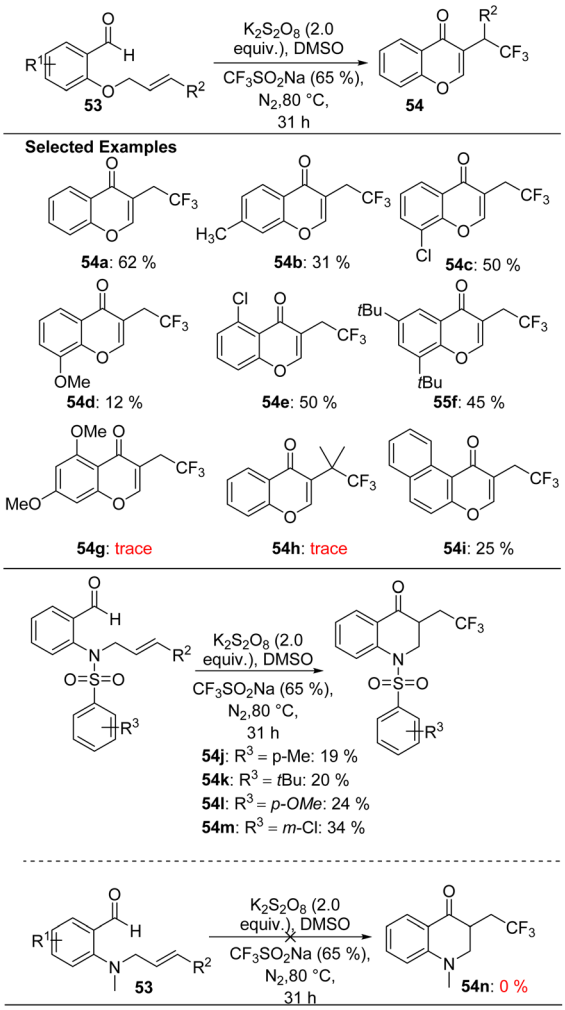

Scheme 39 Substrate scope of aldehydes and nitrogen atom reactants.

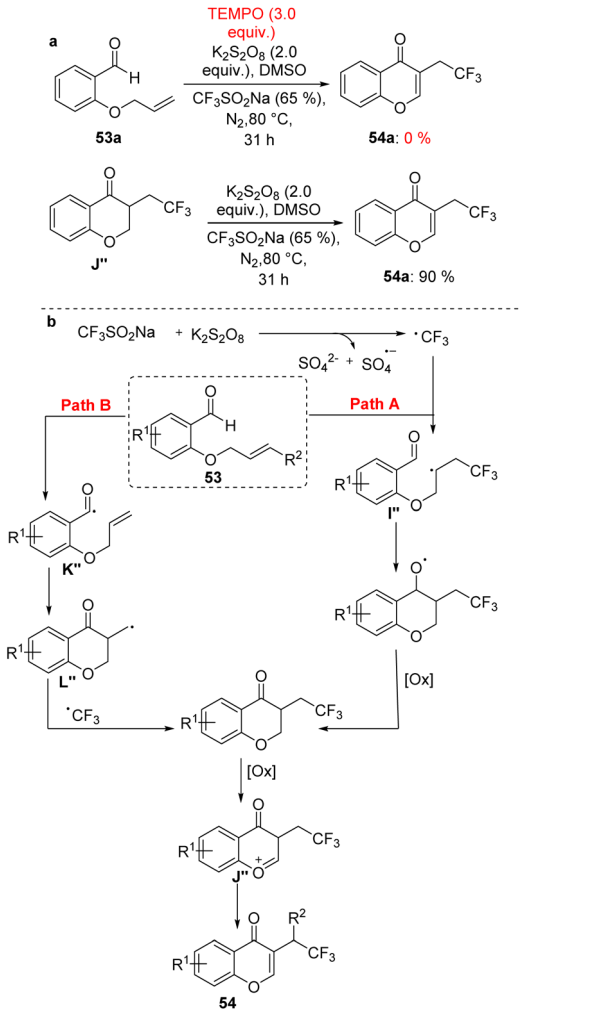

Scheme 40 (a) Control experiments for the synthesis of CF_3-containing 4*H*-chromenones, and (b) proposed mechanism for the synthesis of CF_3-containing 4*H*-chromenones.

where alternative oxidants such as TBHP, DTBP, or H_2O_2 provided lower yields. The optimized conditions involved 0.1 equiv. $K_2S_2O_8$ in air and the presence of water due to the better stabilization of reactive intermediates and irradiated with blue LEDs at room temperature for 24 hours.

The optimized conditions were applied to various N-protected quinoxalinones (methyl, ethyl, allyl, phenyl, *etc.*), which gave 56–85% yield. Even N-unprotected quinoxalinones provided the desired products. Substitution on the aryl ring with groups such as Me, F, Cl, and Br was well tolerated under the reaction conditions although strong electron-withdrawing groups (–NO_2) failed (Scheme 41). These results show the broad compatibility of this method. The reaction showed compatibility with diverse lactams and amides such as pyrrolidones, caprolactams, and imidazolidinones, which provided good yields. Linear amides and urea also participated. Also, drug molecules such as Piracetam underwent amidoalkylation, demonstrating potential pharmaceutical relevance. Overall, both cyclic and acyclic amides proved viable (Scheme 41). The scope of the methodology was extended to N-heteroaromatics, which led to successful amidoalkylation. Quinolines (with various substituents) gave the products in 46–69% yield. Isoquinolines afforded regioselective products. Phthalazine, benzothiazole, and quinoxaline also reacted well (Scheme 42).

Later, the pre-mechanistic studies involving a radical trapping experiment using TEMPO gave traces of **57a**. Similarly, phenol was also used, which inhibited the sulfate radical anion and the hydroxyl radicals, providing the desired product in a very small quantity. These experiments confirmed the radical pathway. The authors performed the reaction using DABCO (a singlet oxygen quencher), which inhibited the reaction. This signifies the involvement of singlet oxygen in the reaction. Moreover, the reaction was also promoted by hydrogen peroxide under a nitrogen atmosphere, suggesting that H_2O_2 is likely generated *in situ* during the process (Scheme 43).

Continuous light irradiation is an essential requirement for the formation of the product. Fluorescence quenching (Stern–Volmer) studies demonstrated that under visible-light irradiation, the excited state of **55a** did not undergo any energy transfer with either NMP or $K_2S_2O_8$, which indicated that these

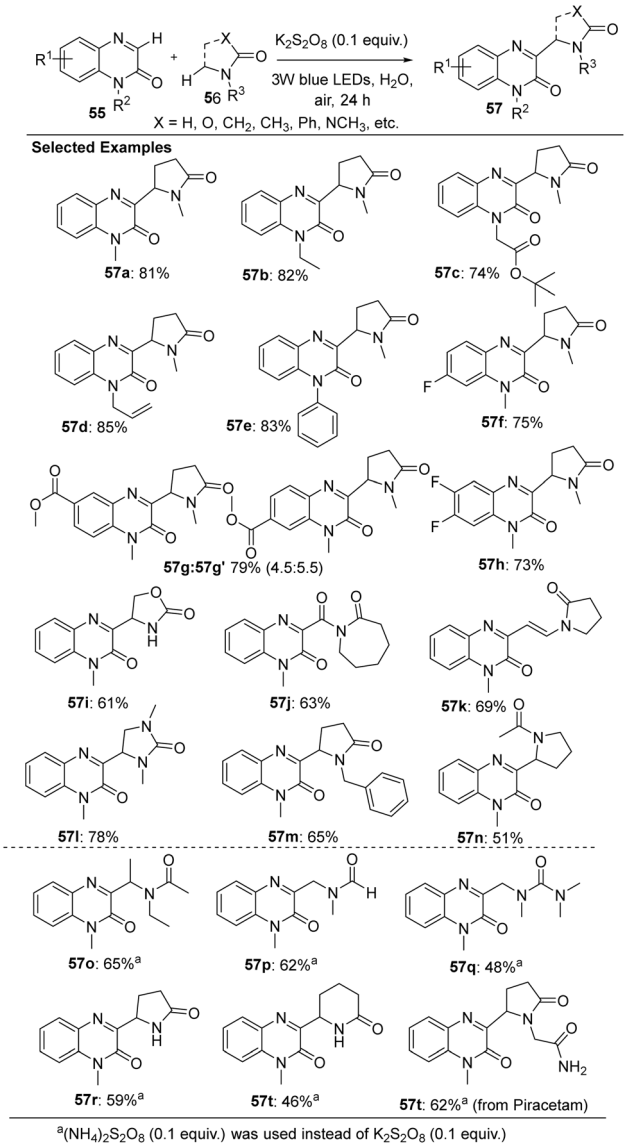

Scheme 41 Substrate scope of quinoxalinones and lactams or amides for amidoalkylation using $K_2S_2O_8$ as the catalyst.

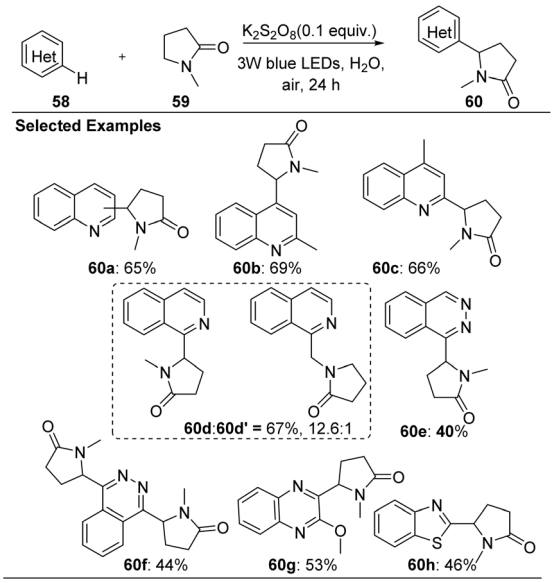

Scheme 42 Substrate scope of N-heteroarenes for amidoalkylation using $K_2S_2O_8$ as the catalyst.

interactions were not involved in the reaction. The proposed mechanism was discussed, where the reaction was initiated with the generation of sulfate radicals under light from $K_2S_2O_8$ (Scheme 44). An N-heteroaromatic substrate (**55a**) was excited by visible light, which produced singlet oxygen. The lactam (**59a**) underwent hydrogen abstraction to form a carbon radical (**59a**′). The radical gets coupled with the N-heteroaromatic (**N**′) at a regioselective position. Oxidation and dehydrogenation yield the amidoalkylated product (**57a**).

Motivated by the efficient application of $K_2S_2O_8$, in 2023, Tian and group highlighted the functionalization of furo[3,2-*c*] coumarins using ynones *via* a cascade radical process, which combined alkylation and cyclization under transition-metal free conditions.[28] The optimization disclosed that $K_2S_2O_8$ is essential for the transformation. The reaction between 1-(4-methoxyphenyl)-3-phenylprop-2-yn-1-one and acetone provided the highest yield (70%) using 2 equivalents of $K_2S_2O_8$ with DCE as the solvent under an Ar atmosphere at 110 °C in 24 h in the α-carbonylation of indanone.

In continuation, various substituted ynones and alkyl acetones were explored under the standard reaction conditions. A variety of electron-rich and electron-deficient groups of different ynones were well tolerated. The broad functionality of various cyclic ketones and acyclic ketones was investigated such as cyclopentane, cyclooctane and *n*-hexane and isohexane, respectively, which provided good yields (Scheme 45). This method introduced diverse alkyl groups into the synthesized coumarin framework products.

To propose the mechanism, the authors performed control experiments, where 1,2-diphentethene, TEMPO, and BHT were added under the standard reaction conditions. They gave traces

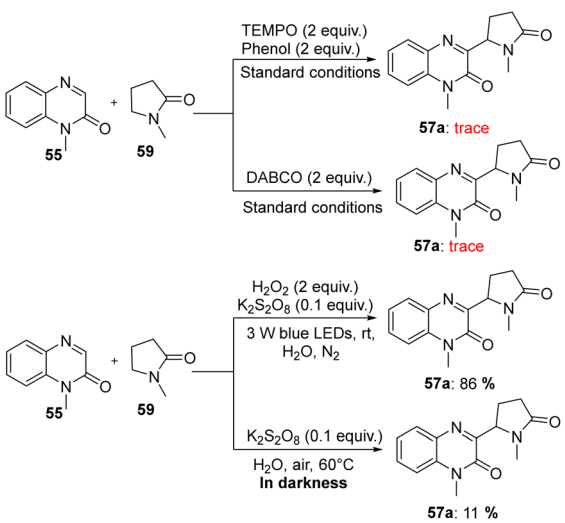

Scheme 43 Pre-mechanistic studies for amidoalkylation.

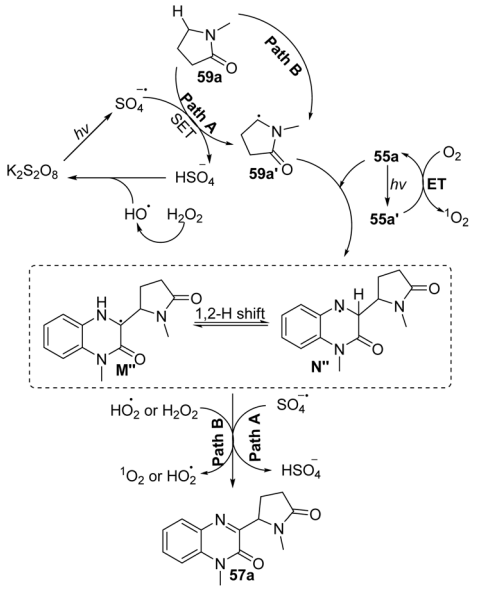

Scheme 44 Plausible mechanism for amidoalkylation using $K_2S_2O_8$ as the catalyst.

of product **63e**, along with the radically trapped intermediate, which was detected by GC-MS. This confirmed the free-radical pathway and involvement of the radical intermediate in the cascade cyclization. They also performed an intermolecular competition reaction with acetone and its deuterated form in a 1 : 1 ratio. This suggested that the activation and cleavage of the αC–H bond in ketone is not the rate-determining step (Scheme 46).

The reaction mechanism was initiated with the thermal decomposition of $K_2S_2O_8$ into sulfate radical anions ($SO_4^{\cdot-}$). The alkyl radical was generated *via* the abstraction of hydrogen from **62a** using the sulfate radical anion. This radical underwent addition to the triple bond of ynone, a vinylic radical intermediate **O″**, which underwent intramolecular cyclization with the ortho hydroxy group furo[3,2-*c*]coumarin (**63e**) after

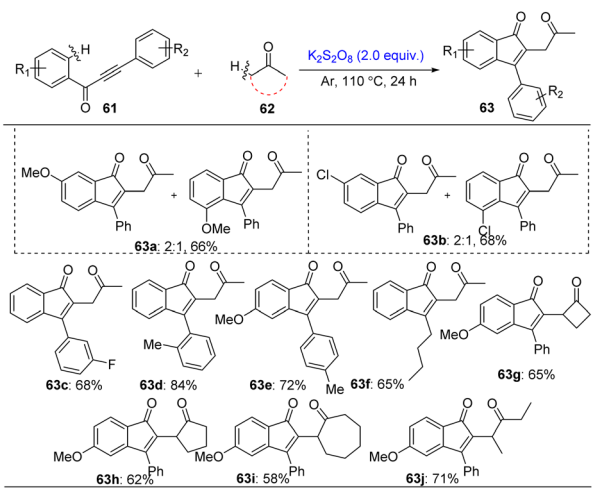

Scheme 45 Substrate scope of substituted ynones and alkyl acetones.

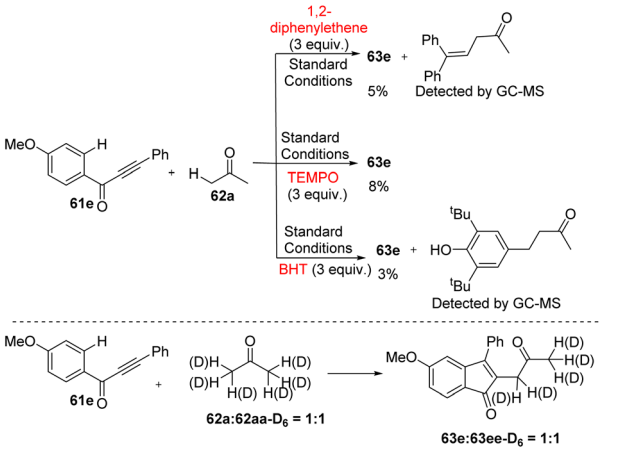

Scheme 46 Mechanistic insights into the radical cascade alkylation or cyclization of ynones and acetone using $K_2S_2O_8$.

oxidation. The role of persulfate aligned well with the goals of green and sustainable chemistry (Scheme 47).

In 2023, Lu *et al.* aimed to develop a metal-free, radical cascade method that enables the cyclization of 1,6-enynes into diiodonated γ-lactams by using a combination of $K_2S_2O_8$ and NaI.[29] The optimized conditions for the reaction are $K_2S_2O_8$, which is crucial for transformation with NaI as a source of iodine, in MeCN/H_2O = 2 : 1 as the solvent for better solubility at 100 °C. The reactions were more effective under air than under O_2 or N_2. Under these conditions, the substrate scope of 1,6-enynes was investigated (Scheme 48). The substituents on the aryl group of the alkyne including electron-donating and electron-withdrawing groups gave good results. Also, the effect of substituents on the N-alkyl group of 1,6-enynes was screened. Substrates with simple alkyl chains or benzyl groups on nitrogen reacted well, affording the products in moderate to good yields. Substrates carrying electron-deficient groups such as sulfone, CF_3, or nitrile on nitrogen also worked efficiently, giving moderate to excellent yields. Even a substrate with a hydroxyl group (**65l**) produced the desired product

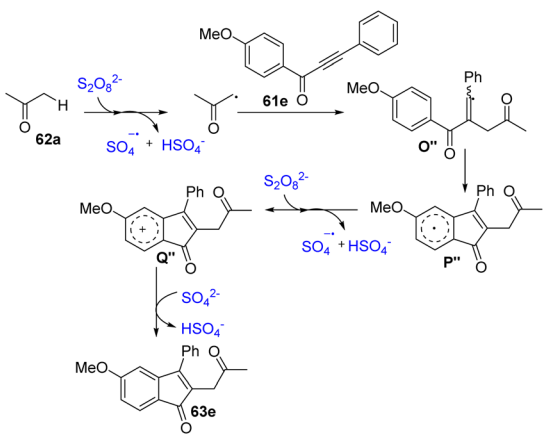

Scheme 47 Proposed mechanism for the formation of furo[3,2-*c*] coumarins using $K_2S_2O_8$.

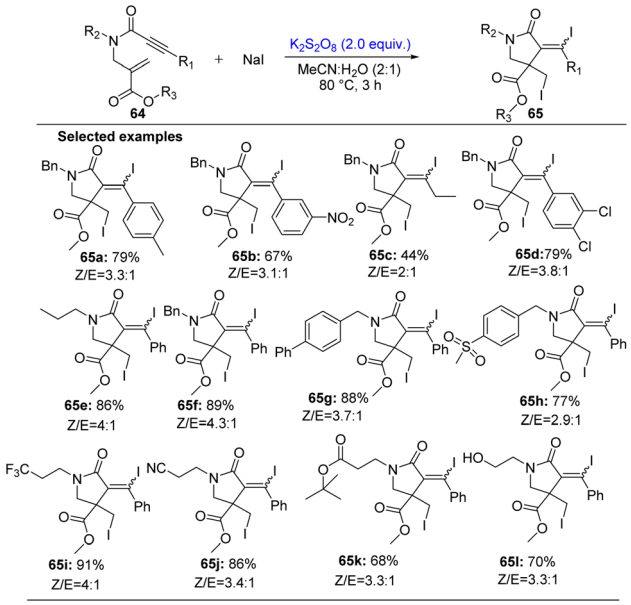

Scheme 48 Substrate scope of 1,6-enynes for diiodinative cyclization.

successfully in good yield. This method promised both structural complexity and synthetic versatility.

As shown in Scheme 49, the reaction was attempted using TEMPO (4.0 equiv.) and BHT (2.0 equiv.), along with the standard conditions, where it was completely suppressed. This confirmed the radical pathway. Later, the standard conditions were used with **64i** and **64i**″, where the respective products were only obtained in trace amounts, which confirmed that the carbonyl group is necessary for the stabilization of the radical and promote the reaction. Also, an iodine radical intermediate was also trapped, which confirmed its presence as an intermediate.

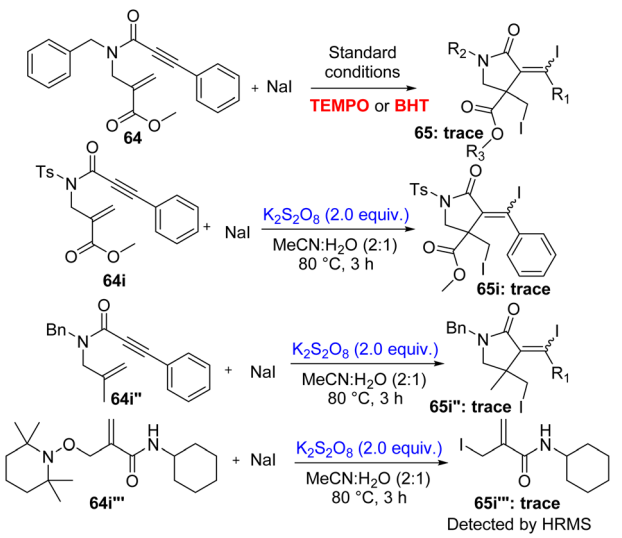

Scheme 49 Control experiments of diiodinative cyclization of 1,6-enynes.

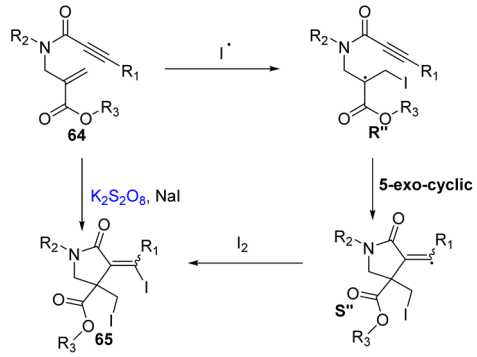

Scheme 50 Proposed mechanism for the diiodinative cyclization of 1,6-enyne.

$K_2S_2O_8$ decomposed to form sulfate radicals, which oxidized iodide into iodine radicals. The iodine radical added to the alkyne moiety of **64**, generating vinyl radical intermediate **R**″. This led to intramolecular cyclization onto the alkene and γ-lactam radical **S**″. Later, it was trapped by iodine and further oxidation led to the diiodonated γ-lactam product (**65**) (Scheme 50).

2.2. C–N bond formation

The utility of $K_2S_2O_8$ as an oxidant has been investigated for promoting C–N bond formation using a variety of coupling partners. These coupling partners include substituted sulfoximines, *ortho*-substituted amines containing thiol or amide groups, aromatic amines such as anilines, and hydrazides and amides. Their corresponding reactions are discussed individually in this section. In some examples shown here, the C–N bond was formed concurrently with a C–C bond or other type of bonds.

In 2018, an approach for C–N bond coupling was designed for the direct functionalization of quinoxalinone at the C3-position using NH-sulfoximines.[30] Sulfoximines are stable, bioactive motifs with growing applications in medicinal and synthetic chemistry.[31] The potential coupling of quinoxalinones with sulfoximines has been explored using potassium persulfate ($K_2S_2O_8$) as the sole oxidant, which offered a simple, efficient, and alternative environmental friendly reagent. The optimization of the reaction was started with quinoxalinone and diphenyl sulfoximine. Initially, the reaction was investigated in the presence of silver acetate, palladium acetate, and copper bromide, which gave low to moderate yields. However, surprisingly, removal of the metal catalyst improved the yield to 90%, indicating that the reaction proceeds efficiently without any metal catalyst. Therefore, the optimized conditions for the C3-functionalization of quinoxalinones with NH-sulfoximines were $K_2S_2O_8$ (2 equiv.) in CH_3CN solvent at 60 °C in 16 hours, which gave excellent yield up to 90%.

In continuation with the standard reaction conditions, the substrate scope was explored with a variation in the substituents in both quinoxalinones and NH-sulfoximines. *N*-Substituted quinoxalinones (ethyl, benzyl, allyl, *etc.*) and electron-withdrawing groups on the aromatic ring (*e.g.*, Br, Cl,

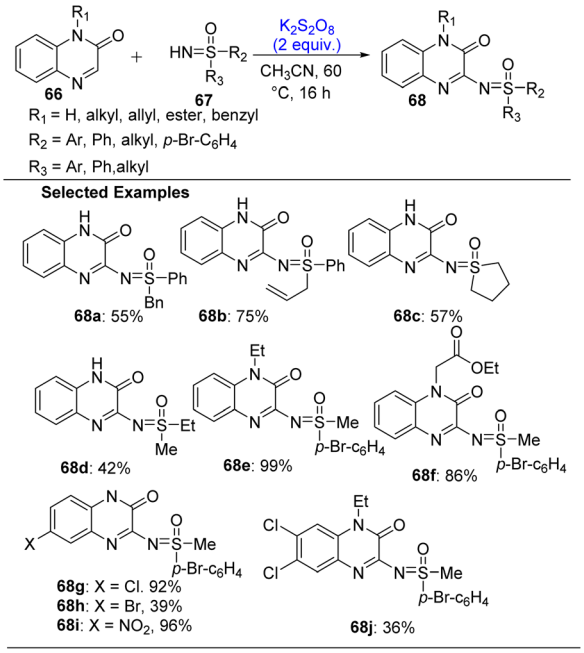

Scheme 51 C–N bond formation at the C3-position of quinoxalinones using NH-sulfoximines.

and NO_2) gave quantitative yields, whereas the disubstituted quinoxalinones showed reduced yields probably due to steric hindrance. In the case of sulfoximines, diaryl, alkyl–aryl, and cyclic along with the functional groups such as methyl, methoxy, chloro, and bromo were well tolerated. However, sulfoximines with strong electron-withdrawing groups gave low yields due to reduced reactivity. This highlights the broad scope of this methodology with great versatility and functional group tolerance (Scheme 51).

The preliminary mechanistic approach was determined by performing the reaction in the presence of BHT and 1,1-diphenylethylene, where no desired product was obtained; instead, the starting materials were recovered (90%). This confirmed the free-radical mechanistic path. The sulfoximination of quinoxalinones was initiated with homolytic cleavage of persulfate to generate sulfate radicals ($SO_4^{\bullet-}$), which abstracts a hydrogen from the NH-sulfoximine (**51**), forming a nitrogen-centered radical **T″**. This radical adds to the C3-position of quinoxalinone, forming a new C–N bond with intermediate **U′**. Further, oxidation yields the *N*-sulfoximidoyl-functionalized quinoxalinone product (**68**) (Scheme 52).

J. K. Laha and colleagues discussed the huge concern of the dependence of India on China for approximately 65% of its active pharmaceutical ingredients (APIs) for affordable healthcare. Although Indian pharmaceutical companies produce generic APIs, research in academic settings is limited. The joint ventures of academic-industry have devoted their efforts to developing cost-effective synthetic methods such as C–H/N–H oxidative coupling, which could boost local API production. This method is green and efficient for forming C–C and C–X bonds but is rarely applied in generic drug synthesis. Therefore, the authors, herein, selected the synthesis of sildenafil (gram scale) under aqueous conditions (H_2O) using arylacetic acid as the acyl source in the formation of the 5-(2-ethoxyphenyl)-1-methyl-3-propyl-1,6-dihydro-7*H*-pyrazolo[4,3-*d*]pyrimidin-7-one intermediate in 67% yield.[32] The chlorosulfonated intermediate further reacted with *N*-methylpiperazine to provide sildenafil in 62% yield. The authors successfully developed an improved synthetic method for the preparation of sildenafil (Viagra™) on the gram scale with this methodology (Scheme 53).

Researchers were motivated by the synthesis of sildenafil using aryl acetic acid and pyrazole carboxamides in the presence of potassium persulfate ($K_2S_2O_8$).[32] The authors developed the methodology with synthetic applicability for the syntheses of substituted benzothiazoles (**69**) (Scheme 54) and quinazolinones (**72**) (Scheme 55) using a variety of aryl acetic acids with **70a** and **70b**, respectively, with 3 equivalents of $K_2S_2O_8$ in water at 80 °C for 6–12 hours. All the reactions proceeded smoothly with good yields.

To explore the reaction mechanism and identify the key intermediates involved in the annulation process, a series of carefully designed experiments was conducted (Scheme 56). (a) The first investigation involved subjecting phenylacetic acid (**69**) to oxidative conditions using potassium persulfate ($K_2S_2O_8$) in water at 80 °C for one hour. The exclusive product formed was benzaldehyde, which suggested that benzaldehyde functions as a reactive intermediate in the overall transformation rather than the heterocyclic product being formed directly from

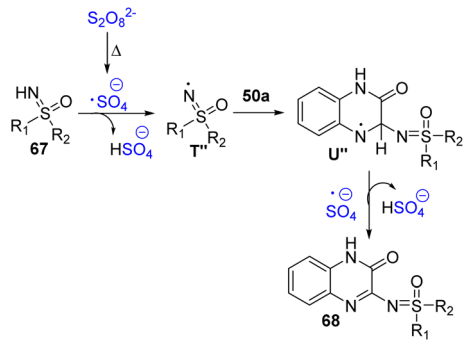

Scheme 52 Proposed mechanism for the C3-functionalization of quinoxalinones using NH-sulfoximines.

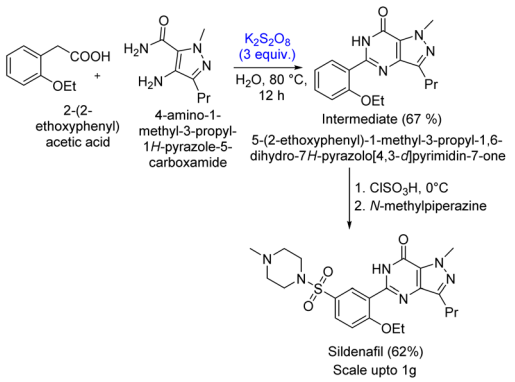

Scheme 53 Potassium persulfate-mediated synthesis of sildenafil.

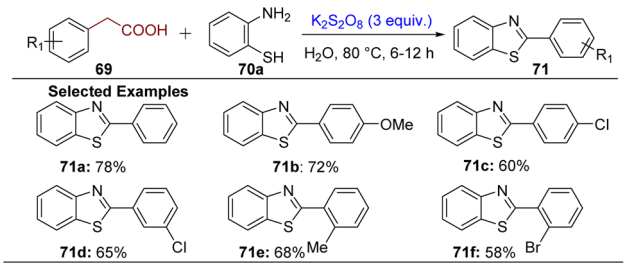

Scheme 54 Synthesis of benzothiazoles.

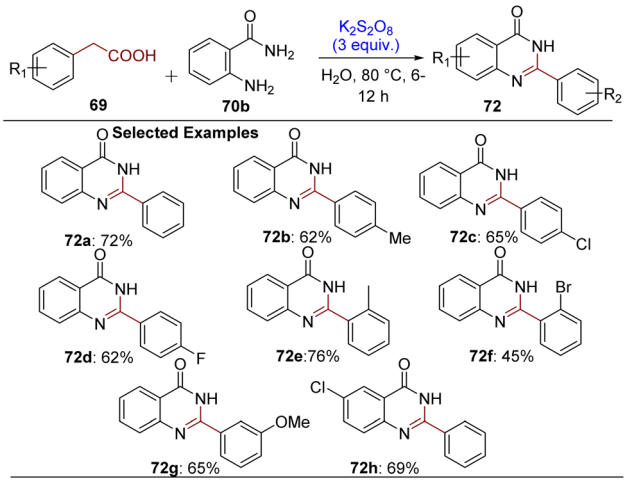

Scheme 55 Synthesis of quinazolinones.

phenylacetic acid. (b) In a subsequent experiment, diphenylacetic acid (**73**) was reacted with 2-aminobenzamide (**70b**) under the same optimized conditions. Contrary to the anticipated annulated product, the reaction only led to the formation of benzophenone. This result further confirmed that the process begins with the oxidative decarboxylation of the

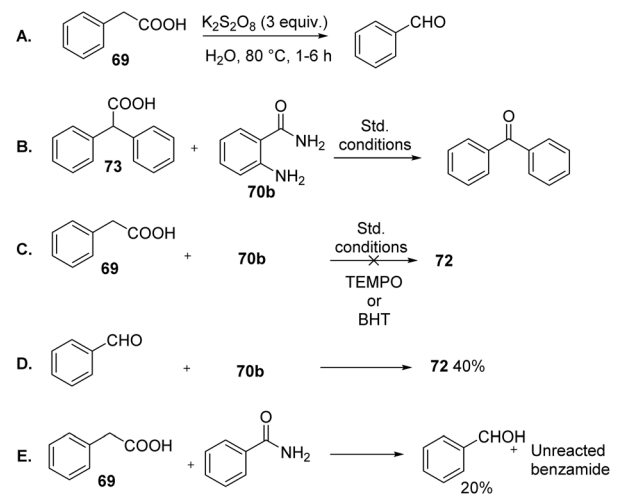

Scheme 56 Control experiments for the synthesis of benzothiazoles and quinazolinones.

acid to form a carbonyl compound, which acts as a precursor in the reaction pathway. The absence of the annulated heterocycle in this case implies that not all carbonyl compounds are suitable for the cyclization, and the nature of the intermediate significantly influences the reaction outcome. (c) To determine whether the transformation involves free radical intermediates, well-known radical trapping agents, TEMPO (2,2,6,6-tetramethylpiperidine-1-oxyl) and BHT (butylated hydroxytoluene) were added to the reaction of phenylacetic acid (**69**) and 2-aminobenzamide (**70b**). In both experiments, the reaction was completely suppressed, and no product formation was observed. This provided compelling evidence that the reaction proceeds through a radical pathway, where free radicals are essential intermediates driving the transformation. (d) To confirm whether benzaldehyde is a viable intermediate, it was reacted directly with 2-aminobenzamide (**70b**) under the standard conditions. The reaction successfully yielded the annulated product (**72**). This supported the hypothesis that benzaldehyde reacts with 2-aminobenzamide to form an imine intermediate, which subsequently undergoes cyclization and oxidation to furnish the heterocyclic product. (e) In another control experiment, benzamide was reacted with phenylacetic acid (**69**) under the same optimized conditions. Interestingly, this reaction only produced benzaldehyde, and benzamide remained unreacted. This finding underscores the significance of using an arylamine (such as 2-aminobenzamide) over a simple amide, given that the amide nitrogen lacks the nucleophilicity required to condense efficiently with the aldehyde. This selectivity confirms that imine formation is specific to arylamines, which then facilitate the next steps in the cascade. Taken together, these detailed experiments confirm that the formation of the annulated heterocycle proceeds through a well-orchestrated sequence involving radical decarboxylation, carbonyl formation, imine condensation, and cyclization, with each step being critical to the successful construction of the final product.

The thermal conditions led to the homolytic cleavage of $K_2S_2O_8$ to form a sulfate radical anion. This assisted the decarboxylation of **53** with the formation of a benzyl radical (**V″**). The formed benzyl radical can follow three competing reaction pathways. In path **A**, benzyl radical **V″** reacts with a hydroxyl radical (from H_2O), resulting in the formation of benzyl alcohol (**W″**). In path **B**, **V″** loses an electron, forming a benzyl carbocation (**X″**). Alternatively, in path **C**, **V″** reacts with an aniline radical cation generated from 70b, leading to the formation of new intermediate **Z″**. Intermediate **X″** produced in path B can itself proceed through two different routes. In path **D**, it undergoes nucleophilic attack by water, leading again to benzyl alcohol. In contrast, path **E** involves nucleophilic attack by an aniline derivative, which also results in the formation of intermediate **Z″**, similar to path C. These various formed intermediates underwent intramolecular cyclization, which ultimately yielded the final annulated product **71**/**72**. The authors mentioned that there are still possible multiple pathways besides that they proposed, which should not be ignored (Scheme 57).

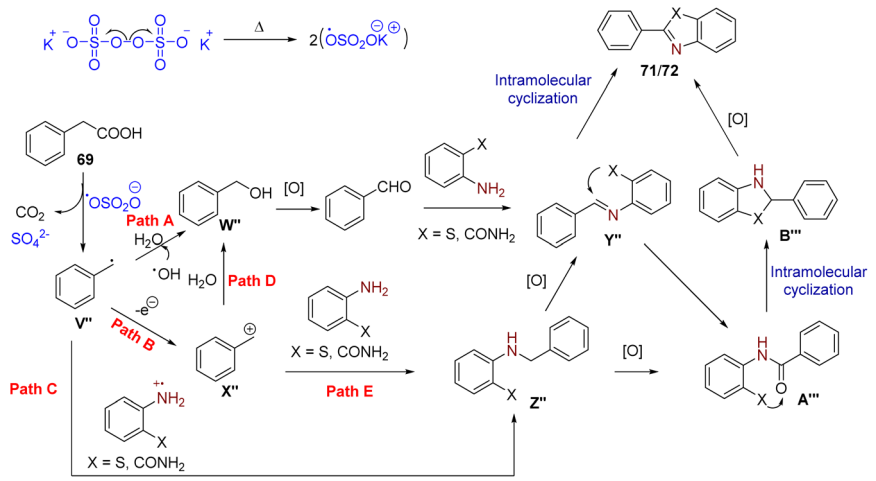

Scheme 57 Mechanism pathway for the synthesis of benzothiazoles and quinazolinones.

In continuation, Laha and colleagues reported that the decarboxylation of aryl acetic acid in the presence of $K_2S_2O_8$ has already been well discussed.[33] However, the phenomenon of the *ortho*-effect in relation to benzoic acid/anilines still has to be investigated in depth. The introduction of a functional group or substituent at the ortho to the carboxylic acid group which could lead to steric hindrance, electronic effects, or specific bonding interactions may significantly influence the chemical and physical properties of a molecule. However, these *ortho*-substitution effects in the case of phenylacetic acid derivatives have not been thoroughly investigated, leaving an unexplored area in understanding how these substitutions might alter the reactivity or behaviour. Henceforth, the authors optimized the reaction between substituted phenylacetic acid (**74**) and 2-

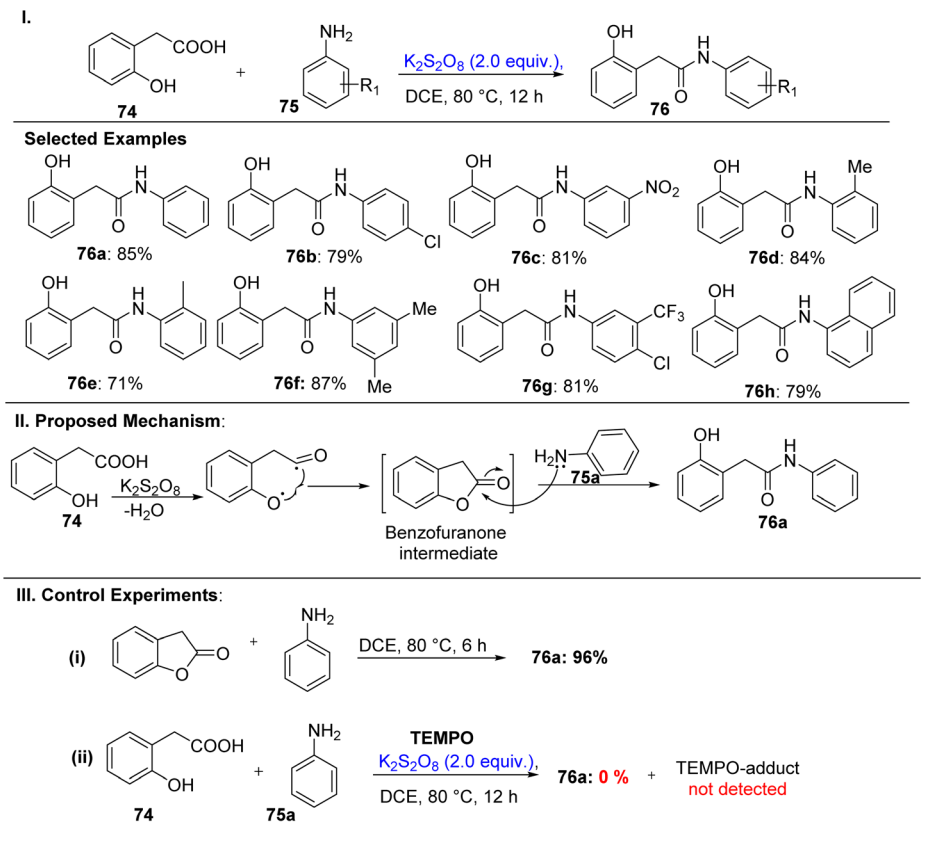

Scheme 58 (I) One-pot synthesis of 2-(2-hydroxyphenyl)-*N*-phenylacetamide derivatives using $K_2S_2O_8$, (II) proposed mechanism, and (III) control experiments.

aminobenzamide (**75b**) using various reaction parameters. It was found that potassium persulfate ($K_2S_2O_8$) with dichloroethane (DCE) as the solvent at 80 °C for 12 hours in an air atmosphere, resulting in good to excellent yields of the annulated product (Scheme 58, **I**). They proved the formation of benzofuranone as an intermediate for the formation of **76** derivatives and proved by performing the reaction of benzofuranone with aniline in DCE at 80 °C to form similar **76** derivatives in high yields. The *ortho*-hydroxyl aryl acetic acid (**74**) in the presence of $K_2S_2O_8$ resulted in a benzofuranone intermediate, and later the attack of aniline (**75a**) on the carbonyl group led to the formation of **76** (Scheme 58, **II**). This confirmed the intramolecular cyclization of **74**, and later intermolecular reaction with an amine. However, the introduction of TEMPO with the standard reaction conditions did not give the desired reaction and no TEMPO-adduct was observed. However, the formation of benzofuranone suggested the free-radical pathway (Scheme 58, **III**). Further, Jaha *et al.*[33] explored the effect of different *ortho*-substitutions containing electron-donating and electron-withdrawing groups to aryl acetic acid under the standard reaction conditions (Scheme 59). Firstly, the homophthalic acid (**74i**) was subjected to the same reaction system, which led to the formation of isobenzofuranone (**76i**) through decarboxylation. The formation of the intermediate was confirmed through mass spectrometry. Next, the *o*-methyl group underwent oxidative reaction (**76j**) only, whereas *o*-nitro led to 21% of *o*-nitro toluidine (**76k**) along with traces of benzaldehyde formation (**76k′**). Overall, in both cases, it was observed that complete decarboxylation was inhibited. In continuation, an earlier report showcased the decarboxylative annulation of biarylacetic acid in the presence of H_2O. However, here, under the standardized conditions, they reported that biarylacetic acid gave 45% of dimerized product (**76l**). It is

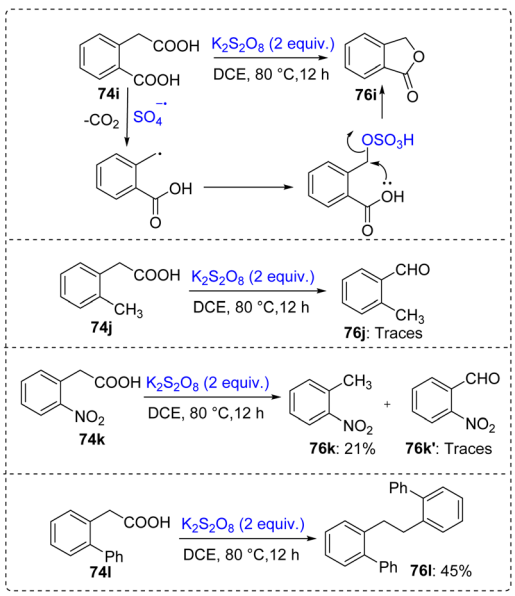

Scheme 59 Effect of *ortho*-substitution in aryl acetic acids using $K_2S_2O_8$.

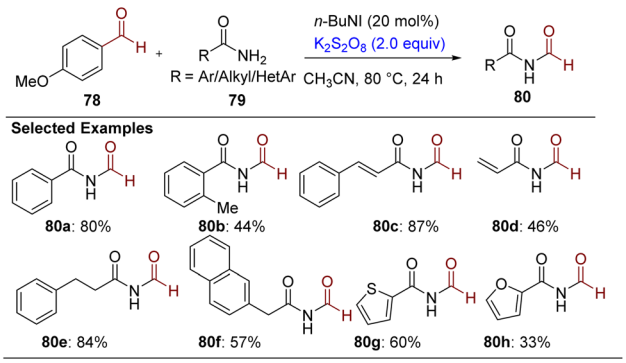

Scheme 60 Transformylation from *p*-anisaldehyde to substituted primary amides by $nBu_4NI/K_2S_2O_8$.

clearly a solvent-dependent reaction. These studies would help to design methods for the synthesis of heterocyclic moieties.

J. Liu and Y. Chen *et al.* introduced a novel and metal-free method for the transformylation of *p*-anisaldehyde to primary amides by using a combination of tetrabutylammonium iodide (nBu_4NI) and potassium persulfate ($K_2S_2O_8$) through Csp^2–Csp^2 bond cleavage.[34] The optimization indicated that the best yield (82%) was furnished using nBu_4NI (20 mol%), $K_2S_2O_8$ (3 equivalent), and acetonitrile as the solvent at 80 °C. The other iodide or ammonium halide sources were less effective. They mentioned that this was the first report on transformylation operated using anisaldehyde. This transformation presented good compatibility with various electron-rich aromatic aldehydes and a range of aromatic and aliphatic primary amides, while secondary amides failed to react, where the starting materials were recovered (Scheme 60).

The control experiments were performed to determine the mechanistic approach for the transformylation (Scheme 61). The reaction of benzamide and 4-methoxyphenyl formate did not give the desired product, where this indicates that 4-methoxyphenyl formate is not a suitable formylation reagent. Also, the coupling between benzamide and 4-methoxybenzoic acid led to the recovery of starting the materials after 24 hours. The optimized reaction was attempted using TEMPO and BHT, which suppressed the reaction completely. Also, the authors also reported that the anion of *p*-methoxyphenyl sulfate was detected by LC-MS analysis. Even oxidation of *p*-anisaldehyde was attempted, which gave 4-methoxybenzoic acid under the reaction conditions. This proved that the transformylation is more kinetically favourable over the oxidation with the standard conditions.

Along with the pre-mechanistic studies and DFT calculations, the plausible mechanism was depicted (Scheme 62). The reaction of *n*-Bu_4NI with $K_2S_2O_8$ led to the formation of bis(tetrabutylammonium) peroxydisulfate, which generated the SO_4^{2-} radical anion at higher temperature. Further, *p*-anisaldehyde was oxidized in the presence of this anion to a phenyl cation radical (**C″**). Later, the other equivalent of $SO_4^{\bullet-}$ underwent addition to the *ipso* position of the carbonyl group of *p*-anisaldehyde, resulting in the formation of **D″**, which is stabilized by a *p*-OMe group. Immediate nucleophilic acyl

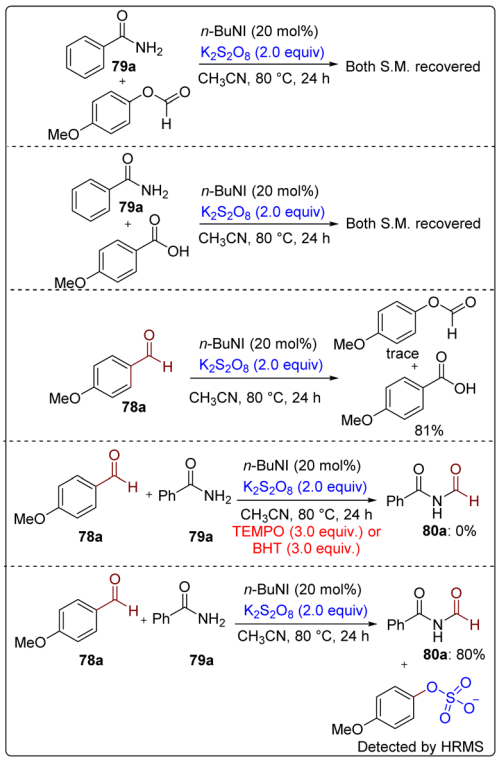

Scheme 61 Control experiments for the transformylation of primary amides by nBu$_4$NI/$K_2S_2O_8$.

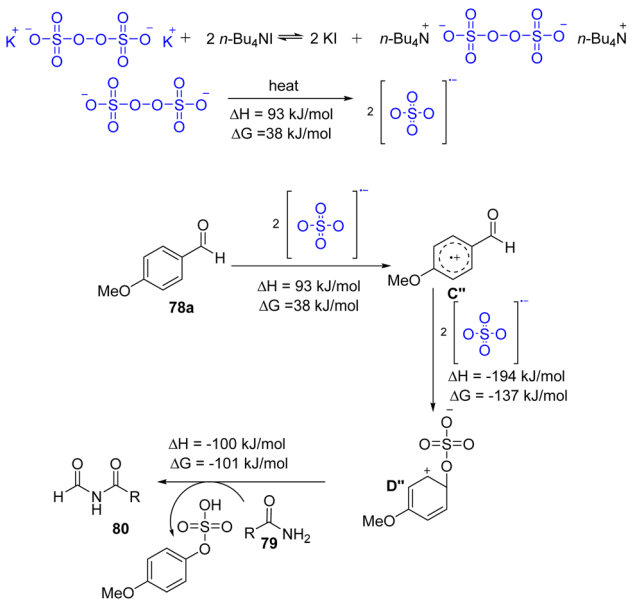

Scheme 62 Plausible mechanism for transformylation from p-anisaldehyde to substituted primary amides by nBu4NI/$K_2S_2O_8$.

substitution on the amide by **D″** furnished product **80** and 4-methoxyphenyl hydrogen sulfate.

Recently, L. Ji and K. Ablajan reported the direct conversion of C(sp^3)–H to C=N bonds under metal-free conditions using $K_2S_2O_8$ for the hydrazonation of methylene in pyrazoline-5-ones with substituted carbazate and benzhydrazides.[35] The authors reported that the earlier methods involved many disadvantages such as harsh conditions, metal catalysts, toxic starting materials, and multistep processes. The standard conditions that gave the highest yield of 78% were 1 mmol of pyrazoline-5-one with 1 mmol of carbazate using $K_2S_2O_8$ (1.0 equiv.) in DMSO at 100 °C for 8 hours.

The optimal conditions were employed to investigate the substrate scope of the methodology (Scheme 63). The substituted pyrazoline-5-ones with substituted carbazate and benzhydrazides gave good yields. But the lowered yield was observed in *ortho*-substituted fluoro group in **83f**. This transformation did not work for the phenyl/acetyl (**83g**) or tosyl substituted hydrazines (**83h**).

A series of control experiments was performed. The reaction was performed under an air and nitrogen atmosphere, where 10% and traces of **83a** was observed, respectively. This indicates that aerial oxidation is considerable here (Scheme 64, eqn (1)). Radical scavengers such as TEMPO and BHT were incorporated under standard conditions, which had no effect on the reaction (Scheme 64, eqn (2)). This confirmed that the mechanism did not follow a free radical pathway. The oxidation of the pyrazoline-5-one methylene group was attempted before hydrazonation, where no oxidized product was observed (Scheme 64, eqn (3)). Also, hydrazide (**82a**) oxidation gave 100% of the diazonium intermediate, which would help to depict the reaction mechanism (Scheme 64, eqn (4)).

Based on the above-mentioned studies, the mechanism was interpreted (Scheme 65). The sulphate radical anion was generated from $K_2S_2O_8$ by heating. It was observed in control experiments that hydrazides (**82a**) are more reactive compared

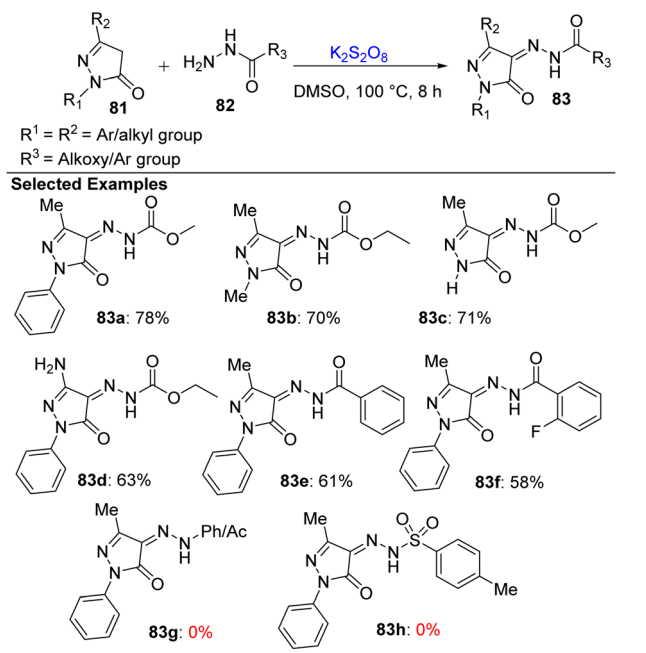

Scheme 63 Substrate scope of pyrazoline-5-ones with substituted carbazate and benzhydrazides.

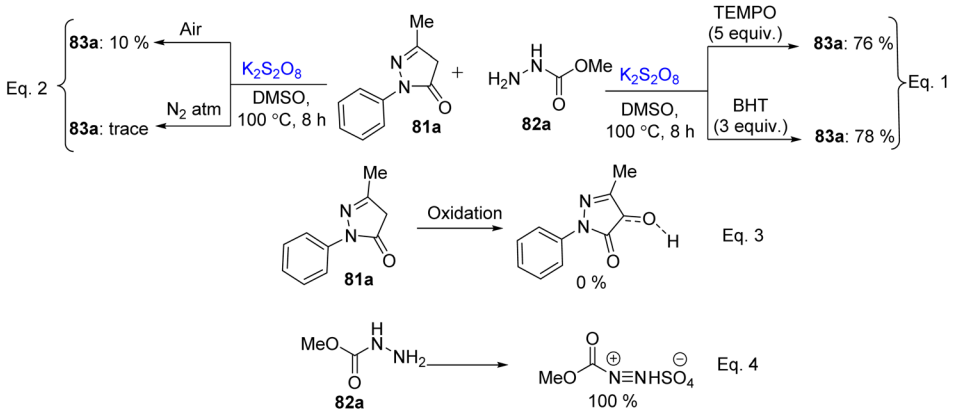

Scheme 64 Control experiments for the hydrazonation of pyrazoline-5-ones.

to 5-methyl-2-phenyl-2,4-dihydro-3*H*-pyrazol-3-one (**81a**), which led to diazonium intermediate (**E″**). The tautomer of **83a** underwent dehydrogenation and subsequent nucleophilic attack at **E″** gave intermediate **F″**. **F″** underwent 1,3-hydrogen migration to furnish the final product **83a.**

In 2020, S. Muthusubramanian and group focused on the synthesis of two types of important chemical compounds, *i.e.*, oxazoles and aminothiazoles, using $K_2S_2O_8$ and $Fe(NO_3)_3$, respectively.[36] This methodology led to the formation of C–N and C–O in an oxazole core. The optimization reaction between (*Z*)-2-azido-3-(4-chlorophenyl)-1-phenylprop-2-en-1-one and potassium thiocyanate (KSCN) using different metal and non-metal catalysts and various solvents was investigated. The optimal conditions were $K_2S_2O_8$ (0.5 equiv.) under reflux conditions with acetonitrile (2 mL) in 6 hours gave the desired product in 97% yield.

They explored the substrate scope with different α-azidochalcone molecules and obtained high yields, irrespective if the molecules had electron-donating or electron-withdrawing groups (Scheme 66). This showed the benefits of the methodology. Conversely, when $Fe(NO_3)_3$ was used instead of $K_2S_2O_8$, it produced aminothiazoles instead of oxazoles.

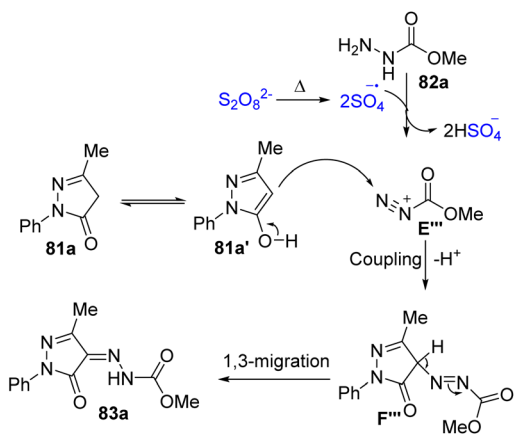

Scheme 65 Plausible mechanism for the hydrazonation of pyrazoline-5-ones.

To confirm the mechanistic pathway for the formation of oxazoles, the following control experiments were performed by the group (Scheme 67). The reaction between α-azidochalcone and KSCN was carried out in the presence of radical scavengers such as TEMPO and BHT. In the first reaction, 45% azirine with 50% TEMPO was observed, and later, the BHT-thiocyanate coupling product was formed through LC-MS analysis, which confirmed the formation of the thiocyanate radical. Later, the absence of $K_2S_2O_8$ did not give the desired product, which indicated the necessity of an oxidizing agent ($K_2S_2O_8$) for the initiation of the radical pathway. These experiments proved that the thiocyanate radical generated from potassium thiocyanate *via* oxidation with potassium persulfate is a key reactive species in this transformation.

A plausible mechanism has been proposed based on control experiments (Scheme 68). Potassium persulfate facilitates the formation of thiocyanate radicals, which preferentially react *via* their nitrogen end with the C=N bond of the azirine

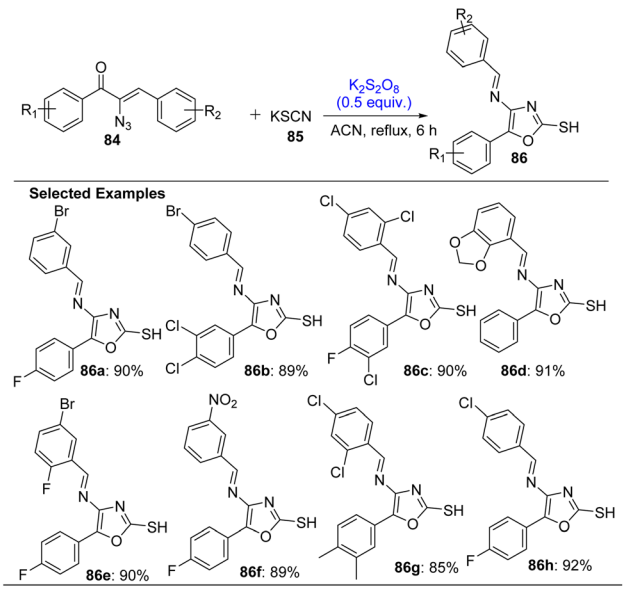

Scheme 66 Substrate scope of oxazoles using $K_2S_2O_8$.

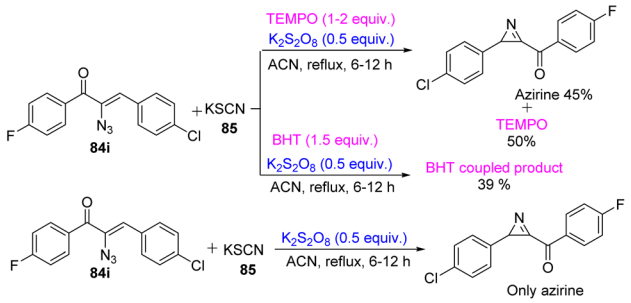

Scheme 67 Control experiments for the formation of oxazoles.

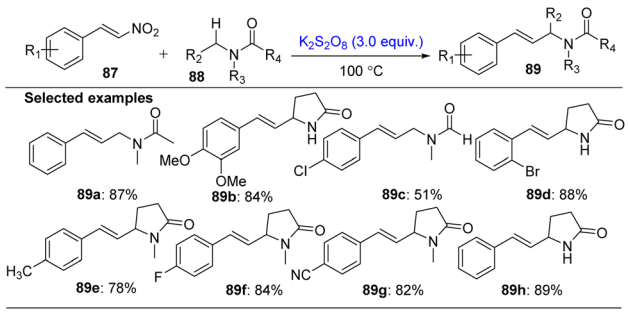

Scheme 69 Substrate scope of substituted nitrostyrenes and *N*-alkyl amides using $K_2S_2O_8$.

intermediate, which is derived from the thermolysis of vinyl azide. This formed intermediate **G‴**, which undergoes homolytic bond cleavage, resulting in **H‴**, and subsequently it undergoes intramolecular cyclization to yield the desired product (**86**).

Direct cross-dehydrogenative coupling (CDC) between terminal alkenes and *N*-alkyl amides is challenging due to side polymerization. In 2021, Li *et al.* reported that activated olefins such as nitro-olefins, cinnamic acids, and alkenyl sulfones were investigated as radical acceptors to form *N*-allylic amides.[37] They are valuable in natural product chemistry and synthesis. The reaction was optimized between (*E*)-(2-nitrovinyl)benzene and DMA (*N*,*N*-dimethylacetamide) with different oxidants, where $K_2S_2O_8$ afforded the desired product in 87% yield at 100 °C compared to other oxidants, which gave poor yields. The optimal conditions for the transformation are 0.6 mmol of $K_2S_2O_8$ with 3 mL of dimethylacetamide (DMA) at 100 °C. With this, the substrate scope for substituted nitro styrene and *N*-alkyl amides was investigated. The methodology was explored for a broad range of nitrostyrenes with electron-deficient (F, Br, and CN) or electron-rich (Me and OMe) substituents, which produced *N*-allylic amides in good yields. Different amides such as *N*-methylpyrrolidone (NMP), pyrrolidone, and dimethyl formaldehyde (DMF) were also tested. NMP and pyrrolidone worked comparatively well, whereas DMF gave lower yields due to side competing reactions (Scheme 69).

Control experiments were attempted, where firstly the reaction of styrene/β-methylstyrene with DMA under the standard reaction conditions gave trace products with the polymerization of styrene. This confirmed that only activated olefins were suitable here. The radical nature of the reaction was confirmed given that the presence of TEMPO suppressed product formation completely. The isomeric β-nitrostyrenes gave only 23% of the desired product (**89a**) even after the reaction time was prolonged. In contrast, (*E*)-(2-nitroprop-1-en-1-yl)benzene did not generate any product (Scheme 70).

The plausible mechanism was proposed by authors, where the reaction initiated with the generation of sulfate radicals from $K_2S_2O_8$, which abstracted hydrogen from the α-C–H of the amide, giving an amide radical (**K‴**). This radical adds to the olefin (**87a**), and subsequently the departure of the leaving-group from **L‴** led to the formation of the *N*-allylic amide product (**89a**) (Scheme 71).

In 2023, Saha *et al.* explored a metal-free and sustainable route using $K_2S_2O_8$ as an oxidant under mild conditions.[38] They reported the synthesis of 2-substituted benzimidazoles by coupling 1,2-diaminobenzenes and primary alcohols. They performed optimization of the reaction using *o*-phenylenediamine and benzyl alcohol as the model substrate. The optimal conditions were 1.5 mmol of persulfate with a mixture of DMF : H_2O (9 : 1) at 80 °C, where H_2O accelerated the formation of the product, with 82% yield after 4 h of reaction. This confirmed that $K_2S_2O_8$ in aqueous DMF was the best setup

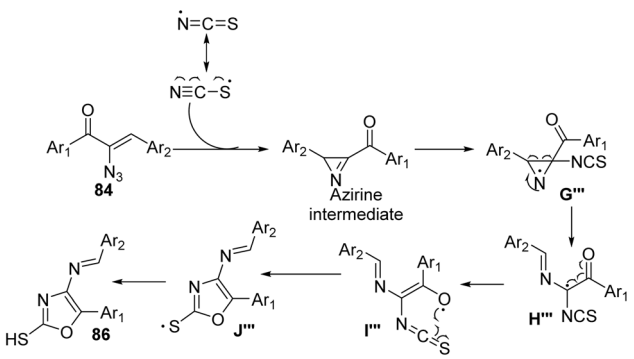

Scheme 68 Plausible mechanism for the synthesis of oxazoles.

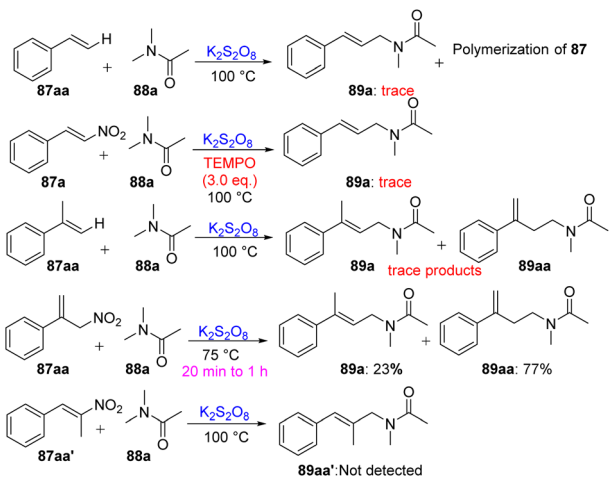

Scheme 70 Control experiments for *N*-allylic amides using $K_2S_2O_8$.

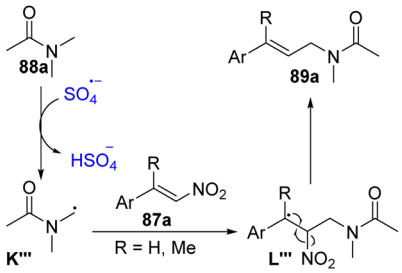

Scheme 71 Proposed mechanism for the synthesis of *N*-allylic amides using $K_2S_2O_8$.

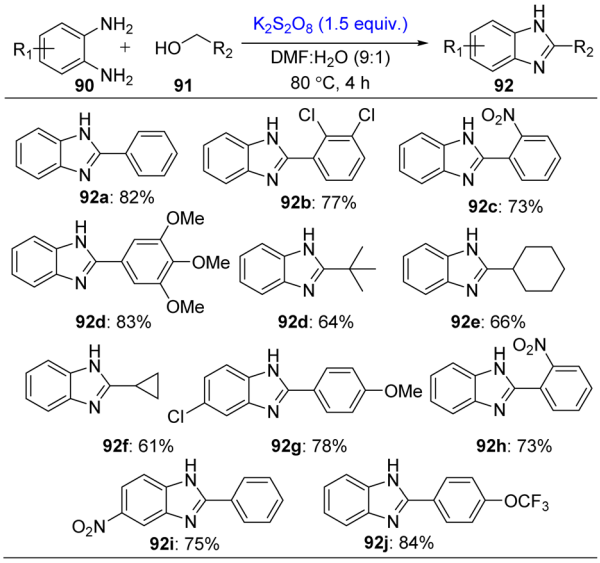

Scheme 72 Substrate scope of 1,2-diaminobenzenes and primary alcohols using $K_2S_2O_8$.

for efficient synthesis. The optimized conditions were carried with unsubstituted/substituted 1,2-diaminobenzenes and substituted benzyl phenols, which gave quantitative yields. Also, aliphatic alcohols (**92e** and **92f**) were well tolerated under the reaction conditions (Scheme 72). The authors also focused on the practicability of the method with gram-scale synthesis, which afforded >80% yield.

The pre-mechanistic studies showed the radical pathway when the reaction was completely inhibited with radical scavengers such as TEMPO and BHT. Even the reaction of **90a** with benzaldehyde under the standard conditions along with BHT gave 84% of **92a**, which eliminated the involvement of any radical process (Scheme 73).

The plausible mechanism initiated as $K_2S_2O_8$ generated sulphate radicals at 80 °C. These radicals oxidize **91** to form aldehyde. Then, aldehyde condenses with 1,2-diaminobenzene, forming an imine intermediate to intermediate **M'''**, which undergoes oxidation to form cyclic benzimidazole (**92**). In the reaction mechanism, water plays a significant role in the stabilization and conversion of the imine intermediate to the desired product **92**. In addition, the authors performed

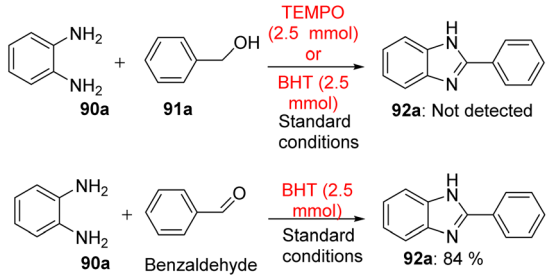

Scheme 73 Control experiments for the synthesis of 1,2-diaminobenzenes using $K_2S_2O_8$.

photophysical analysis and DFT studies, which provided valuable insights into the electronic properties of benzimidazoles. This suggested their potential applications in light-emitting and electronic materials (Scheme 74).

In 2024, Liu *et al.* explored cross-dehydrogenative coupling (CDC) with a greener approach, for the C–N coupling of aldehydes with amides using a dual *n*-$Bu_4NI/K_2S_2O_8$ system.[39] For optimization, the reaction of acetamide and benzaldehyde was investigated. The combination of 10 mol% *n*-Bu_4NI with 2 equiv. $K_2S_2O_8$ in acetonitrile at 80 °C gave *N*-acetylbenzamide in 66% yield.

n-Bu_4NI and $K_2S_2O_8$ alone did not form imides. Alternatively, other chloride and bromide salts of tetrabutylammonium gave negligible yields, showing a specific iodide effect. The optimization was further explored with alternative oxidants such as TBHP, H_2O_2, and DBPO, which failed to provide the desired products. In the solvent screening, toluene, THF, and DMF gave lower yields, whereas DMSO was completely inactive.

Employing the standard conditions, the coupling of electron-rich aldehydes and benzamide was explored, which revealed that *p*-anisaldehyde gave the highest yield (80%) of **95a** (Scheme 75). Further, both simple alkyl and aromatic amides, including

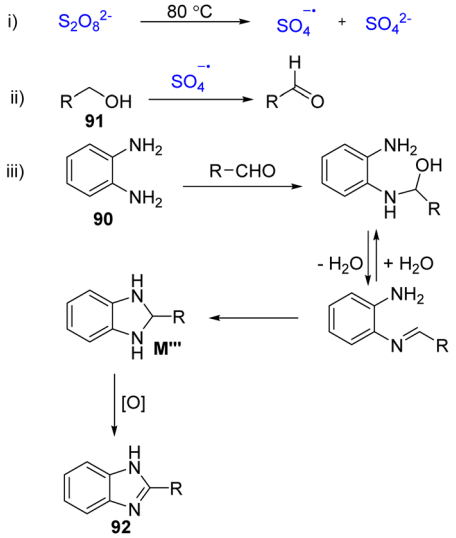

Scheme 74 Plausible mechanism for the synthesis of cyclic benzimidazole using $K_2S_2O_8$.

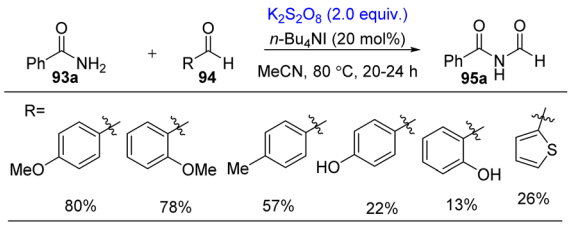

Scheme 75 Substrate scope of electron-rich aldehydes using *n*-$Bu_4NI/K_2S_2O_8$.

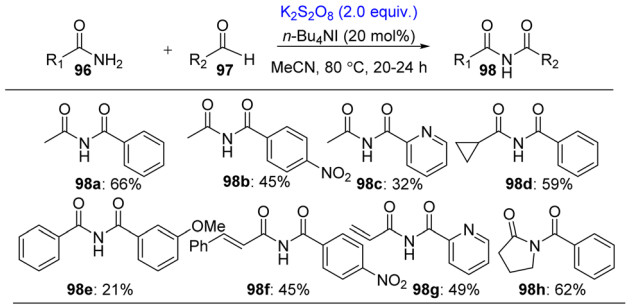

Scheme 76 Substrate scope of amides and aldehydes using $K_2S_2O_8$.

secondary ones such as pyrrolidin-2-one (**98h**), gave good yields, showing broad applicability. Even alkenyl and aromatic amides were well tolerated under the reaction conditions (Scheme 76). In some cases, mixtures of imides and transformylation products were formed depending on the aldehyde used.

The addition of TEMPO trapped a benzoyl radical, proving a radical pathway. The mechanism was researched experimentally and *via* DFT calculations. The generated radicals from $K_2S_2O_8$ abstracted a hydrogen atom from **96i** to form acyl radical intermediate **N‴**. This further reacts with sulfate to form sulphuric anhydride intermediate **O‴**. It undergoes nucleophilic acyl substitution with amides, furnishing **98** (Scheme 77). In the case of electron-rich aldehydes, sulfate radicals oxidized the aldehyde to a cation radical, which favored transformylation. DFT calculations confirmed that the key radical and substitution steps were energetically consistent with the observed reactivity.

Recently, Rana *et al.* and group developed the $K_2S_2O_8$-mediated synthesis of 3-substituted isoindolin-1-ones, which is

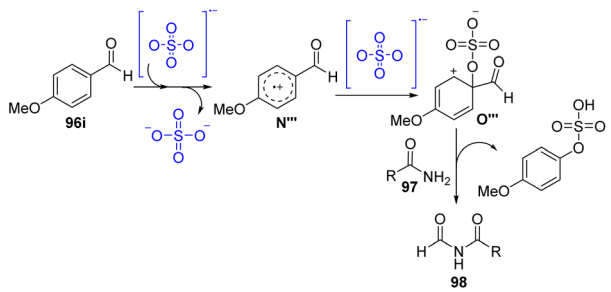

Scheme 77 Proposed mechanism for substituted amides using $K_2S_2O_8$.

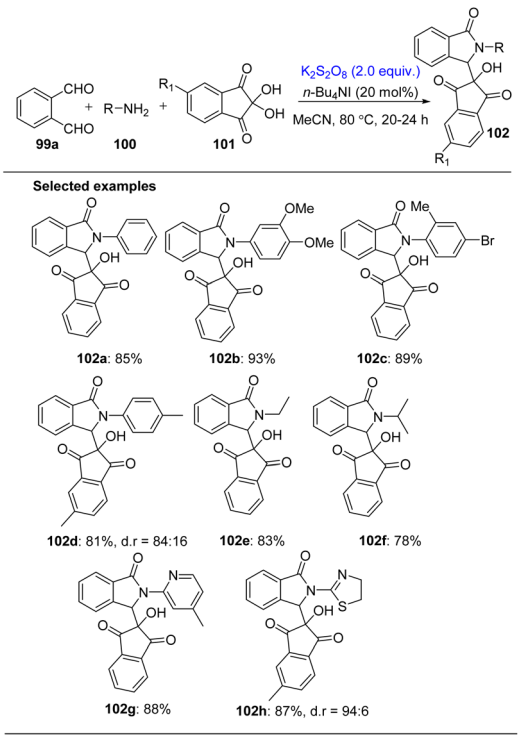

Scheme 78 Substrate scope of substituted anilines and ninhydrin using TBAB/$K_2S_2O_8$.

a metal-free, green approach.[40] They are of great synthetic and biological importance. The optimization was conducted by the authors using phthalaldehyde, substituted anilines, and ninhydrin (2,2-dihydroxyindane-1,3-dione). The optimal conditions were $K_2S_2O_8$ (2 equiv.) and tetrabutylammonium bromide (TBAB) (20 mol%) in dichloroethane (DCE) at 80 °C within 8 h, which provided 3-substituted-2-arylisoindolin-1-one in good yields. They proved that both $K_2S_2O_8$ and TBAB (*n*-BuNI) were essential for the formation of the desired product. This work showed the huge role of the phase transfer catalyst (PTC) for the enhancement of the reaction efficiency. Employing the optimal conditions, the substrate scope of substituted anilines and ninhydrin was investigated. Aromatic anilines with electron-rich and electron-poor groups provided quantitative yields. Also, aliphatic and heteroaryl groups were well tolerated. In some cases, such as **102d** and **102h**, they showed diastereoselectivity with excellent yields (Scheme 78).

Later, control experiments were performed, as illustrated in Scheme 79. Radical scavengers such as TEMPO and BHT were used, along with the standard conditions, which completely inhibited the product formation and provided the radical trapped intermediates, as detected by HRMS. In the absence of ninhydrin, the reaction with phthalaldehyde (**99a**) and *p*-toluidine (**100d**) with the standard conditions along with BHT concluded the generation of radicals in 2-substituted isoindolinone derivatives. The carbocation intermediate is likely to be formed during the reaction.

The mechanism proposed by the authors is mentioned in Scheme 80. They proposed a radical pathway mechanism.

Initially, the reaction of $K_2S_2O_8$ and TBAB produced $SO_4^{-\bullet}$, which facilitated the condensation of phthalaldehyde with *p*-toluidine, producing a diol intermediate (**Q‴**). This led to hydrogen abstraction, resonance stabilization, dehydration, and tautomerization, leading to the formation of isoindolinone radical intermediate **T‴**. **T‴** underwent cyclization and hydrogen abstraction with the production of the target molecule 2-hydroxy-2-(*p*-tolyl)isoindolin-1-yl-indene-1,3-dione (**102d**).

2.3. C–S bond formation

Different C–S bond formation reactions were also reported in the literature using $K_2S_2O_8$ in last six years. The reports of C–S bond formation involved disulphide, thiol, ammonium thiocyanate and potassium thiocyanate. These sulphur nucleophiles enabled the establishment of C–S bonds under oxidative conditions, which led to structurally varied organosulfur compounds with synthetic and pharmaceutical importance. In these transformations, different additives such as molecular iodine and glucose were employed, which enhanced the efficiency of the reaction or by generation of *in situ* reactive intermediates.

In 2018, Wu *et al.* developed a protocol for the $K_2S_2O_8$-mediated thiolation of allenylphosphine oxides, where disulfides react with α-allenylic compounds to form S, P-bifunctionalized butadienes.[41] Using **103a** and diphenyl disulfide (**104a**), the optimization was conducted, where the molar equivalent of substrates was varied along with the employment of different oxidants and solvents. The best choice for the formation of the desired product was a 1 : 1.5 ratio for **103a** and **104a**, respectively, with 3 equivalents of $K_2S_2O_8$ in the presence of NMP/H_2O (1 : 1, 2 mL) at 80 °C in 12 hours. This gave the highest yield of 82% for **105a**. Employing these standard conditions, the substrate scope for allenylphosphine oxides was investigated by altering the substituents at the C-terminal with alkyl, aromatic and cycloalkyl groups with heteroatoms, which furnished the respective products in the range of 61–84%, as shown in Scheme 81 (**105a–105d**). The allene derivatives with electron-rich species preferably gave higher yield (55%) of **71e** with the *E* isomer. Further, the substituents (EDGs/EWGs/heterocyclic moieties) in disulfides were explored, which gave good yields of the products. This methodology was not good enough to support aliphatic disulfides as sulphide nucleophile sources, given that it gave a sluggish reaction.

Pre-mechanistic experiments were conducted to understand the reaction pathway (Scheme 82). A radical scavenger (TEMPO) was added to the reaction between allenylphosphine oxide and diphenyl disulfide, where the yield of the product dropped suddenly, indicating a radical-based mechanism. This suggested that the reactive species initiate from the oxidation of the disulfide instead of the allenyl compound. The authors confirmed this through HRMS analysis, which detected radical-

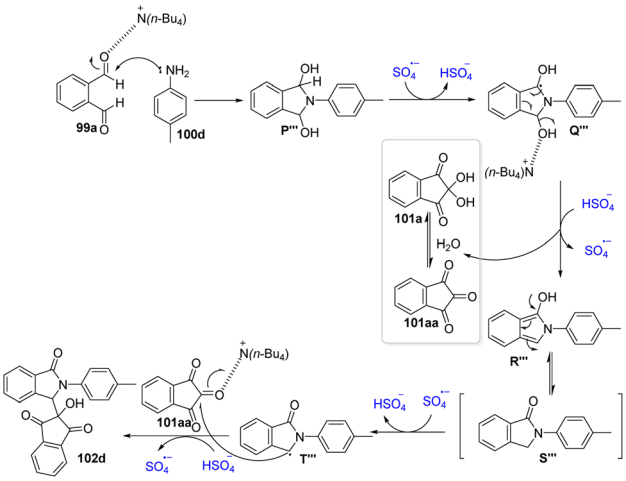

Scheme 80 Proposed mechanism for the synthesis of 3-substituted isoindolin-1-ones using TBAB/$K_2S_2O_8$.

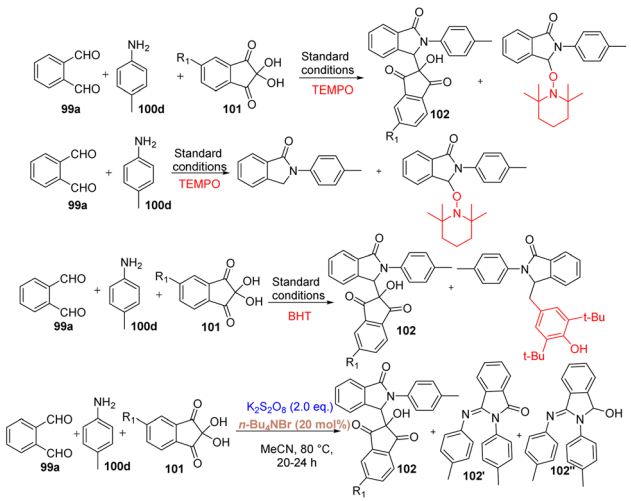

Scheme 79 Control experiments for the formation of 3-substituted isoindolin-1-ones using TBAB/$K_2S_2O_8$.

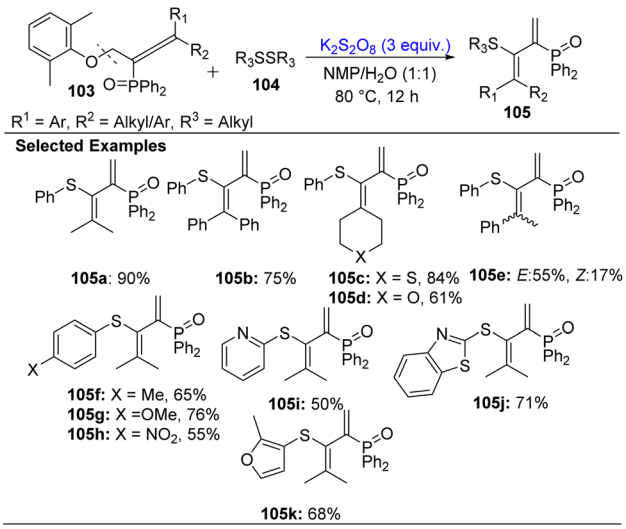

Scheme 81 Substrate scope for thiolation of allenylphosphine oxides.

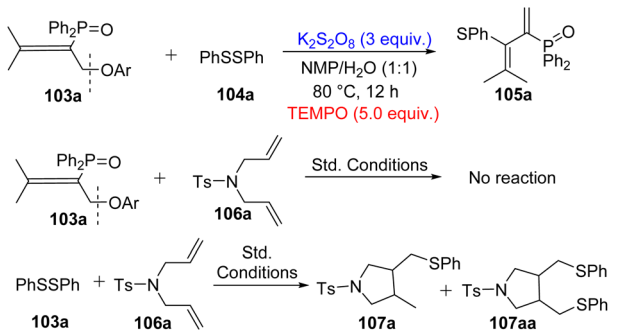

Scheme 82 Control experiments for the thiolation of allenylphosphine oxides.

derived products (**107a** and **107aa**) when diphenyl disulfide reacted with *N*-Ts-diallylamine (**106a**). This supported the formation of a thiyl radical through the oxidation of $K_2S_2O_8$.

The experimental findings and previous studies helped to propose the mechanism. It initiated with the generation of phenylthiyl radicals (PhS˙) from **104a** *via* activation by the sulfate radicals produced from $K_2S_2O_8$. These thiyl radicals then add to the central carbon of **103a**, forming an alkenyl radical intermediate. This intermediate quickly undergoes β-elimination to yield the final product **105a**. Meanwhile, the ArO˙ by-product is further oxidized by $SO_4^{\bullet-}$ to form an ArO^- anion (Scheme 83).

In 2021, Yadong Sun and colleagues presented a metal-free and efficient approach for constructing 1,2,3-thiadiazoles from tosylhydrazones and ammonium thiocyanate using a combination of iodine and potassium persulfate under mild conditions.[42] This protocol leads to the formation of C–S to S–N bonds as 1,2,3-thiadiazoles. These are important N- and S-containing heterocycles with diverse biological and pharmaceutical applications. The best conditions through the optimization of the reaction between **108a** and **109** were 0.25 mmol of iodine as an additive, $K_2S_2O_8$ (1 mmol) in eco-friendly ethanol as the solvent (2 mL). With the optimized conditions in hand, the R substitutions of N-tosylhydrazones were explored including electron-rich or halo groups, heterocyclic, and polycyclic moieties. Also, 4-methyl-*N*′-((2*Z*,3*E*)-4-phenylbut-3-en-2-ylidene)benzenesulfonohydrazide (**108h**) was found to be compatible under the reaction conditions. They all gave qualitative yields (Scheme 84). It was also observed that substrates with strong electron-withdrawing such as NO_2 or NH_2 groups were incompatible with this methodology.

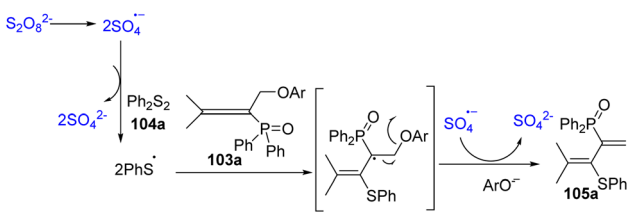

Scheme 83 Plausible mechanism for the thiolation of allenylphosphine oxides.

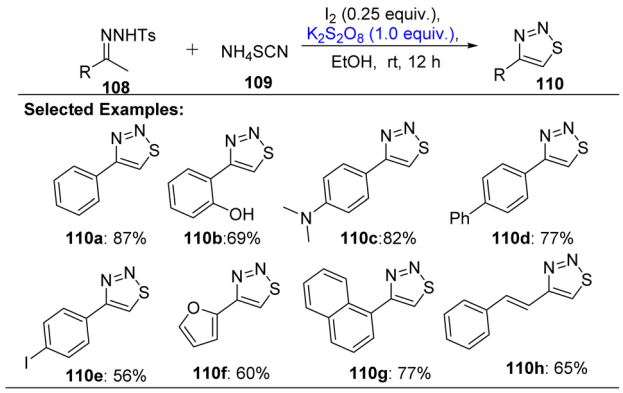

Scheme 84 Substrate scope of tosylhydrazines for the synthesis of 1,2,3-thiadiazines.

To elucidate the mechanism, a few control experiments were investigated (Scheme 85). Firstly, the one-pot reaction between acetophenone, tosylhydrazines, and ammonium thiocyanate under standard conditions was attempted, which gave 83% yield of **110a**. Next, the reaction of (*E*)-*N*′-(2-iodo-1-phenylethylidene)-4-methylbenzenesulfonohydrazide with NH_4SCN also produced the same product in 78%. Later, the reaction between 1-phenyl-2-thiocyanatoethan-1-one and NH_4SCN which also furnished **110a** with 76%. These reactions indicated the possible intermediates could be **U**‴ and **W**‴. Also, the addition of radical scavengers TEMPO and BHT to the reaction only slightly affected the yield of **110a** which ruled out the radical-pathway.

The reaction mechanism began with *N*-tosylhydrazone (**108a**) reacting with iodine to form an α-iodoacetophenone (**U**‴). The iodide ions formed in the reaction are regenerated back to iodine by potassium persulfate. The iodo group from the **U**‴ compound loses hydrogen iodide (HI), forming a new reactive intermediate (**V**‴). When ammonium thiocyanate is introduced, it reacts with this intermediate to form **W**‴, which rearranged into a more stable form **X**‴. This rearranged compound underwent ring formation to generate **Y**‴, releasing

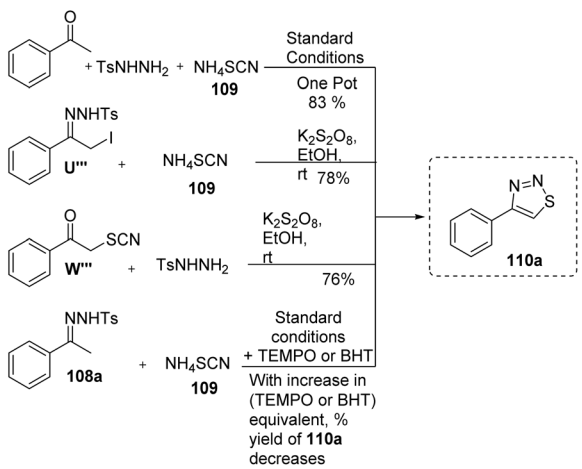

Scheme 85 Control experiments for synthesis of 1,2,3-thiadiazines.

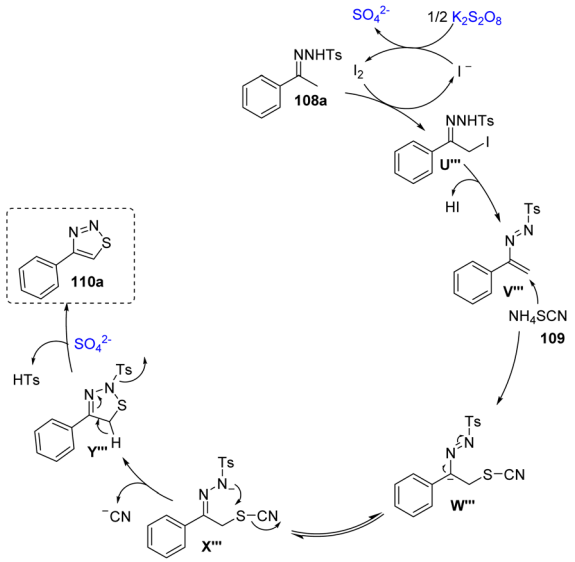

Scheme 86 Proposed mechanism for the formation of 1,2,3-thiadiazines.

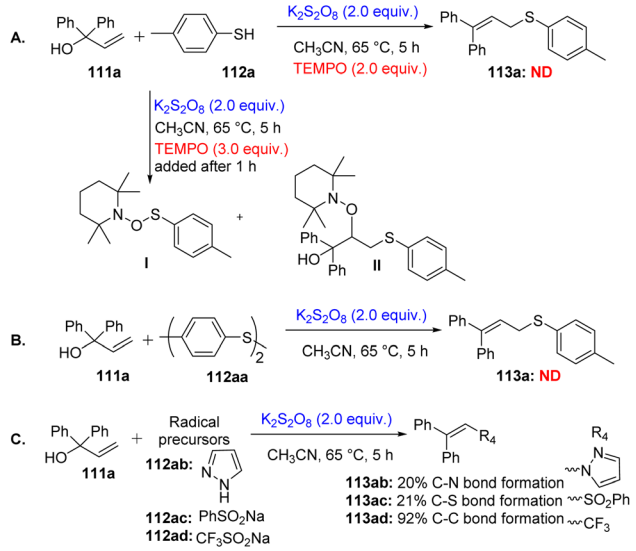

Scheme 88 Control experiments for the dehydrative coupling of allyl alcohols with substituted thiophenols.

a cyanide ion with the help of a base. Finally, the tosyl group is removed, resulting in the formation of the 1,2,3-thiadiazole product (**110a**). The authors also mentioned the possible release of the toxic HCN gas as a byproduct (Scheme 86).

In 2021, Guo *et al.* reported the synthesis of allyl sulfides using aryl/alkyl/heterocyclic sulphides as nucleophiles to allyl alcohols using $K_2S_2O_8$.[43] Allyl sulfides are important organo-sulfur compounds because they can be used to make many different types of chemical structures found in natural substances, medicines, and compounds with biological activity. The reaction of 1,1-diphenylprop-2-en-1-ol (**111a**) with 4-methylthiophenol (**112a**) was optimized, and the best yield of the desired product was obtained using 2 equivalents of $K_2S_2O_8$ in 2 mL of acetonitrile at 65 °C within 5 hours. With the optimized conditions in hand, varying substituents of allyl alcohols and aryl/alkyl/heterocyclic sulphides gave yields ranging from 54–84% (Scheme 87).

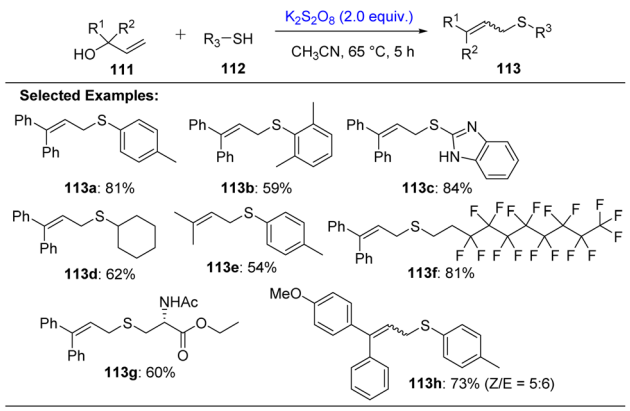

Scheme 87 Substrate scope for dehydrative coupling of allyl alcohols with substituted thiophenols.

Later, pre-mechanistic studies were performed, where no product (**113a**) was detected after the reaction between **111a** and **112a** under the standard conditions with 2 equivalent of TEMPO. A similar reaction was tested separately under the standard conditions but the radical scavenger TEMPO was added after 1 h of reaction, where TEMPO-linked species (**I** and **II**) were detected through HRMS (Scheme 88A). This proved that thiophenol is converted into radical form and would react with **113a**, which might be present in the reaction to form the product. Further, the product was not achieved when the reaction between 4-methyl disulfide (**112a**) and **111a** was performed the under standard reaction conditions, which suggested that disulfide is not key intermediate for the formation of allyl sulfide (Scheme 88B). Also, 1H-pyrazole, sodium benzenesulfinate, and sodium trifluoromethanesulfinate were used as radical precursors for the formation of **113ab** (20%), **113ac** (21%), and **113ad** (92%), where C–N, C–S, and C–C bonds were formed, respectively. These reactions indicated that the reaction might occurred *via* a radical pathway, and also showed the substrate scope for this metal-free approach (Scheme 88C).

The tentative mechanism according to the control studies and literature reports is shown in Scheme 89. Single electron

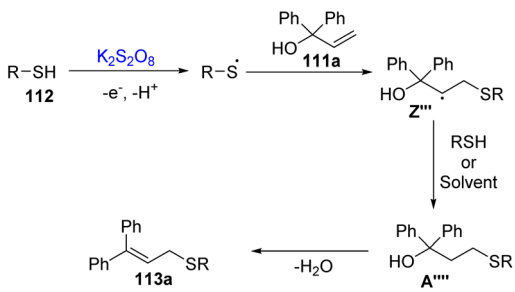

Scheme 89 Proposed mechanism for allyl sulfide formation.

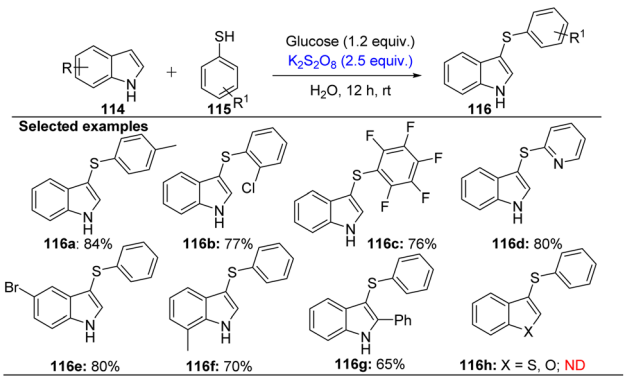

Scheme 90 Substrate scope for indoles and thiophenols.

transfer (SET) and deprotonation of thiophenol furnished the thiyl radical. Carbon radical **Z‴** is formed after the addition of the thiyl radical to **111a**. **Z‴** abstracts a proton from thiophenol/solvent to form intermediate **A‴′**, and its dehydration produces the final product **113a**.

The versatility of $K_2S_2O_8$ encouraged the synthesis of various bioactive molecules such as arylthio compounds. Recently, in 2023, Jeyakumar *et al.* explored the synthesis of (3)-S-arylthioindoles using $K_2S_2O_8$-glucose from indole and thiophenols in aqueous media.[44] The reaction was optimized using model substrates **114** and **115a** by testing different oxidants, including $(NH_4)_2S_2O_8$, $PhI(OAc)_2$, $Na_2S_2O_8$, DDQ, and $K_2S_2O_8$, in both polar protic and aprotic solvents, along with various additives such as glucose, galactose, mannose, and maltose. The best conditions were 1.5 mmol of persulfate and 0.72 mmol of glucose in 4 mL of water. These optimized conditions were employed to explore the substrate scope for substituted indole and thiophenols, where all gave quantitative yields (Scheme 90). All the substrates were found to be well tolerated under the reaction conditions. However, other heteroaryl groups such as benzothiophene and benzofuran did not provide the target products.

The radical scavengers TEMPO and BHT supported the free-radical mechanistic approach. Based on the control experiments and previous reports on persulfate-glucose mediated reactions, the mechanism has been depicted, where this reagent system led to the formation of a thiophenol radical and indole-stabilized radical **C‴′**. The combination of the thiophenol radical with **C‴′** forms radical intermediate **D‴′**, which undergoes 1,3-H shift to form the target product **116i** (Scheme 91).

Last year, Sharma *et al.* disclosed the dual C–H sulfenylation of imidazopyridines using potassium thiocyanate catalyzed by potassium persulfate under visible light to furnish symmetrical and unsymmetrical imidazopyridine sulfanes.[45] The authors reported a metal-free approach over the traditional methods involving toxic chemicals, smelly thiols, and expensive metal catalysts. By prioritizing green chemistry, sulfur-containing imidazopyridines (C–S–C) were achieved with cleaner and light-driven method. The model substrates imidazopyridine (**117a**) and indole (**118a**) were used to find the effect of different light sources in the presence of potassium thiocyanate (KSCN), potassium persulfate ($K_2S_2O_8$), and the base DBU. The reaction was checked for different solvents such as DMSO, DCM, AcCN, and water. Also, the reaction product yield decreased when DBU was replaced with other bases such as Cs_2CO_3 and K_3PO_4, and even an alternative to $K_2S_2O_8$, *i.e.*, TBHP, gave no product. The reaction was carried out for varying reaction times. The optimized conditions were 2 mmol of $K_2S_2O_8$, 1 mmol of DBU, and irradiation from blue LEDs at room temperature in AcCN : H_2O (1 : 1) solvent system for 20 h. With the established protocol, the effect of substitutions on 2-phenylimidazo[1,2-*a*]pyridine and indole was minimum, and there were no electronic and steric effects on the formation or yield of the desired products (Scheme 92). The reaction of **117a** and 3-methyl indole failed to give the expected product.

Further, the reaction of substituted 3-phenyl imidazo[1,5-*a*] pyridines (electron rich/electron poor) with indole was carried out, resulting in the desired products with good yields varying from 71% (Scheme 93A). Also, the reactions with azaindole, benzothiazole, and another molecule of imidazopyridine furnished the respective products in quantitative yield of thioether

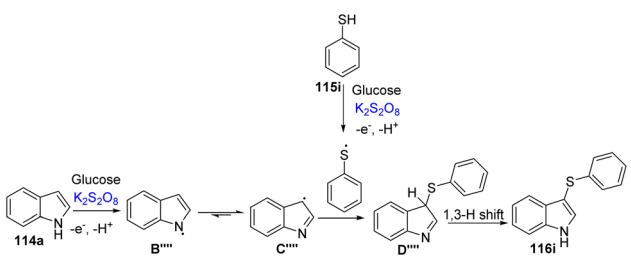

Scheme 91 Proposed mechanism for the synthesis of (3)-S-arylthioindoles.

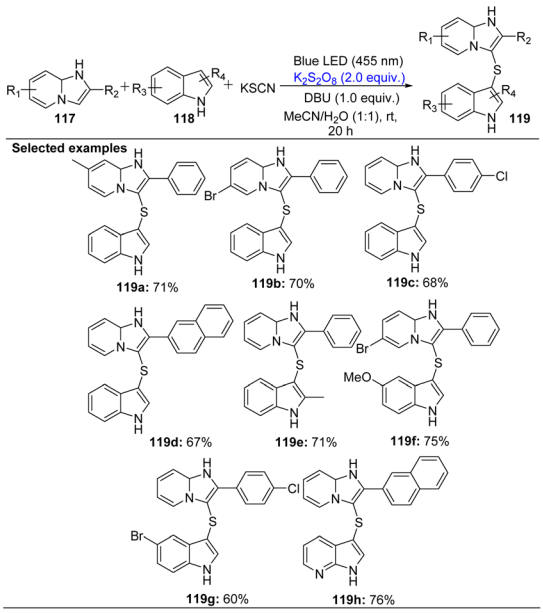

Scheme 92 Substrate scope for 2-phenylimidazo[1,2-*a*]pyridine and indole.

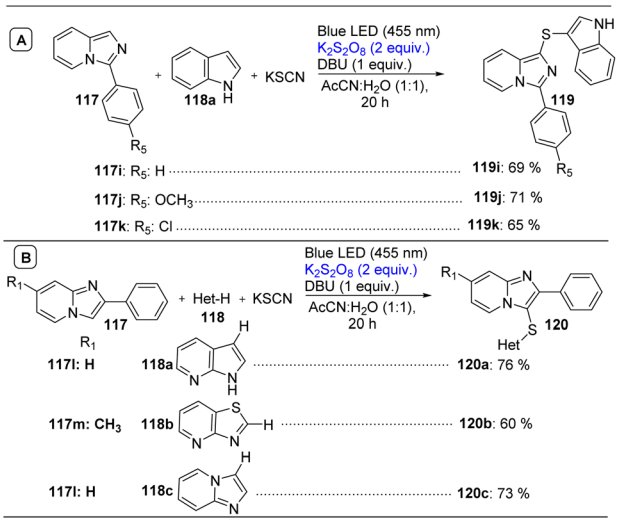

Scheme 93 (A) Reaction of 3-phenyl imidazo[1,5-*a*]pyridines with indole. (B) Reaction of 2-phenylimidazo[1,2-*a*]pyridine with diverse nucleophiles.

products under the standard reaction conditions (Scheme 93B). Alternatively, this methodology was not compatible with thiophene, furan, pyrrole, and N-protected indoles as nucleophiles.

Control experiments were performed by the authors to elucidate the reaction mechanism (Scheme 94). The reaction of **117l**, **118a**, and potassium thiocyanate (KSCN) predominantly formed disulfide (**H′′′′**) and imidazole-linked thiocyanate (**E′′′′**) in 75% and 21%, respectively, which were detected by HRMS after 9 hours. The reaction was conducted in the absence of DBU, where **E′′′′** was formed in 90%, which indicated its importance in the conversion to **H′′′′**. Later, **L′′′** was used for the reaction with indole, which provided the target compound in 79%. Also, radical inhibitors such as TEMPO supported the radical pathway reaction mechanism (Scheme 68).

These studies led to the depiction of the reaction mechanism (Scheme 95). The mechanism began when $K_2S_2O_8$ under blue

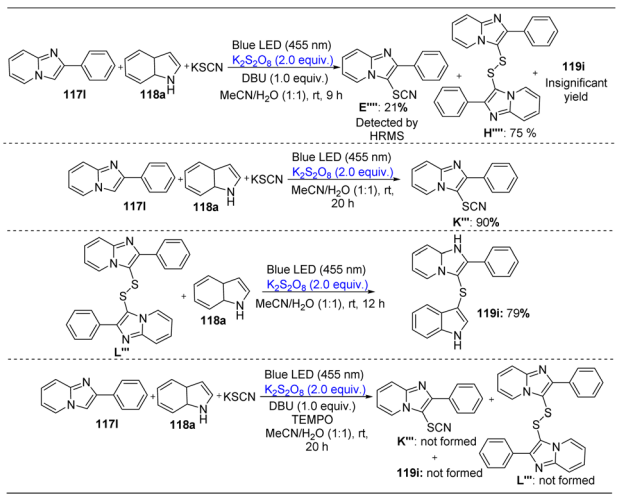

Scheme 94 Control experiments for the formation of imidazopyridine sulfanes.

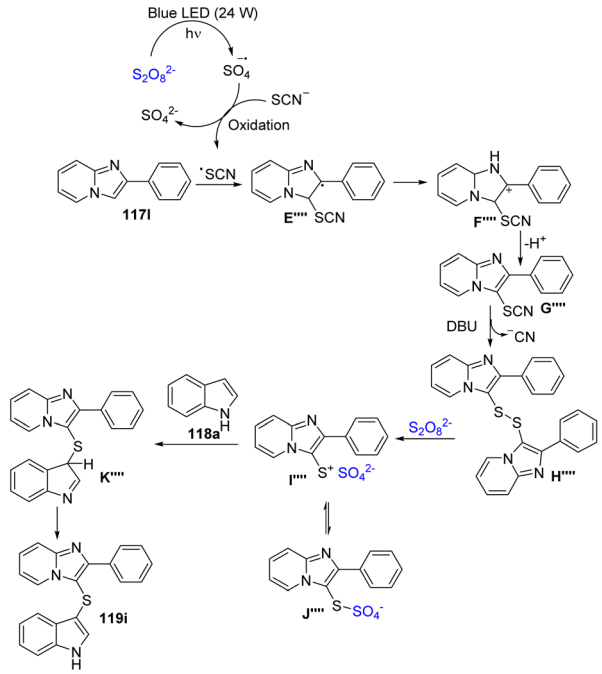

Scheme 95 Proposed mechanism for the synthesis of imidazopyridine sulfanes.

LED light at RT generated $SO_4^{-\bullet}$. The $SO_4^{-\bullet}$ radical oxidized the thiocyanate ion, forming a thiocyanate radical, which reacts with imidazopyridine (**117l**), leading to the formation of a thiocyanate compound (**E′′′′**). It was treated with the base DBU, and a cyano group was removed, resulting in the formation of a diimidazopyridinyl disulfide intermediate (**H′′′′**). This intermediate reacts with persulfate and generated sulfenylated imidazopyridine radicals (**I′′′′** and **J′′′′**). These radicals then coupled with indole to form a new intermediate (**K′′′′**), which finally loses a proton to give the final C-3 sulfenylated product (**119i**).

2.4. C–Se bond formation

The efficient role of $K_2S_2O_8$ was observed for the construction of C–Se bonds. Only one study has been reported on the formation of C–Se bonds and another described the selenylation of pyrazoles, where both C–N and C–Se bonds were formed using persulfate as the oxidant in the past six years. Diselenides were used as the source of organoselenium.

In 2022, Xiaoxiao Li and Zhigang Zhao with their colleagues opted for a greener and sustainability method for the transformation of allenamides to 1,2-diselenides, overcoming the previous approaches using potassium persulfate.[46] The preliminary step of optimization involved the reaction of 4-methyl-*N*-phenyl-*N*-(propa-1,2-dien-1-yl)benzenesulfonamide (1.0 mmol) **120a** with diphenyl diselenides **121a** (3.0 mmol), which led to the standard conditions of 1 mmol of $K_2S_2O_8$ in the presence of acetonitrile (2 mL) at room temperature under an Ar atmosphere, where the desired product was obtained in 74% with a ratio of $Z:E$ (3 : 1) within 4 h. The optimized conditions were investigated for the substrate scope of allenamides and

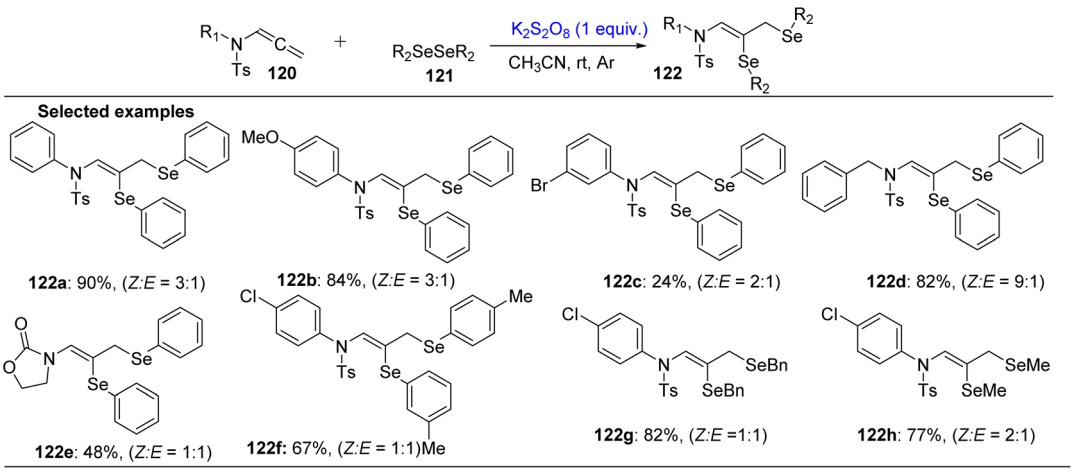

Scheme 96 Substrate scope of allenamides and diselenides.

dialkyl/diaryl/dibenzyl diselenides. Electron-rich and unsubstituted allenamides gave good yields compared to electron-poor allenamides with a ratio of $Z:E$, as mentioned in Scheme 96. Even heterocyclic allenamides also sustained the reaction conditions and provided **122e** in 48%. Most of substituted diphenyl diselenides gave moderate to good yields. However, the reaction did not work for 2-Cl and 3-Cl substituted diselenides. Further, dibenzyl diselenide and dimethyl diselenide extended the methodology and provided quantitative yields of the desired products. The authors confirmed the stereochemistry and exact configuration of (*Z*)- and (*E*)-1,2-diselenides using single-crystal X-ray analysis of **122f**.

The protocol was attempted in the presence of TEMPO and BHT radical scavengers, which indicated the probable free radical mechanistic approach. The proposed mechanism (Scheme 97) suggested that the presence of $K_2S_2O_8$ produced PhSe$^{\bullet}$ from PhSeSePh (**121a**). This radical attaches to the terminal carbon of allenamide **120a**, creating an alkenyl radical intermediate (**L**$''''$). Then, this intermediate reacts with another PhSe$^{\bullet}$ to form the target product **122a**. The probability of addition to the central carbon is less because the alkenyl radical intermediate ($\Delta E = 0$ eV) is more stable than allylic radical intermediate **M**$''''$ ($\Delta E = 1.06$ eV).

Last year, Peglow *et al.* reported the one-pot $K_2S_2O_8$-mediated, acid-promoted synthesis of 4-selanylpyrazoles using 1,1,3,3-tetramethoxypropane and aryl hydrazines, with the method also enabling the synthesis of 4,5-bis-selenylated derivatives.[47] Based on previous literature studies, acetic acid was used for the generation of 4-selanylpyrazoles. Further, the overall reaction was optimized for the formation of 4,5-bis-selenylated derivatives, using 1,1,3,3-tetramethoxypropane and phenyl hydrazine using a range of organic and inorganic oxidants. 4-Selanylpyrazoles were *in situ* generated from 1,1,3,3-tetramethoxypropane (0.5 mmol) and aryl hydrazines (0.5 mmol), which react with phenyl diselenide (0.25 mmol) in the presence of 1.5 mmol of $K_2S_2O_8$ at 120 °C within 90 min as the standard reaction conditions. Under the optimized conditions, the substrate scope was explored for pyrazoles and diselenides. Different substituents of pyrazoles were well tolerated under the reaction conditions, and also a variety of diselenides also gave moderate to good yields (Scheme 98).

Pre-mechanistic studies were performed for the proposal of the mechanism (Scheme 99). An increased equivalent of $(PhSe)_2$ and $K_2S_2O_8$ at higher temperature of 140 °C provided the bis-selenated product (91%) with traces of **125a** from *in situ*-formed **124aa**. The authors mentioned that **125a**′ is an unprecedented product, which they characterized and described in detail using NMR (Scheme 99A). Also, the radical scavenger TEMPO with 3.0 equivalent was used, along with the

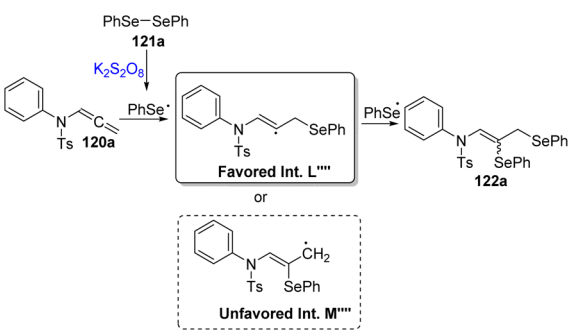

Scheme 97 Mechanism for diselenation of allenamides.

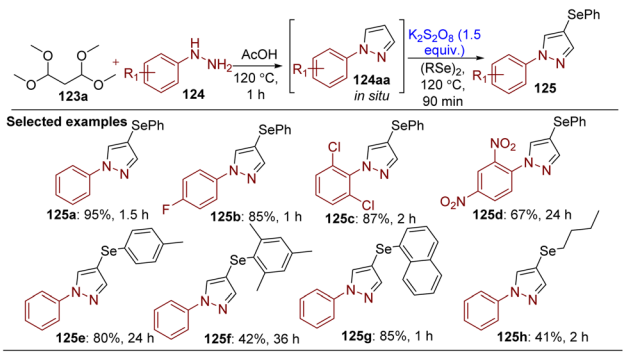

Scheme 98 Substrate scope for 1H-pyrazoles and diselenides.

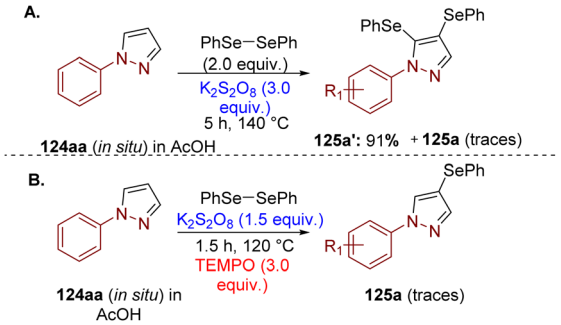

Scheme 99 Control experiments for selenylation.

standard reaction conditions, which proved the radical pathway (Scheme 99B).

Further, the mechanism showed two stages, where initially in the first stage, 1-aryl-4-(organylselanyl)-1*H*-pyrazoles were generated using acetic acid (Scheme 100). Later, the phenyl selenide radical was produced using persulfate and attacked at the C4 of 1-phenyl-1*H*-pyrazole, resulting in the formation of radical intermediate **N**′′′′, which then underwent oxidation to form cationic intermediate **O**′′′′ by sulphate radical anion. At last, the deprotonation of **O**′′′′ led to the final product **125a**.

2.5. C–P bond formation

The persulfate-mediated formation of the C–P bond has been least explored since 2018 to the present to the best of our knowledge under metal-free oxidative transformations by $K_2S_2O_8$. Here, diaryl phosphites have been explored for the construction of C–P bonds in chroman-4-ones.

Guanqun Xie *et al.* developed a metal-free, green, and efficient method to synthesize phosphinoylchroman-4-ones by using $K_2S_2O_8$.[48] The formation of C–P bonds in phosphine oxides of chroman-4-one from 2-(allyloxy)benzaldehyde and diphenyl phosphine oxide using 3.0 equivalent of $K_2S_2O_8$ with a DMSO/H_2O solvent system in the ratio of 4 : 1 at 80 °C in 18 hours gave the best results. These standardized conditions were

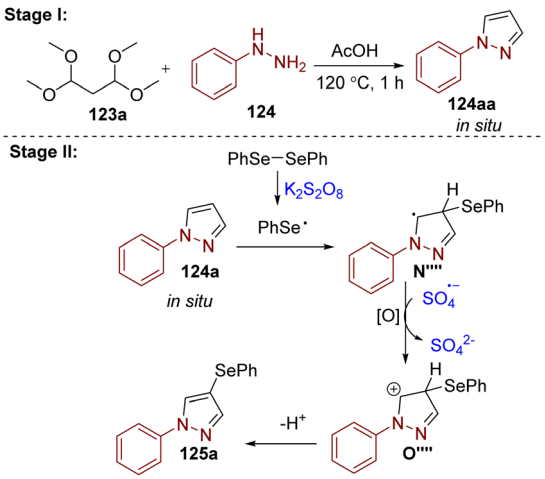

Scheme 100 Mechanism for the selenylation of C4-1*H*-pyrazoles.

exposed to a variety of 2-(allyloxy)benzaldehydes and diaryl phosphine oxides, which gave quantitative yields, whereas dialkyl phosphine oxides did not gave the desired products. Also, an indanone derivative was also found to give comparable yields. Strong electron-deficient groups such as the nitro group failed to produce the desired products. Alkoxy phenyl phosphine oxides (**127i**) and dialkoxy phosphine oxides (**127j**) were investigated and well tolerated the reaction conditions. *N*-Allyl-*N*-(2-formylphenyl)-4-methylbenzenesulfonamide (**126k**) was also attempted to expand the methodology and clearly supported, which gave moderate yields (40–44%) (Scheme 101).

The mechanism was proposed after attempting the reaction with TEMPO and BHT by the authors, involving a free-radical pathway. $K_2S_2O_8$ breaks down under heat to produce $SO_4^{\bullet-}$. These radicals then react with diphenylphosphine oxide (**127a**), forming a phosphorus-centered radical (**P**′′′′). This radical adds to the double bond of **126a** and generates the **Q**′′′′ radical, which then attacks the aldehyde group within the same molecule. This intermediate was detected through NMR by the authors. This produced an oxygen-centered radical (**R**′′′′), which underwent 1,2-hydrogen abstract transfer (HAT) to form a benzyl radical (**S**′′′′). Finally, another $SO_4^{-\bullet}$ abstracted a proton from **S**′′′′ to give the final product **128a** (Scheme 102).

3. Miscellaneous

Owing to the unique and interesting properties of the inexpensive oxidant potassium persulfate, it has been used in metal-free oxidative, nitration and *N*-nitrosation reactions.

In 2024, Fernandes *et al.* presented an efficient and environmentally benign scheme for the conversion of 1-arylbutadienes into cinnamaldehydes through oxidative C–C bond cleavage using either potassium persulfate ($K_2S_2O_8$) or azobisisobutyronitrile (AIBN) in the presence of molecular oxygen (Scheme 103).[49] Here, we are concerned about the transformation conducted with persulfate. The reactions proceeded under metal-free conditions and tolerated diverse electron-rich, electron-poor, and heteroaryl substituents. The optimization studies identified 0.5 equivalent of $K_2S_2O_8$ in aqueous acetonitrile at 80 °C as the most effective conditions. Control experiments and trapping studies demonstrated that the reaction proceeded *via* radical pathways. This approach offered a practical and selective alternative to traditional oxidative cleavage methods.

In 2019, Naseem Ahmed *et al.* introduced a direct and eco-friendly method for the oxidative deoximation of flavanone and chalcone oximes using $K_2S_2O_8$ under mild conditions to furnish the respective carbonyl compounds in good to excellent yields.[50] The most effective system was found through optimization, *i.e.*, acetonitrile at 80 °C with 1.5 equivalents of $K_2S_2O_8$ (Scheme 104). This method was acceptable for broad application not only for flavanone and chalcone oximes but also a range of ketoximes and aldoximes, including sterically hindered and functionalized substrates, generating their corresponding ketones or aldehydes. The substrates bearing electron-deficient groups generally gave higher yields than those with electron-rich groups. The mechanistic insights suggested that the reaction

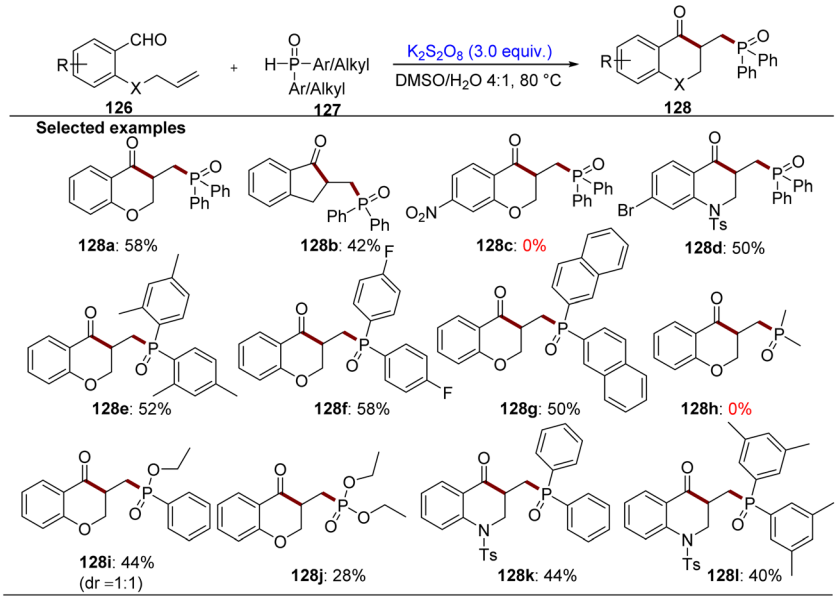

Scheme 101 Substrate scope for phosphine oxide-functionalized chroman-4-ones.

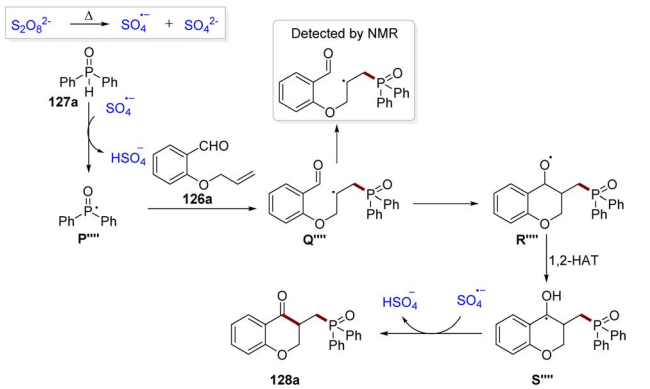

Scheme 102 Proposed mechanism for the synthesis of phosphine oxide-functionalized chroman-4-ones.

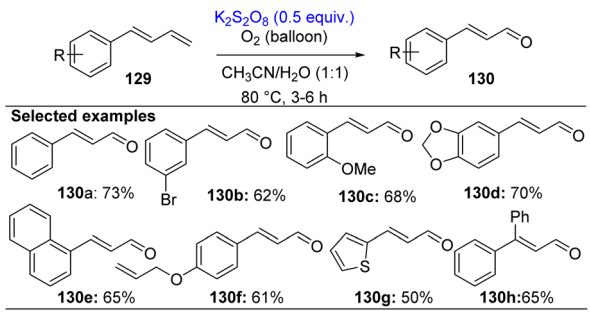

Scheme 103 Oxidative cleavage of 1-arylbutadienes into cinnamaldehydes by $K_2S_2O_8$.

proceeds *via* the formation of a nitrone-type intermediate, cyclization, and consequent hydrolysis to release the carbonyl product and hydroxylamine, with H_2SO_4 by-product, which is a crucial. The mechanism did not follow a free-radical pathway. The methodology is beneficial given that it requires a short reaction time, minimal work-up, and tolerance towards different functionalities.

In the same year, Singh *et al.* presented a direct and metal-free method for nitrating olefins using $NaNO_2$ as the NO_2 source, trifluoroacetic acid (TFA) as the proton donor, and $K_2S_2O_8$ as the oxidant under open-air conditions (Scheme 105).[51] Through optimization, stereoselective *E*-nitroolefins were generated efficiently from styrenes and mono-substituted alkenes, while α,α-disubstituted olefins produced *E*/*Z* mixtures using a DCM–water solvent system in ratio of 2 : 1 with TFA (1 equiv.) and $NaNO_2$ (2 equiv.), along with $K_2S_2O_8$ (2 equiv.). The method tolerated a broad range of electron-donating, electron-withdrawing, and heteroaryl substrates, providing good yields. The reduced selectivity for aliphatic olefins was noticed. The mechanistic analyses suggested the reaction proceeded without any effect of TEMPO, which implied that radical intermediates play a significant role in the elimination to form the nitroolefin.

In 2018, Kandasamy and group disclosed an efficient protocol for the *N*-nitrosation of secondary and tertiary amines using nitromethane (CH_3NO_2) as the nitrosating agent, activated by $K_2S_2O_8$ and DBU under mild conditions (Scheme 106).[52] Through proper optimization, 60 °C was the best temperature for the provision of the desired product in quantitative yields across varying substrates including dialkyl, cyclic, benzyl, and aryl secondary amines, as well as tertiary amines *via* dealkylative nitrosation. Cheap, stable, and readily available reagents were used with the avoidance of acids or toxic nitrosating reagents. The protocol was well tolerated for diverse functional groups. $K_2S_2O_8$ promoted the formation of the nitrosonium ion from nitromethane and attack to the secondary amine or dealkylative nitrosation afforded the desired product.

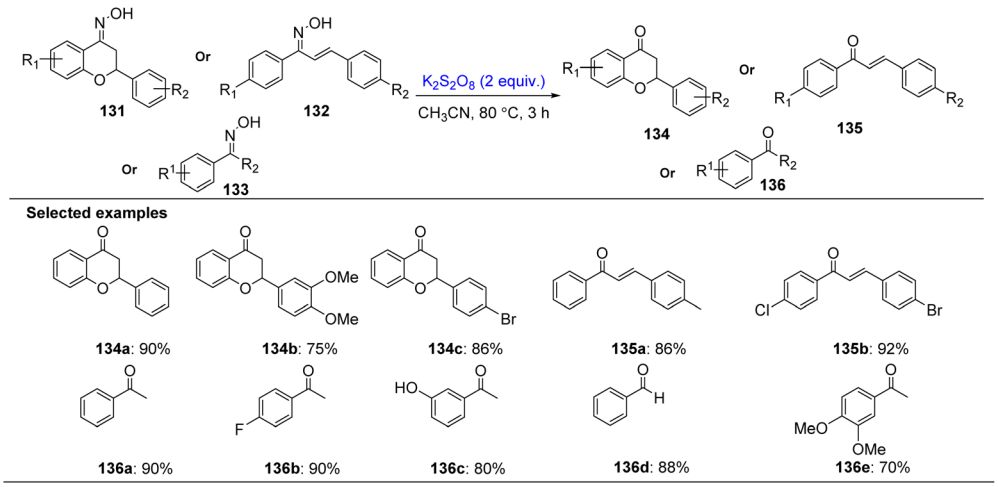

Scheme 104 Oxidative deoximation of flavanones and chalcones oximes using $K_2S_2O_8$.

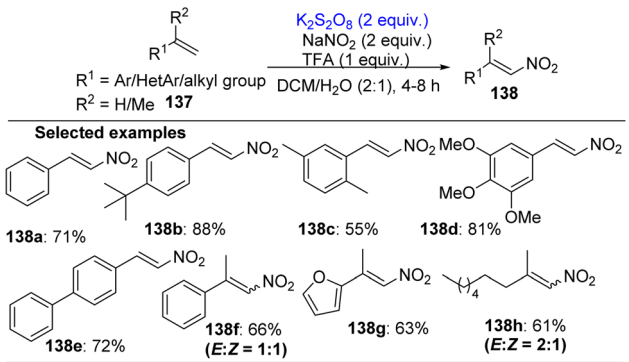

Scheme 105 Nitration of olefins assisted by $K_2S_2O_8$–$NaNO_2$–TFA.

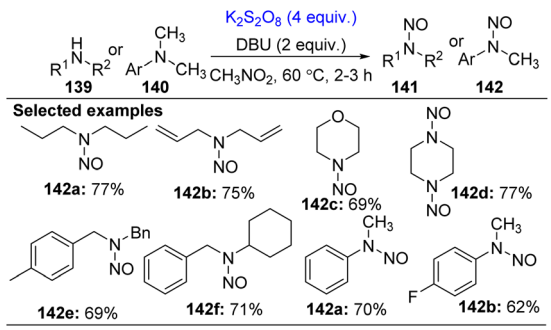

Scheme 106 *N*-Nitrosation of secondary amines or dialkylative nitrosation assisted by $K_2S_2O_8$.

4. Conclusions

Over quite a few years, $K_2S_2O_8$ has been developed as a prevailing, multipurpose, and environmentally friendly oxidant in organic synthesis due to its high redox potential and ability to generate sulfate radical anions under mild conditions. The homolytic cleavage of the peroxo (O–O) bond in the peroxydisulfate anion and production of two highly reactive sulfate radical anions ($SO_4^{-\bullet}$). This sulfate radical is responsible for diverse transformations such as C–H functionalization, oxidative coupling, radical cyclization, C–C and C–heteroatom bond formation, as well as selective oxidations in both aqueous and organic media. The reactivity of persulfate could be harnessed under controlled conditions for various catalytic and oxidative transformations and its effectiveness strongly influenced by temperature, solvent, pH, and surrounding matrix components. The possible activation of persulfate for different functionalities containing substrates was attempted using heat, light, ultrasound, or additives, which has made it a key reagent in green synthetic methodologies. Several studies have revealed that $K_2S_2O_8$ can be successfully utilized for heterocycle construction and C–C and C–heteroatom bond formation.

The future scope of potassium persulfate-facilitated reactions is promising for the development of sustainable synthetic strategies. Researchers have been actively focused on finding novel methods for the construction of new bonds by exploiting the applications of $K_2S_2O_8$. Advancements are expected in planning and executing more selective with catalytic systems for its activation, along with visible light and electrochemical approaches. Its role in tandem and cascade reactions could be further explored for efficient one-pot innocuous methodologies. Furthermore, integration with continuous-flow technology and its application in the large-scale production of pharmaceutically important molecules may significantly enhance its role in industry. The combination of $K_2S_2O_8$ with greener solvents would further support its role as a key oxidant in the next generation of environmentally friendly chemical routes.

Author contributions

R. V. contributed to the planning, execution and drafting of the article. P. C. contributed to the proposal, conception, supervision and execution of the study and drafted and edited the manuscript. Both the authors thoroughly read the final manuscript draft and have agreed for its submission.

Conflicts of interest

There are no conflicts to declare.

Data availability

This is a review article. There are no new data available.

Acknowledgements

R. V. thanks the Institute of Chemistry, Academia Sinica, Taipei, Taiwan. P. C. would like to thank R&D, Department of Higher Education, U. P. for funding (Letter No. 2/2025/361/Sattar4-2025-003-4 (33)/2023).

References

1 (*a*) C. Lee, H. Kang and S. Hong, NiH-catalyzed C–N bond formation: insights and advancements in hydroamination of unsaturated hydrocarbons, *Chem. Sci.*, 2024, **15**, 442–457; (*b*) S. Wang, L. Wang, J. Cui, L. Zhang, Q. Zhang, C. Ke and S. Huang, Recent progress in C–S bond formation *via* electron donor–acceptor photoactivation, *Org. Biomol. Chem.*, 2025, **23**, 1794–1808; (*c*) K. A. Jannath, and H. A. Saputra, A Review on Recent Developments in Transition Metal and Heteroatom-Doped Carbon Catalysts for Oxygen Reduction Reaction, *Electrochem. Sci. Adv.*, 2024, **5**, e202400033; (*d*) M. Elagawany, L. Maram and B. Elgendy, Synthesis of 3-Aminoquinazolinones *via* a $SnCl_2$-Mediated ANRORC-like Reductive Rearrangement of 1,3,4-Oxadiazoles, *J. Org. Chem.*, 2023, **88**(24), 17062–17068; (*e*) J. He, M. Wasa, K. S. L. Chan, Q. Shao and J.-Q. Yu, Palladium-Catalyzed Transformations of Alkyl C–H Bonds, *Chem. Rev.*, 2017, **117**, 8754–8786; (*f*) L. Ping, D. S. Chung, J. Bouffard and S.-G. Lee, Transition Metal-Catalyzed Site-and Regio-Divergent C–H Bond Functionalization, *Chem. Soc. Rev.*, 2017, **46**, 4299–4328.

2 (*a*) O. N. Farinde, V. Satheesh, K. K. Shrestha, C. R. Rhinehalt, V. G. Landge and M. C. Young, Oxidative Mizoroki–Heck reaction of unprotected cinnamylamines at ambient temperature under air, *Org. Chem. Front.*, 2023, **10**, 3982–3988; (*b*) J. Ni, M. Lanzi and A. W. Kleij, Unusual DBU-catalyzed decarboxylative formation of allylic thioethers from vinyl cyclic carbonates and thiols, *Org. Chem. Front.*, 2022, **9**, 6780–6785; (*c*) Q. Wang, S. Wu, Y. Wang, J. Sun, Y. Han, C. Yan and L. Wang, Photo-induced 1,2-alkylarylation/cyclization of alkenes, alkyl halides and N-alkylindoles *via* an EDA-complex, *Org. Chem. Front.*, 2023, **10**, 2907–2912.

3 F. Minisci, A. Citterio and C. Giordano, Electron-Transfer Processes: Peroxydisulfate, a Useful and Versatile Reagent in Organic Chemistry, *Acc. Chem. Res.*, 1983, **16**, 27–32.

4 D. Y. Naumov, A. V. Virovets, N. V. Podberezskaya, P. B. Novikov and A. A. Politov, Redetermination of the Crystal Structure of Potassium Peroxodisulfate ($K_2S_2O_8$), *J. Struct. Chem.*, 1997, **38**, 922–929.

5 S. Mandal, T. Bera, G. Dubey, J. Saha and J. K. Laha, Uses of $K_2S_2O_8$ in Metal-Catalyzed and Metal-Free Oxidative Transformations, *ACS Catal.*, 2018, **8**, 5085–5144.

6 (*a*) Z. Xia, Z. Ye, T. Deng, Z. Tan, C. Song and J. Li, Benzylic C–H Radical Sulfation by Persulfates, *Angew. Chem.*, 2025, **64**(10), e202413847; (*b*) Z. Xia, T. Deng, C. Song and J. Li, Decarboxylative sulfation by persulfates, *Chem. Sci.*, 2025, **16**, 11568–11573.

7 S. Pari, A. Wang, I. H. Li and B. M. Wong, Sulfate Radical Oxidation of Aromatic Contaminants: A Detailed Assessment of Density Functional Theory and High-Level Quantum Chemical Methods, *Environ. Sci.: Processes Impacts*, 2017, **19**, 395–404.

8 G. F. P. de Souza, J. A. Bonacin and A. G. Salles, Visible-Light-Driven Epoxyacylation and Hydroacylation of Olefins Using Methylene Blue/Persulfate System in Water, *J. Org. Chem.*, 2018, **83**(15), 8331–8340.

9 (*a*) R. A. Sheldon, The E factor 25 Years On: The Rise of Green Chemistry and Sustainability, *Green Chem.*, 2017, **19**, 18–43; (*b*) X. Zhang, G. Dhawan, S. Muthengi, S. Liu, W. Wang, M. Legris and W. Zhang, One-pot and catalyst-free synthesis of pyrroloquinolinediones and quinolinedicarboxylates, *Green Chem.*, 2017, **19**, 3851–3855; (*c*) N. Eghbali, J. Eddy and P. T. Anastas, Silver-Catalyzed One-Pot Synthesis of Arylnaphthalene Lactones, *J. Org. Chem.*, 2008, **73**, 6932–6935.

10 (*a*) J. Li and D. Z. Wang, Visible-Light-Promoted Photoredox Syntheses of α, β-Epoxy Ketones from Styrenes and Benzaldehydes under Alkaline Conditions, *Org. Lett.*, 2015, **17**, 5260–5263; (*b*) A. Loupy, S. Chatti, S. Delamare, D.-Y. Lee, J.-H. Chung and C.-H. Jun, Solvent free Chelation-assisted Hydroacylation of Olefin by Rhodium(I) Catalyst under Microwave Irradiation, *J. Chem. Soc., Perkin Trans. 1*, 2002, **10**, 1280–1285.

11 M. Jouffroy and J. Kong, Direct C-H Carbamoylation of Nitrogen-Containing Heterocycles, *Chem.–Eur. J.*, 2019, **25**, 2217–2221.

12 (*a*) S. V. Amosova, A. S. Filippov, V. A. Potapov and A. I. Albanov, Regio- and stereoselective one-pot synthesis of new heterocyclic compounds with two selenium atoms based on 2-bromomethyl-1,3-thiaselenole using phase transfer catalysis, *Catalysts*, 2022, **12**, 1236; (*b*) T. Balakrishnan and S. Damodarkumar, The kinetics and mechanism of induced thermal decomposition of peroxomonosulphate by phase transfer catalysts, *J. Chem. Sci.*, 2000, **112**, 497–505.

13 S. Sultan, M.-u.-S. Bhat, M. A. Rizvi and B. A. Shah, Visible Light-Mediated [2 + 2] Cycloaddition Reactions of 1,4-Quinones and Terminal Alkynes, *J. Org. Chem.*, 2019, **84**, 8948–8958.

14 Y.-N. Wang, Q. Li, Y.-L. Fang, L.-H. Gao, S.-Z. Song, Y. Dong and W.-T. Wei, Potassium-Persulfate-Promoted Regioselective Azidation/Cyclization of 1,6-Enynes, *Asian J. Org. Chem.*, 2019, **8**, 1–5.

15 S. Bhattacharjee, S. Laru, P. Ghosh and A. Hajra, Potassium Persulfate Mediated Chemodivergent C-3 Functionalization

of 2H-Indazoles with DMSO as C1 Source, *J. Org. Chem.*, 2021, **86**, 10866–10873.

16 H. K. Indurthi, S. Das, P. Saha and D. K. Sharma, $K_2S_2O_8$-Mediated C-3 Formylation of Imidazopyridines Using Glyoxylic Acid, *Eur. J. Org Chem.*, 2023, **26**, e202300829.

17 J. K. Laha and M. K. Hunjan, $K_2S_2O_8$ activation by glucose at room temperature for the synthesis and functionalization of heterocycles in water, *Chem. Commun.*, 2021, **57**, 8437.

18 Y. Zhong, M. Jiang, B. Yang, Q. Wang and D. Zhu, Umpolung Conversion of Phosphine Chlorides as Transient Nucleophilic Phosphines for Nickel-Catalyzed Cross-Coupling with Isocyanates, *ACS Catal.*, 2025, **15**, 14813–14822.

19 J. K. Laha, U. Gulati, Saima, T. Schulte and M. Breugst, pH-Controlled Intramolecular Decarboxylative Cyclization of Biarylacetic Acids: Implication on Umpolung Reactivity of Aroyl Radicals, *J. Org. Chem.*, 2022, **87**, 6638–6656.

20 H. K. Indurthi, S. Das, P. Saha, S. N. Koli and D. K. Sharma, Potassium persulfate-glucose mediated synthesis of 3,3′-Bis(indolyl)methanes from arylacetic acid and indoles in water, *J. Mol. Struct.*, 2024, **1307**, 137959.

21 H. Chen, Z. Sun, H. Yang, F. Mao, X. Yan, X. Li and X. Xu, Potassium Persulfate/Tributylamine-Mediated Alkylation/Annulation of N-Arylacrylamides with Alkyl Iodides, *Synlett*, 2023, **34**, 63–66.

22 B. Trinadh and B. Viswambharan, Potassium persulfate mediated oxidative dearomatization and C-H functionalization of indoles in water: Green and transition metal free approach for the synthesis of indolone derivatives, *Tetrahedron*, 2023, **142**, 133527.

23 Z. Chen, X. Huang, J. Sun, Y. Liu and Z. Li, Metal-free Cascade Radical Cyclization of N-Methylacrylyl-2-phenylbenzimidazole: Construction of Aryldifluoromethylated Benzimidazole[2,1-a]iso-Quinoline-6(5H)-ketone, *Asian J. Org. Chem.*, 2022, **11**, e202200255.

24 Á. M. Pálvölgyi, F. Scharinger, T. Bauhoff and K. B. Schröder, Visible Light-Driven, Persulfate-Mediated Hydrocarboxylation of Vinylsulfones, *Adv. Synth. Catal.*, 2023, **365**, 3069–3074.

25 Y.-M. Xiao, Y. Liu, W.-P. Mai, P. Mao, J.-W. Yuan and L.-R. Yang, A Novel and Facile Synthesis of Chroman-4-one Derivatives via Cascade Radical Cyclization Under Metal-free Condition, *ChemistrySelect*, 2019, **4**, 1939–1942.

26 F. Gao, F.-X. Meng, J.-Y. Du, S. Zhang and H.-L. Huang, One-Step Synthesis of Trifluoroethylated Chromones via Radical Cascade Cyclization–Coupling of 2-(Allyloxy)arylaldehydes, *Eur. J. Org Chem.*, 2020, 209–212.

27 J. Zhou, Q. Ren, N. Xu, C. Wang, S. Song, Z. Chen and J. Li, $K_2S_2O_8$-catalyzed highly regioselective amidoalkylation of diverse N-heteroaromatics in water under visible light irradiation, *Green Chem.*, 2021, **23**, 5753.

28 S.-W. Tian, F.-T. Xiong, B.-Q. Xiong, L.-J. Zhong, K.-W. Tang and Y. Liu, $K_2S_2O_8$-Mediated Radical Cascade Alkylation/Cyclization of Ynones: Access to Oxoalkyl-Substituted Indenones, *ChemistrySelect*, 2023, **8**, e202302484.

29 Y. Lu, J. Zhang, X. Duan, B. Yang, C. Zhao, L. Gu, C. Chen, H. Zhu, Y. Ye, Z. Luo and Y. Zhang, $K_2S_2O_8$-Mediated Radical Cyclization of 1,6-Enyne for the Synthesis of Diiodonated γ-Lactams, *J. Org. Chem.*, 2023, **88**, 2393–2403.

30 L. Sumunnee, C. Pimpasri, M. Noikham and S. Yotphan, Persulfate-promoted oxidative C–N bond coupling of quinoxalinones and NH-sulfoximines, *Org. Biomol. Chem.*, 2018, **16**, 2697–2704.

31 (*a*) M. Reggelin and C. Zur, Sulfoximines: Structures, Properties and Synthetic Applications, *Synthesis*, 2000, **1**, 1–64; (*b*) C. P. R. Hackenberger, G. Raabe and C. Bolm, Synthetic and Spectroscopic Investigation of N-Acylated Sulfoximines, *Chem.–Eur. J.*, 2004, **10**, 2942; (*c*) C. R. Johnson, Applications of Sulfoximines in Synthesis, *Aldrichimica Acta*, 1985, **18**, 3.

32 J. K. Laha, U. Gulati, Saima, A. Gupta and H. K. Indurthi, Improved, gram-scale synthesis of sildenafil in water using arylacetic acid as the acyl source in the pyrazolo[4,3-d]pyrimidin-7-one ring formation, *New J. Chem.*, 2021, **45**, 2643–2648.

33 J. K. Laha, U. Gulati and Saima, Effect of *ortho*-substitution on persulfate-mediated decarboxylation and functionalization of arylacetic acids, *New J. Chem.*, 2023, **47**, 15137.

34 X. Liu, S. Hee, N. G. Sapir, A. Li, J. Liu and Y. Chen, n-Bu_4NI/$K_2S_2O_8$ Mediated Csp^2-Csp^2 Bond Cleavage -Transformylation from p-Anisaldehyde to Primary Amides, *Adv. Synth. Catal.*, 2024, **366**, 2489–2494.

35 L. Ji and K. Ablajan, Metal-Free $K_2S_2O_8$-Mediated Direct Hydrazonation of Methylene in Pyrazoline-5-ones, *Asian J. Org. Chem.*, 2024, **13**, e202300577.

36 M. B. Harisha, P. Dhanalakshmi, R. Suresh, R. R. Kumar and S. Muthusubramanian, Access to highly substituted oxazoles by the reaction of α-azidochalcone with potassium thiocyanate, *Beilstein J. Org. Chem.*, 2020, **16**, 2108–2118.

37 M. Li, L. Zheng, L. Ma and Y. Chen, Transition Metal-Free Oxidative Cross-Coupling Reaction of Activated Olefins with N-Alkyl Amides, *J. Org. Chem.*, 2021, **86**, 3989–3998.

38 P. Saha, P. Kour, R. Kumar and D. K. Sharma, $K_2S_2O_8$ mediated metal free oxidative coupling of alcohols with 1,2-diaminobenzenes for synthesis of benzimidazoles, photophysical and DFT studies, *J. Mol. Struct.*, 2023, **1294**, 136431.

39 X. Liu, S. Hee, N. G. Sapir, A. Li, S. Farkruzzaman, J. Liu and Y. Chen, n-Bu_4NI/$K_2S_2O_8$-Mediated C-N Coupling Between Aldehyde and Amides, *Eur. J. Org Chem.*, 2024, **27**, e202400067.

40 S. Rana, R. Karmakar, U. Shee and C. Mukhopadhyay, Metal-Free $K_2S_2O_8$ Mediated Synthesis of 3-(Substituted)-2-Arylisoindolin-1-One Derivatives With Cascade C-N/C-C Bond Formations Via Radical Cyclization, *Eur. J. Org Chem.*, 2024, **27**, e202400080.

41 K. Luoa, L. Zhanga, K. Weia, W.-C. Yanga and L. Wu, Latent Radical Cleavage of α-Allenylic C–O Bonds: Potassium Persulfate Mediated Thiolation of Allenylphosphine Oxides, *Synthesis*, 2018, **50**, 2990–2998.

42 Y. Lu, Y. Sun, A. Abdukader and C. Liu, Diiiodine/Potassium Persulfate Mediated Synthesis of 1,2,3-Thiadiazoles from N-Tosylhydrazones and a Thiocyanate Salt as a Sulfur Source

under Transition-Metal-Free Conditions, *Synlett*, 2021, **32**(10), 1044–1048.

43 G. Guo, Y. Yuan, S. Wan, X. Cao, Y. Sun and C. Huo, $K_2S_2O_8$ promoted dehydrative cross-coupling between α, α-disubstituted allylic alcohols and thiophenols/thiols, *Org. Chem. Front.*, 2021, **57**, 8437.

44 N. Kumar, R. Venkatesh, S. Singh and J. Kandasamy, Potassium Persulfate-Glucose Mediated Synthesis of (3)-S-Arylthioindoles from Indole and Thiophenols in Water, *Eur. J. Org Chem.*, 2023, **26**, e202300679.

45 P. Saha, V. Kumar and D. K. Sharma, Visible light-driven, persulfate-mediated dual C–H sulfenylation of imidazopyridines using thiocyanate salt, *New J. Chem.*, 2024, **48**, 18651.

46 X. Tan, K. Zhao, X. Zhong, L. Yang, Y. Dong, T. Wang, S. Yu, X. Li and Z. Zhao, Synthesis of 1,2-diselenides via potassium persulfate-mediated diselenation of allenamides with diselenides, *Org. Biomol. Chem.*, 2022, **20**, 6566.

47 T. J. Peglow, J. P. S. S. C. Thomaz, L. S. Gomes and V. Nascimento, Potassium Persulfate Promoted the One-Pot and Selective Se-Functionalization of Pyrazoles under Acidic Conditions, *ACS Omega*, 2024, **52**, 51295–51305.

48 Q. Liu, W. Lu, G. Xie and X. Wang, Metal-free synthesis of phosphinoylchroman-4-ones via a radical phosphinoylation–cyclization cascade mediated by $K_2S_2O_8$, *Beilstein J. Org. Chem.*, 2020, **16**, 1974–1982.

49 R. A. Fernandes, R. S. Ranjan and P. Choudhary, $K_2S_2O_8$-Mediated or Azobisisobutyronitrile-Catalyzed Regioselective Aerobic Oxidative Cleavage of 1-Arylbutadienes to Cinnamaldehydes, *Org. Lett.*, 2024, **26**, 6247–6252.

50 M. Waheed, N. Ahmed, M. A. Alsharif, M. I. Alahmdi and S. Mukhtar, $K_2S_2O_8$-Mediated Efficient Oxidative Deoximation of Flavonoid Oximes under Mild Reaction Conditions, *ChemistrySelect*, 2019, **4**, 7572–7576.

51 S. Ambala, R. Singh, M. Singh, P. S. Cham, R. Gupta, G. Munagala, K. R. Yempalla, R. A. Vishwakarma and P. P. Singh, Metal-free, room temperature, acid-$K_2S_2O_8$ mediated method for the nitration of olefins: an easy approach for the synthesis of nitroolefins, *RSC Adv.*, 2019, **9**, 30428–30431.

52 S. Azeez, P. Chaudhary, P. Sureshbabu, S. Sabiah and J. Kandasamy, Potassium persulfate promoted *N*-nitrosation of secondary and tertiary amines with nitromethane under mild condition, *Asian J. Org. Chem.*, 2018, **7**(10), 2113–2119.